Ultra-high Field MRI Bio-effects and Safety Assessment

A Multidisciplinary Approach

Dissertation

zur Erlangung des akademische Grades

Doktoringenieurin

(Dr.-Ing.)

von MSc. **Mahsa Fatahi**

geb. am 26.05.1985 in Teheran, Iran

genehmigt durch die Fakultät für Elektrotechnik und Informationstechnik

der Otto-von-Guericke-Universität Magdeburg

Gutachter:

Prof. Dr. rer. nat. Georg Rose (Otto-von-Guericke-Universität Magdeburg)
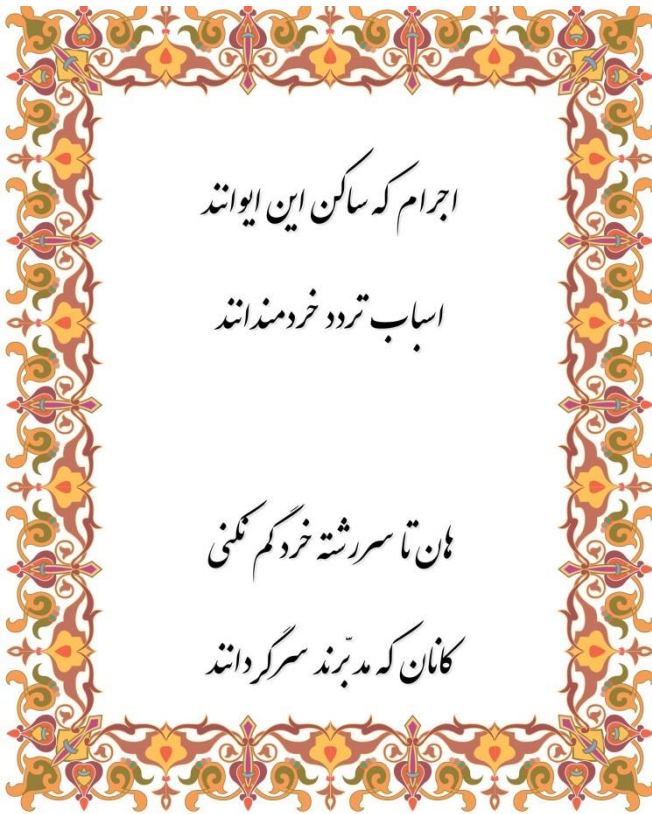
Prof. Dr. rer. nat. habil. Oliver Speck (Otto-von-Guericke-Universität Magdeburg)

Prof. Dr. sc. techn. M. E. Ladd (German Cancer Research Center, Heidelberg)

Promotionskolloquium am 31.07.2017

This doctoral dissertation is lovingly dedicated to my dear parents for their infinite love and support.

Mahsa Fatahi

Magdeburg, Germany

اجرام که ساکن این ایواند

اسباب تردد خردمنداند

هان تا سر رشته خرد گم نکنی

کانان که مدبّرند سرگردانند

The stars and planets in the skies
Allow the wise to fantasize;

Hold on to Wisdom as your guide
Schemers suffer schematicide

Hakim Omar Khayam Neyshabouri (1048-1131)
Persian polymath, astronomer, mathematician and poet

Acknowledgment

Undertaking this PhD has been a truly life-changing experience for me and it would not have been possible to do without the support and guidance that I received from many people.

Firstly, I would like to express my sincere gratitude to my advisor Professor. Dr. rer. nat. habil. Oliver Speck, for giving me the chance to be part of his research team and for his continuous support. He also gave me the freedom to pursue research in different areas, while focusing on this dissertation project. I also would like to thank Professor. Dr. rer. nat. habil. Geroge Rose.

This present work would not have been successfully completed without the supportive and professional academic environment, I found myself in. I would like to thank the excellent ''MRI-DNA'' expert team, Professor. Dirk Reinhold, Professor. Dirk Roggenbuck, Dr. Björn Friebe, Dr. Annika Reddig and Dr. Frank Godenschweger. I very much enjoyed the collaboration with such a great team.

For the genetic damage investigation studies, in particular, I am really grateful for the excellent guidance, crucial advice and hints from Dr. Vijaylaxmi. Her scientific backup was fundamental and her enthusiastic approach to work helped push me forward.

Further, I'd like to thank all friends and co-workers at BMMR Group, especially the ''frequent flyers'', who generously helped with the in-vivo experiment. Tobias, Frank, Sebastian, Uten, Myung-Ho, Falk, Daniel, Michel, Hendrick and Allessandro, thank you very much!

The survey-based study would not have been possible without the support of the HiMR project fellows and supervisors. I would like to express my gratitude to Professor Mark Ladd and his team at DKFZ, Professor. Peter Jezzard and Professor Karla Miller at Oxford Centre for Functional MRI of the Brain (FMRIB), for hosting my secondment and welcoming me into their research group.

Abstract

We are continuously surrounded by appliances that emit electromagnetic fields (EMFs). The pace in the development of EMF technologies is breathtaking, and the number of commercial EMF applications and their users are ever increasing. Much of our daily exposure to EMFs, both in the workplace and by the general public, is no longer consists of a single frequency, but is rather a multi-frequency exposure with different characteristics. Despite a large number of published reports by different expert groups regarding the biological effects caused by non-ionizing EMFs during the last decades, the question of whether they can cause biological detrimental effects to health is still open. Possible genotoxic and carcinogenic effects of magnetic resonance imaging (MRI), especially with high and ultra-high field strengths, have been among the main questions and concerns in the last decades. Both theoretical considerations and empirical evidence indicate that direct damage to genetic material caused by non-ionizing EMFs of a single frequency, per se, is not likely. However, the question of whether the combined EMFs generated by MRI scanners, can enhance the effects of genetic-damaging agents remains still unanswered and there is still no consensus in the scientific community even about the existence of harmful effects generated by MRI scanners.

In this thesis a profound insight into ultra-high field magnetic resonance imaging (UHF MRI) bio-effects and safety is given using a multidisciplinary research approach in three different themes. A series of experiments, starting from *in vitro* exposure of the human blood cells to *in vivo* exposure of human subjects, and from a single exposure to multiple repeated exposures, was designed to quantitatively and qualitatively assess the potential biological effects induced by UHF MRI. The results of these experimental studies are reported in Part I. The other safety aspect of UHF MRI relates to the occupational exposure level. Part II of the thesis aims to fill the knowledge gap between safety concerns in actual exposure and perceived risks in 7 Tesla (T) MRI environments during routine MRI research procedures. Part II relates to the measurement of the 7 T MRI occupational exposure and identifies the worst case scenarios of maximum exposure.

Part III focuses on retrospective, self-reported perceptions of safety, and the prevalence of UHF MR-related sensory effects. The results reported in this part of the thesis, are based on a comprehensive survey among healthy individuals who occupationally work with and around 7 T MRI scanners in 8 different MRI centres across Europe.

Zusammenfassung

Wir sind ständig von Geräten umgeben, die elektromagnetische Felder (EMFs) aussenden. Das Tempo, mit der die Entwicklung dieser Technologien voranschreitet, ist atemberaubend, und die Zahl kommerzieller EMF Anwendungsfelder sowie deren Nutzer vergrößern sich weiter. Ein Großteil der täglichen EMF-Exposition, sowohl am Arbeitsplatz als auch in der Öffentlichkeit, besteht nicht nur aus einer einzigen Frequenz, sondern ist vielmehr eine Mehrfrequenzbelastung mit unterschiedlichen Merkmalen. Trotz der großen Zahl an Veröffentlichungen durch verschiedene Fachgruppen zu den biologischen Auswirkungen nicht-ionisierender EMF in den letzten Jahrzehnten bleibt die Frage offen, ob sie schädlichen Einfluss auf unsere Gesundheit haben. Mögliche genotoxische und karzinogene Effekte der Magnetresonanztomografie (MRT), insbesondere bei hohen und ultrahohen Magnetfeldstärken, gehören zu den Hauptfragen und -bedenken der letzten Jahrzehnte. Sowohl theoretische Überlegungen als auch empirische Nachweise deuten darauf hin, dass direkte Schäden durch nicht-ionisierende EMF einer einzigen Frequenz, per se, unwahrscheinlich sind. Allerdings bleibt die Frage offen, ob die in der MRT erzeugten EMF Kombinationen die Auswirkungen von genetisch bedingten Schädigungen verstärken können. Es gibt derzeit noch keinen Konsens in der Wissenschaft, ob durch MRT-Geräte überhaupt schädliche Effekte hervorgerufen werden. In dieser Arbeit soll ein tiefgreifender Einblick in die biologischen Effekte und die Sicherheit von Ultrahochfeld-Magnetresonanztomografie (UHF MRT) mittels eines multidisziplinären Ansatzes in drei Themenfeldern gegeben werden: Um qualitativ und quantitativ die potentiellen biologischen Effekte durch UHF MRT zu untersuchen und zu bewerten wurde eine Reihe von Experimenten, beginnend mit in vitro-Exposition menschlicher Blutzellen bis zur Exposition von Versuchspersonen im MRT, sowohl in einmaligen Exposition als auch in mehrfach wiederholten Expositionen, entworfen. Die Ergebnisse dieser experimentellen Studien werden in Teil I dargelegt. Ein weiterer Sicherheitsaspekt liegt in der berufsbedingten Strahlenexposition. Teil II der Arbeit hat das Ziel, die Wissenslücke zwischen den Sicherheitsbedenken in der tatsächlichen Exposition und den gefühlten Risiken bei 7 Tesla (T) MRT-Umgebungen

während des routinierten Arbeitsablaufs in der Forschung zu füllen. Teil III konzentriert sich auf retrospektiv selbst berichtete Wahrnehmungen der Sicherheit und die Prävalenz UHF MRT-bedingter sensorischer Empfindungen. Die Ergebnisse dieses Teils der Arbeit basieren auf einer umfassenden Befragung gesunder Personen, die mit 7 T MRT-Scannern und in deren Umgebung in 8 verschiedenen MRT-Zentren in ganz Europa arbeiten.

Contents

PART II: EXPOSURE ASSESSMENT IN (ULTRA) HIGH FIELD MRI ENVIRONMENTS

4 Evaluation of Exposure to (Ultra) high Static Magnetic Fields during Research Activities with MRI Scanners………..……………………..71

PART III: TRANSIENT AND SENSORY EFFECTS

5 Transient and Sensory Effects of Exposure to UHF MR…………….90

6 General Discussion, Conclusions and Future Research..................... 103

Appendix

1 Introduction

1.1 Exposure to Electromagnetic Fields

All living organisms are constantly exposed to a broad range of naturally present electromagnetic fields (EMFs) that exist over the surface of the Earth. Superimposed on the Earth's magnetic field, are human made EMFs. As technology advances, global emissions of such EMFs are likely to further increase [1]. The best known examples in everyday life are EMFs produced during electricity production, transmission and distribution; mobile phone communication services; cordless telephones, wireless networks; and medical applications. Typical sources of EMFs in medical applications are X-ray scanners, magnetic resonance imaging (MRI) scanners, hyperthermia, diathermy and transcranial magnetic stimulation. A detailed overview of the EMFs spectrum can be found in section 1.2.

1.2 Electromagnetic Spectrum

Electromagnetic radiation is emitted energy that travels through a medium or space with wave-like and particle-like properties [2]. The EM spectrum is continuous and divided into

the different frequency ranges, which reflect differences in the physical behavior such as absorption and reflection in different materials, Figure (1.1). All types of EM radiation share the same physical properties of divergence, interference, coherence, and polarization; however, they differ in terms of energy [2].

EMF fields are classified into ionizing and non-ionizing, based on their ability to ionize an atom or a molecule [3]. Ionizing radiation contains enough energy to physically alter the atoms and change them into charged particles called ions. It is well known that medical applications using ionizing radiation such as x-ray-based imaging and computed tomography (CT) can lead to adverse health effects, such as carcinogenic damage in human cells. Therefore, the 'as low as reasonably achievable' (ALARA) principle is widely accepted and implemented for ionizing-based medical applications [4]. On the other hand, non-ionizing radiation is a general term for that part of the EM spectrum with weak photon energy, which is not able to break atomic bonds in exposed materials.
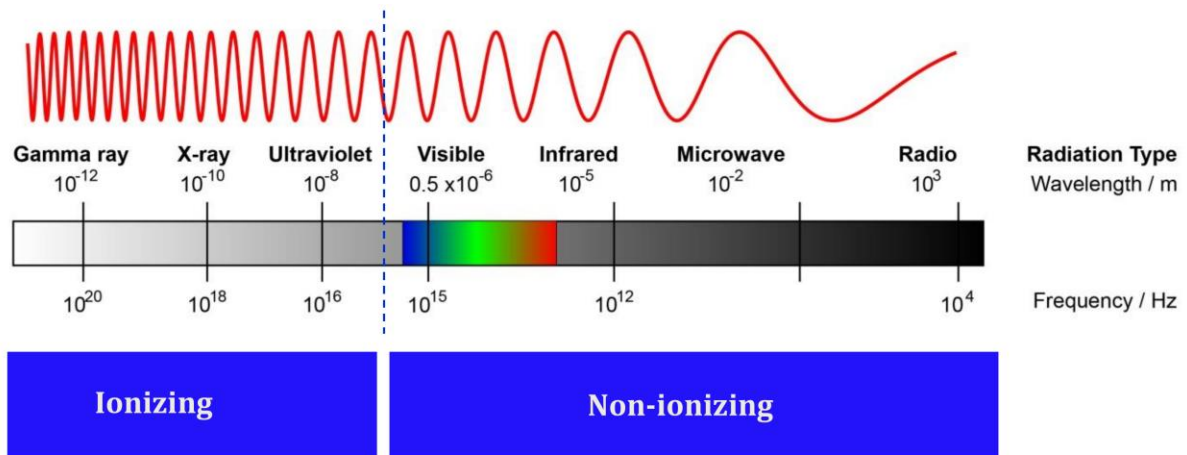
Figure 1.1: Schematic representation of the electromagnetic spectrum. It shows various properties across the range of frequencies and wavelengths. The division between Ionizing and non-ionizing radiation is generally accepted to be at wavelengths around 100 nm (10^{-7}) of the EM spectrum. (Image source: EM Spectrum Properties, retrieved February 1, 2017 from www.sciencemadesimple.co.uk)

The work described in this thesis is limited to non-ionizing radiation. Therefore, the EMFs referred to in this thesis, represent non-ionizing EMFs.

The spectrum of non-ionizing radiation can be further divided into several categories according to frequency or wavelength: extremely low frequencies (ELF) electromagnetic fields, intermediate frequencies (IF) electromagnetic fields, radio frequency (RF) electromagnetic fields, infrared (IR) radiation, visible (VIS) light, and ultraviolet (UV) radiation.

There is no doubt that the exposure levels from all sources of EMFs must be limited to prevent adverse health effects in humans. For this purpose a number of national and international organizations such as the International Commission on Non-Ionizing Radiation Protection (ICNIRP) and the International Electro-technical Commission (IEC) have issued guidelines for limiting EMFs exposures for the general public and occupational staff to protect them from potential adverse health effects associated with exposure to human made EMFs.

Recently, a debate has arisen on potential bio-effects of MRI. MRI is a powerful, non-invasive, diagnostic medical imaging technique widely used to acquire detailed information about internal anatomies and functions of different organs, in both healthy and diseased bodies. It utilizes non-ionizing electromagnetic fields of three different frequency bands: the static magnetic field (SMF), the gradient magnetic fields (GMF) in the kHz range, and the pulsed Radio frequency (RF) in the MHz range. However, MR imaging is generally considered to be a safe and powerful diagnostic tool, but potential long-term biologic effects on humans is still an open question.

Since MRI is used within clinical and research environments, there are multiple groups of patients, medical and research staff, manufacturers, and regulatory bodies who deal with MRI and each have their own interests and demands. However, they all have a common interest which is the safety of MRI.

Over the past decades, there has been an increased demand in MRI magnets with higher field strength, which are being developed and used. This has increased the already existed uncertainties in long term effects induced by MRI.

In order to assess and verify the effects of MRI on health, biological studies, as well as epidemiological studies, have to be taken into account. Evidence of an effect can be only shown when the results of both types of studies are collected, compared and assessed. On the other hand, research on the potential health effects of MRI can only cease, when either the health effects have been established or it is concluded that further studied cannot change the overall pattern and subsequently reduce the uncertainties. Since the available data on this topic is inconsistent to draw definitive conclusions, further research on the MRI long term adverse effects is essential.

1.3 Outline of the Thesis

In this thesis, several different aspects of the ultra-high field (UHF) MRI safety, such as biological, technical and subjective safety are studied. These aspects are relevant for patients, subjects, as well as staff and policy makers. A multidisciplinary approach used in this thesis allowed a broad view on the safety-related topics, which are usually investigated separately.

These aspects are investigated by means of experimental and survey-based studies and focus is placed on three main themes (Figure 1.2):

Part I. Biological aspect: biological effects of ultra-high fields MRI

Part II. Technical aspect: exposure assessment in high and ultra-high field MRI environments

Part III. Psychological aspect: sensory and transient effects of ultra-high fields MRI

Part I: Biological effects

Chapter 2 describes in detail the known interaction mechanisms for EMFs with human bodies and safety issues in MRI and provides an overview of relevant EMF safety guidelines.

Chapter 3 provides background on genetic material and genetic endpoints. An extensive review of available literature on genetic damage associated with MRI exposure is presented.

The results of the experimental studies on the potential genetic damage after exposure to high and ultra-high field MRI are reported at different levels: *in vitro* analysis, analysis of frequently whole-body exposure, and *in vivo* analysis.

Part II: Exposure assessment

Chapter 4 links Part I and part II. This chapter aims to fill gaps about actual exposures and the perceived risks and safety of 7 T MRI during routine MRI research procedures by investigation into occupational exposure. It also reports the results from the evaluation of the exposure levels in (ultra) high field MRI environments during research activities.
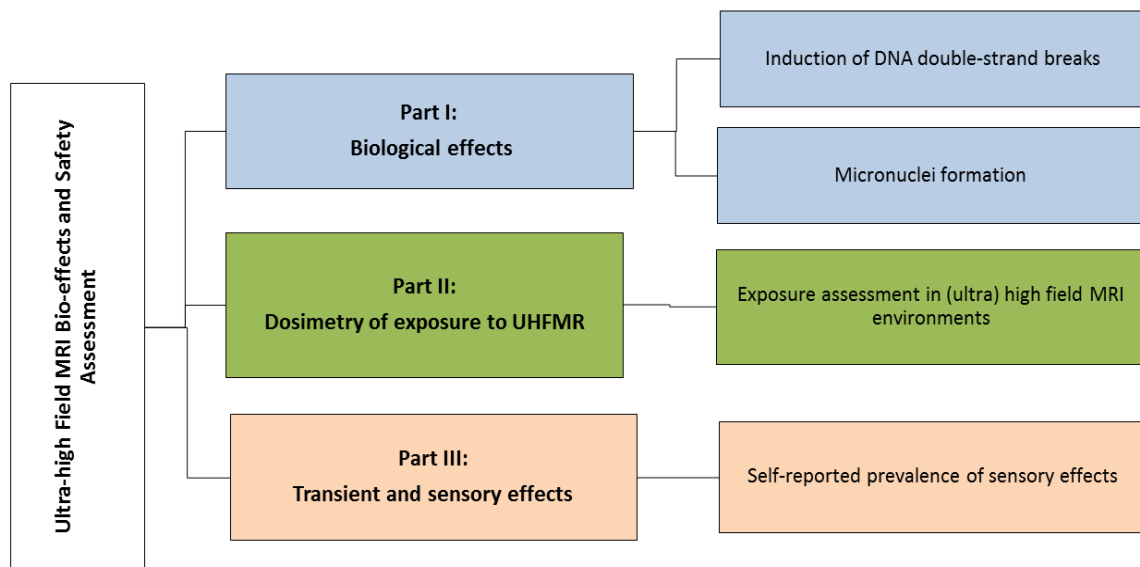
Figure 1.2: The structure of the thesis consists of three parts.

Part III: Transient and sensory effects

Chapter 5 reports the results of a multi-centre questionnaire-based study, and explores self-reported prevalence of sensory effects associated with exposure to high and ultra-high fields MRI scanners. The perceived safety of respondents in MRI environments is also investigated.

Chapter 6 provides a general discussion of the main findings. It also covers suggestions for future research, in which methodological considerations and potential implications are addressed.

Part I

Biological Effects of Exposure to Ultra-high Field Magnetic Resonance Imaging

2 Background in Electromagnetic Exposure and Safety Issues in Magnetic Resonance Imaging

2.1 Introduction

The enormous expansion in the use of MRI during the last decades is due to the incredible flexibility of this technique. Owing to its wide contrast range, use of non-ionizing electromagnetic fields, have relatively low health risk for patients and workers [5]. As a result, MR imaging has become the gold standard diagnostic tool for soft tissue imaging, and has had a very high clinical impact. MRI can provide excellent, detailed images of soft tissue with a wide contrast range. It also provides a functional and dynamic imaging modality, which is similar to nuclear medicine techniques. It can be used to measure blood flow in vessels or tissue perfusion, or changes in blood oxygenation levels.

2.2 Magnetic Resonance Imaging (MRI)

All atoms with an odd number of protons and/or neutrons have a spin correlating with an intrinsic magnetic moment *m* that is directly proportional to the quantized angular momentum *J*.

$$m = \gamma \cdot J = \gamma \cdot \hbar \cdot m_z \tag{2.1}$$

Where $\hbar$ is the reduced Planck's constant - Planck's constant *(h)* divided by 2π - and the gyromagnetic ratio γ is a proportional constant and characteristic for each nucleus and m_z is the z-component of the magnetic moment.

Nuclei possess only discrete energy levels, according to quantum mechanics. When a nucleus is affected by an external magnetic field B0, the moment *m* experiences a precession about the field direction of B0. The Larmor precession occurs at a specific frequency, called the *Larmor frequency*, which depends on the strength of the external magnetic field and the characteristics of the nucleus. The angular precession frequency $\omega 0$ is proportional to the external field strength and can be expressed by

$$2\pi f0 = \omega 0 = \gamma B0 \tag{2.2}$$

According to quantum mechanics, the proton has only two possible states (Figure 2.1) with the values mz $=\pm 1/2$ and the two energy states, parallel $\uparrow$ or anti-parallel $\downarrow$ in respect to B0, depend on the internal energy E. In thermal equilibrium and without an external magnetic field, the numbers of protons in each state of energy are evenly distributed. The energy gap ΔE between those two discrete energy bands E−and E+.

$$\Delta E := E_{+} - E_{-} = \gamma \cdot \hbar \cdot B0 = \hbar \cdot \omega 0 \tag{2.3}$$
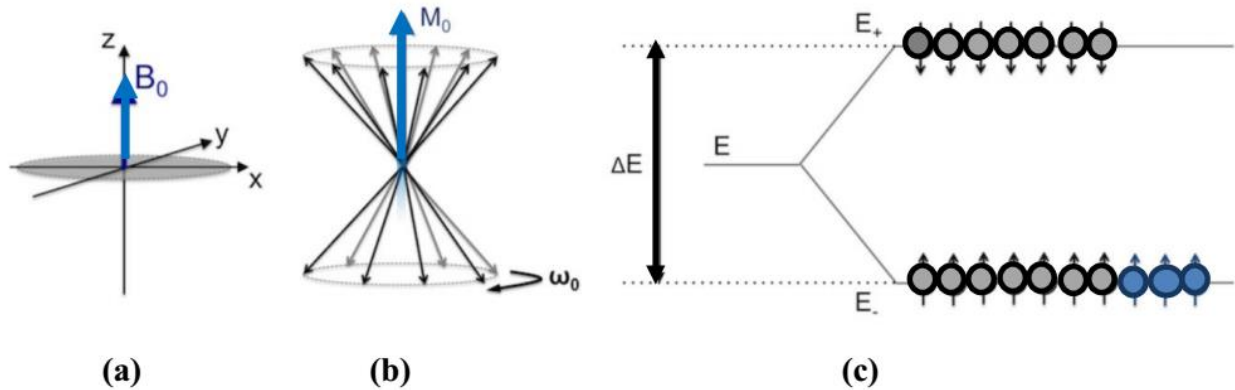
Figure 2.1: Schematic representation of the discrete states and precessing spins for Hydrogen. **(a)** An external magnetic field B0 (z-axis of the MRI coordinate system). **(b)** Each nucleus experiences a torque and precesses with the Larmor frequency about the axis of B0. The proton has only two discrete states, E− and E+ and a small surplus of spins (c) The two discrete energy bands E− and E+ are illustrated. The energy gap (ΔE) is directly proportional to B0 and the transition between E− and E+ is also determined by Equation 2.2 and 2.3 [6].

When applying an alternating magnetic field with the Larmor (resonance) frequency, energy is absorbed by the nuclear spins and re-radiated during the relaxation. This forms the basic principle of MR imaging.

Therefore, in order to create an MRI image, three types of electromagnetic fields are used; a static magnetic field (B0), a gradient magnetic field, and a radio frequency magnetic field. Table 1 presents the typical range of magnetic field exposures in MRI scanners.

- The static magnetic field (B0) is used to line up all hydrogen atoms in the body in one spatial direction. Clinically established scanners have field strengths of 1 T, 1.5 T or 3 T, with development towards 7 T, 9.4 T and beyond.

- A pulsed time gradient is used to spatially and temporally apply different effective magnetic fields to encode the position of the protons. It is applied as switching magnetic fields with frequency components up to about 100 kHz.

- A pulsed radio frequency is used to energize and excite the hydrogen proton at the Larmor resonance frequency. This energy is re-emitted by the nucleus (relaxation) and detected by a receiver coil right after the termination of the pulsed radio frequency. It is applied as a circularly polarized RF fields with frequencies of, e.g., 42, 64, 128, 298 MHz, depending on the magnetic flux density.

Table 2.1: Typical range of magnetic fields used in MRI scanners

Field	Range	Frequency	Applies
Static magnetic field	0.2- 7 T	0 Hz	Always
Spatial gradient	0- 25 T/m	0 Hz	Always, movement within it acts like a time-varying field
Gradient fields	0- 70 mT/m	0-10 KHz	During image acquisition, multiple trapezoidal pulses of few milliseconds duration
Radiofrequency	0- 50 μT	10-300 MHZ	During image acquisition, amplitude modulated pulses of few milliseconds duration

The combined effect of static, gradient magnetic fields and pulsed radiofrequency fields, as used in MRI has been getting attention only since 2007. However, the observations so far reported are controversial [7-17]. Currently the most basic question is whether or not there are "non-thermal" mechanisms that produce adverse health effects in individuals chronically exposed to MRI. If such effects do exist, then it must be determined what the effects are, and how they are produced.

Knowledge of potential mechanisms explaining possible interaction phenomena is widely demanded, not only for its predictive value for governing bodies for future legislation to ensure safety of patients and workers, but also as a necessary prerequisite for the stepwise approach to reach the highest MRI field for human application.

In this chapter the known interaction mechanisms of the EMFs with a human body is described, and focus is placed on the electric and magnetic fields generated by an MRI scanner.

2.3 Interaction of Electromagnetic Fields Used in MRI with Biological Systems

The basics of electromagnetic interaction with the materials were elucidated more than a century ago, and stated as the well-known Maxwell's equations [2]. However, it is very difficult to apply these equations to biological systems, due to the extreme complexity and multiple properties of living organisms. Nevertheless, there are several known mechanisms for the interaction of EMFs with living systems.

Electric and magnetic fields often occur together in EMF exposures; however, human body tissue responds in radically different ways to applied electric and magnetic fields. Electric fields are associated with the presence of electric charge, whereas, magnetic fields result from movement of electric charges (electric current) [18]. Electric fields are more pronounced at the surface of an electrically charged object. Due to the high conductivity of tissue in a human body, relative to the air, exposure to an electrical field leads to the buildup

of surface charge on the body than an internal field. In contrast, magnetic fields can easily penetrate the body; therefore the magnetic field strength is virtually the same inside the body as outside.

2.4 Interaction of Static Magnetic Fields with a Human Body

Interest in the biological effects of static magnetic fields has increased with the invention of MRI at the beginning of the 80s [19]. In the last two decades, several studies were carried out to examine the potential hazards associated with exposure to a strong static magnetic field. The majority of these studies did not report adverse effects on human health. However, It is known that the static magnetic field interacts with a human body at the molecular, cellular tissue, and organ level through three established physical mechanisms [18-21]. They are magnetic induction, magneto-mechanical and electronic interactions.

2.4.1 Magnetic Induction

Magnetic induction can be derived from two phenomena: Electrodynamic interactions and induced electric fields and currents.

Electrodynamic interactions with moving electrolytes: Static fields exert Lorenz forces on an electric charge (q) moving with v velocity in a direction perpendicular to the flux density of B, with the amplitude of $F = q(v \times B)$. This interaction results in a change in the direction of the charges without change in velocity. Therefore, static magnetic fields do not deposit energy into the tissues [18]. However, such interaction is the basis of magnetically induced potential associated with flowing blood in a human body. A detailed assessment of the effects of electric field on cardiovascular function shows that the fields of up to 8 T are unlikely to affect the heart rate and function [18, 20, 22]. However, as no experimental studies have been published above 8 T, this conclusion would not necessarily be true for higher fields. According to theoretical calculations, the electrodynamic-related diminution in blood flow could be 10% in the aorta in the presence of a10T field [23].

Induced electrical field and currents: According to Faraday's law of induction, the time-varying magnetic fields ($\frac{\partial \vec{B}}{\partial t}$) can induce electric current ($\vec{E}$) in living tissue.

$$\vec{\nabla} \times \vec{E} = -\frac{\partial \vec{B}}{\partial t} \tag{2.4}$$

Currents may also be induced by movement in a static magnetic field. The magnitude of the induced currents and associated electric fields is affected by the velocity of the movement and amplitude of the gradient. These gradient-induced electric fields, at sufficiently high values, can stimulate nerves and muscles. Calculations suggest that such induced electric fields can be substantial during normal movement around the fields >2-3 T [24]. Such effect may account for the numerous reports of transient sensory effects such as; vertigo and nausea experienced by MRI patients and workers [18, 25-27], which is addressed in chapter 5. The most established effect of induced currents below the threshold for nerve and muscle stimulation is the induction of magnetophosphenes. Magnetophosphenes are the perception of faint and flickering visual sensation which is most likely associated with transient electric field peaks due to sudden changes in the velocity of the head [18].

2.4.2 Magneto-mechanical Effects

There two basic mechanisms through which static magnetic fields exert mechanical force and torque on objects.

Magneto-orientation (Torque on magnetic dipole moment): It is known that in a static field, paramagnetic material experience a torque that orients them in a configuration that minimizes their free energy within the field. In other words, the rotational motion of a substance occurs in a uniform manner until achieving a minimum energy state. Although, this force is negligible in biological material due to very small ($\sim 10^{-5}$) magnetic susceptibility [18, 21], an effect cannot be excluded. A Magnetic dipole with moment $\vec{m}$ in an external magnetic field $\vec{B}$ experiences a torque.

$$\vec{N} = \vec{m} \times \vec{B} \qquad\qquad (2.5)$$

And the potential energy associated with the system is:

$$\vec{U} = -\vec{m}.\vec{B} \qquad\qquad (2.6)$$

The field has a tendency to rotate the dipole toward alignment with the field. To be precise this phenomena occurs in materials with intrinsic magnetization or with anisotropic susceptibility. An example of biological material that can be oriented magnetically is deoxygenated sickle erythrocytes. It has been shown that these cells, which contain deoxygenated hemoglobin that is paramagnetic, aligned in 0.35 T static fields with the long axis of the sickle cell oriented perpendicular to the magnetic flux lines [18, 28].

Magneto-mechanical translation (Force on magnetic dipole moment): Another mechanism through which static magnetic fields exert mechanical force and torques on objects involves a translational force.

$$F = (m.\nabla)\, B \qquad\qquad (2.7)$$

Magneto-mechanical translation happens in the presence of a gradient, when a static magnetic field produces a net translational force. The direction of the force is identical, or opposite to that of the gradient. Such force is very dominant in ferromagnetic materials, which have a strong magnetic susceptibility. The amplitude of the force is proportional to the product of the magnetic flux density (B, in teslas) multiplied by its gradient (dB/dx). For the biological material this force is as large as the force of gravity when the product of flux density and the field gradient (B.dB/dt) $> 1000 \; T^2 m^{-1}$[29]. The force exerted on a paramagnetic or ferromagnetic material provides the physical basis for a range of useful biological and biochemical processes, [30] such as targeting of drugs encapsulated in magnetic micro-carries [31], the removal of microorganisms from water [32, 33], and separation of deoxygenated erythrocytes from white blood cells [34]. It has been suggested that this latter adverse effect could retard the rate of blood flow when the B.dB/dt exceeds $100 T^2 m^{-1}$[35].

2.4.3 Electron Spin Interactions

Several metabolic reactions involve an intermediate state comprising a radical pair, usually in a single state, with the spin of one unpaired electron anti-parallel to the spin of the other. These spin correlated radical pair may recombine and prevent the formation of reaction products [36-39]. The rate and the extent to which the radical pair converts to parallel spin in which recombination is no longer possible, is affected by the magnetic field. Although the biological significance of this effect is not clear yet, the effect has been suggested by some studies [18, 39] to be a source of navigational information which helps birds during migration.

2.5 Interaction of Time-Varying Gradient Fields with a Human Body

The gradient magnetic fields, which consist of three orthogonal gradients of the z-axis magnetic field, are used to select the region of diagnostic interest and to spatially encode the MR signals. They produce weak magnetic fields, which are switched on and off during image acquisition, and superimposed on the static magnetic field. Gradient coils are designed to produce line gradients within a region around the iso-centre of the scanner. These time-varying fields which lead to an induced electric field, at sufficiently high values, could stimulate nerves and at very high levels could generate cardiac stimulation or even ventricular fibrillation [40]. Clinical MR systems generate gradient field strengths in the region of 25-50 mT/m and maximum slew rates (the peak field amplitude divided by the rise time) of 100 - 200 T/m/s within the imaging field of view. Gradient fields in UHF MRI systems can be as high as 100 mT/m and the slew rate can be 800 T/m/s [41].

Many authors have investigated peripheral nerve stimulation perception thresholds for various combinations of axes on whole-body MR gradient systems [42-46]. The threshold induced electric field strengths for direct nerve stimulation could be as low as a few volts per meter and it is likely to be constant over a frequency range between a few hertz and a few kilohertz [29].

The primary cause of the acoustic noise associated with MRI is the switching gradients that impose Lorentz forces and vibrations, and mechanically couples into the system structure. Patients typically experience elevated sound pressure levels of 80–119 dB [47] which can be reduced by implementation of a proper hearing protection such as headphones and earplugs.

2.6 Interaction of Radio-frequency Magnetic Waves with a Human Body

The main effect, and, in most cases, limiting factor, of acute RF exposures is the energy absorption of the body which is associated with some degree of local tissue heating [2, 48-49]. Local tissue heating is caused by the periodical movement stimulation of dipole molecules and charge carriers. They can move and rotate freely (e.g. water molecules in water, body fluids or tissues containing water). During this process, the field components exert an action of force on charged groups of the dipole molecules, and charge carriers resulting in a torque affecting the whole molecules, causing the charge carriers to rotate. Heat is generated by friction between rotating molecules and/or moving charge carriers of other atoms [50].

The deposition and distribution of energy and temperature rise within the body is highly non-uniform and depends on the intensity and distribution of the RF and the electromagnetic and thermal properties of the tissue, e.g. thermal conductivity, permittivity, electrical conductivity, heat capacity and local blood perfusion [19, 51-58].

The term utilized to describe the absorption of radiofrequency energy is the specific absorption rate (SAR), which it is normally measured in W/kg and applies to the whole body, whereas local SAR which is applied to partial body, is averaged over any 10 g of body tissue.

Several studies have been carried out over the past decades to determine the adverse effect of RF on a human body. However, these experiments do not apply directly to the conditions that occur during MRI procedures due to the special pattern of RF absorption and the coupling of radiation to biological tissues. This pattern is highly dependent on several anatomical

features, such as the body size, the sensitivity of tissues, as well as the duration of the exposure. Therefore, the results obtained in experiments with animals or *in vitro,* cannot strictly predict thermoregulatory ability or physiological adverse effects in human subjects exposed to RF radiation during MR examinations [59-61].

With regard to non-thermal interactions, according to ICNIRP [30], ''it is in principle impossible to disprove their possible existence, but the plausibility of the various non-thermal mechanisms that have been proposed is very low''.

2.7 MRI Related-Electromagnetic Fields Exposure Guidelines

A number of international organizations and agencies regularly assess the state of knowledge in science regarding EMF bio-effects. The scientific assessment normally leads to recommendations to governments, suggested as guidelines for limiting exposure to electromagnetic fields for protection against all established adverse health effects. The currently applied limits for EMF are mostly developed by the following organizations:

- Institute of Electrical and Electronic Engineers/International Committee on Electromagnetic Safety (IEEE/ICES)
- International Electrotechnical Commission (IEC) [62]
- European Committee for Electrotechnical Standardisation (CENELEC)
- Food and Drug Administration (FDA) [63]
- Institute of Electrical and Electronic Engineers (IEEE) [64]
- International Commission on Non-Ionizing Radiation Protection (ICNIRP) [30,65]
- European Commission (SCENIHR, Scientific Committee for the Emerging and Newly Identified Health Risks) [66]
- European Health Risk Assessment Network on Electromagnetic Fields Exposure (EFHRAN)
- The World Health Organization (WHO)

All the guidelines agreed that exposed people can be grouped into three categories, and there are three approach modes for the operation of MRI equipment in line with IEC [62, 67], and ICNIRP [18, 30, 65]. Three categories are:

1. Patients for diagnosis, volunteers engaged in clinical trials

2. Staff (workers)

3. General public, including visitors/educational visitors

And three approach modes are listed below:

- **Normal mode** of operation when risk of ill effects to the patient is minimized.

- **Controlled mode (first level)** of operation when the exposure is higher than the normal mode. Although the risks are minimal, some people may experience some effects at this level, such as sensory disturbance or transient discomfort due to peripheral nerve stimulation. Scanning in this mode requires patient monitoring [18, 30, 65].

- **Research or experimental mode (second level)** when exposure is only restricted to prevent harmful effects. Scanning in this mode will require approval of a research ethics committee and patient monitoring [18, 30, 65-67].

For MRI scanners, to date only scanners with maximum field strength of 3 T have received the Food and Drug Administration (FDA) clearance for purely clinical scanning without the requirement for institutional reviewing board (IRB) approval. Scanning for purely clinical purposes above 3 T requires IRB approval. However, in 2003, the FDA in the Unites State declared that MRI up to 8T constituted a non-significant risk device for adults, children, and infants of one month and older [63]. European regulations for MRI adhere to the International Electrotechnical Commission IEC-60601-2-33 standard and in which magnetic field strengths of 3 T or less constitute the normal operating mode, field strengths between 3 T and 4 T constitute the first level controlled operating mode, and above 4 T, the second level controlled operating mode (effectively requiring IRB-approval). In 2009, the International Commission on Non-Ionizing Radiation Protection (ICNIRP), states that,'' The current information does not indicate any serious health effects resulting from acute exposure to static magnetic fields up to 8 T''[18].

An accepted standard for ensuring basic safety in MRI is the IEC standard 60601-2-33, which was updated in June 2015 [62]. The summary of MRI-related restrictions is listed in Table 2.2. It should be noted that the guidelines recommended by the international organizations include a large safety margin to limit exposure to EMFs, and these are based on the known and established adverse effects, shown in several biological and epidemiological studies.

2.7.1 Established Biological Effects versus Established Health Effects

It is important to distinguish between an "adverse effect" and a "biological effect "while referring to the guidelines. The IEEE [64] defines an adverse health effect as:
 "A biological effect characterized by a harmful change in health that is supported by consistent findings that the effect was published in the peer-reviewed scientific literature, the evidence of the effect being demonstrated by independent laboratories and, where there is consensus in the scientific community that the effect occurs for the specified exposure conditions" and, "The biological effects are alterations of the structure, metabolism, or function of a whole organism, its organs, tissues, and cells. Biological effects can occur without harming health and can be beneficial".

2.7.2 Basic Restrictions versus Reference Levels

Protection against acute health effects is assured if the dose inside human bodies does not exceed "basic restrictions". Basic restrictions are limits for personal protection, which specify the maximum exposure allowed in the whole body or in parts of the body with respect to the emissions from field-generating devices and systems. Compliance with the basic restrictions can be validated only in part by direct measurements [18, 30].

In general, dose assessment inside the human body is difficult and cannot be performed for all types of exposure. Therefore, practical "reference levels" for external exposure are defined and used to determine whether exposure limits are met.

Table 2.2: Static magnetic field restrictions for the whole-body according to ICNIRP [18, 30] and IEC [62, 67]

❖	Normal mode	Controlled mode	Research mode
ICNIRP	≤ 4 T	4-8 T	> 8 T
IEC	≤ 3 T	3-8 T	> 8 T

2.8 Ultra-high Field MRI Safety Considerations

Due to the signal to noise advantages of high field MRI systems, increases in the static magnetic field are inevitable in MRI scanners [20]. As the field strength increases, the signal to noise ratio in an image increases approximately linearly. This is because the signal increases quadratically (as it depends on both the polarization of the tissue and induction), whereas the noise only increases linearly (as it depends only on induction) [6]. On the other hand exceeding a SMF of 3 T, is impaired by high SAR, which constitutes one of the reasons, why UHF MRI has not been implemented into routine diagnostic imaging yet [4, 68-69]. There are currently more than 70 ultra-high field (7 T and above) MRI systems installed around the world [70]. A few recent review articles provide a comprehensive overview of the current status of high field MRI [68, 70]. Over the last few years an initiative to design and build MRI scanners with much higher fields (14-20 T) than currently exist, has been underway, but safety has yet to be demonstrated. Human subject safety is therefore a prerequisite for the establishment of MRI systems with higher and higher fields.

3 Genetic Damage Investigations of Exposure to High and Ultra-high Field Human MRI Scanners

The work presented in this chapter has been partly published in the following articles:

Fatahi M, Reddig A, Friebe B, et al. DNA double-strand breaks and micronuclei in human blood lymphocytes after repeated whole body exposures to 7 T Magnetic Resonance Imaging. NeuroImage. 2016 Jun 30;133:288-93.

Reddig A, **Fatahi M**, Roggenbuck D, Ricke J, Reinhold D, Speck O, Friebe B. Impact of in Vivo High-Field-Strength and Ultra-High-Field-Strength MR Imaging on DNA Double-Strand-Break Formation in Human Lymphocytes. Radiology. 2016 Sep 30:160794.

Reddig A, **Fatahi M**, Friebe B, et al. Analysis of DNA double-strand breaks and cytotoxicity after 7 Tesla magnetic resonance imaging of isolated human lymphocytes. PloS one. 2015 Jul 15;10(7):e0132702.

Vijayalaxmi, **Fatahi M**, Speck O. Magnetic resonance imaging (MRI): A review of genetic damage investigations. Mutation Research/reviews in Mutation Research. 2015 Jun 30;764:51-63.72

3.1 Objectives and Motivation

MRI technology has a very good safety record. The highest energy of electromagnetic waves used in MRI deposited in tissue, is at the order of magnitude below the ionization limit molecule, which breaks chemical bonds and is known to cause biological damage. However, there are structures in biological materials that may be affected by very low energy, such as the hydrogen bonded structures in which very low energy may cause displacement of protons [2]. Such effects, if any, must be discovered, acknowledged and taken into consideration for the safety of the patients, volunteers, clinicians and research staff working with MRI scanners.

Despite the numerous investigations evaluating the extent of genetic damage in animal and human cells exposed *in vitro* and *in vivo* to SMF, GMF and RF, each one independent of the other, very little attention has been given to assess the potential combined effects of such exposures. Due to the combined pattern of EMFs used in MRI, the conclusions from previous studies may or may not be applicable to MRI exposure. In an MRI scan, during image acquisition, the body is exposed to different waveforms, duration and amplitudes of all three different frequency ranges of electromagnetic fields. Nonetheless, there have been a limited number of investigations which examine whether *in vitro* and/or *in vivo* exposure of cells to EMFs used in MRI can cause significant genetic damage. These studies, which have previously been critically reviewed elsewhere in a review article [71], are summarized in section 3.4 of this thesis.

This chapter is comprised of three sections. Section (I) provides a background on genetic material and genetic endpoints. Section (II) reports the observations from recent studies reported in peer-reviewed scientific publications. It also addresses unresolved issues and gaps in knowledge in MRI genotoxicity assessments. Some hypothesized and potential interaction mechanism(s) are discussed in this section. Section (III) describes experimental studies on the genetic damage investigation at three different levels: *in vitro;* whole-body exposure; frequent exposure; and *in vivo*. The impact of different magnetic field strengths on the human blood cells under controlled conditions is assessed and the results are reported.

Section I: Background

3.2 Genetic Material

The term *genome* was created in 1920 by Hans Winkler, Professor of Botany at the University of Hamburg [72]. The Oxford Dictionary suggests the name is a blend of the words *gene* and *chromosome* [73]. The human genome is a chemical sequence that contains all the basic information of human bodies. It consists of tightly coiled Deoxyribonucleic acid (DNA) and associated proteins (Figure 3.1). A nucleosome is a basic unit of DNA packaging, which consists of 146 base pairs of DNA wrapped around the core histone octamer.
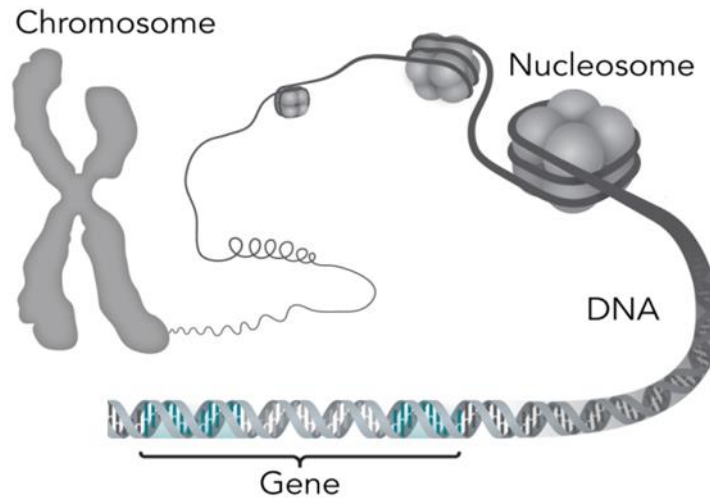
Figure 3.1: A schematic representation of a chromosome, nucleosome, DNA and gene. (Image source: chromosome, Credit: Thomas Splettstoesser/Wikipedia/CC BY-SA 4.0, retrieved December 15, 2016 from https://commons.wikimedia.org/wiki/Category:DNA

A histone octamer contains two copies of the four core histone proteins H2A, H2B, H3 and H4 [74]. Histone proteins are schematically presented in Figure 3.2.
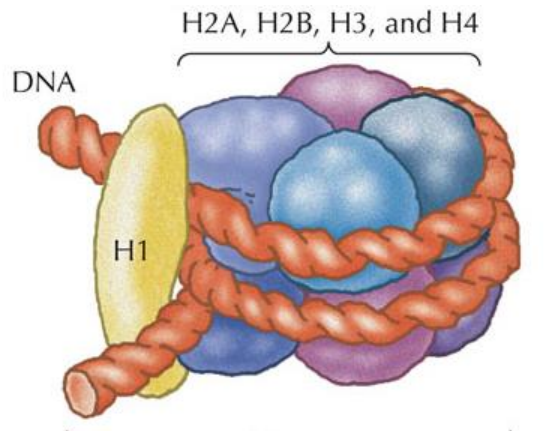
Figure 3.2: Schematic representation of the domain structures for the histone family. The histone contains a core of histone molecules, including pairs of H2A, H2B, H3, and H4, wrapped by double-helix DNA and held together by histone H1. (Image source: The Cell, Forth edition, 2006, retrieved 15 January 2017, from http://oregonstate.edu/instruction/bi314/summer09/genome.html).

3.2.1 Deoxyribonucleic Acid (DNA)

A DNA is a double-stranded molecule held together by weak bonds between two base pairs of nucleotides, which carry the genetic instructions used in the growth, development, reproduction and functioning of all known living organisms. A DNA molecule contains many genes, the fundamental physical and functional unit of heredity. The simplified illustration of DNA is shown in Figure 3.3. Each strand is composed of one sugar, one phosphate (gray ribbons) and a nitrogenous base. Two strands of the helix are arranged in an anti-parallel manner. The upper end of one strand is labeled five prime (5'), and the lower end of the same strand is labeled three prime (3'). This is opposite in the other strand. As a result, the 5' end of one strand matches up with the 3' end of the other strand on each end of the double helix. The two strands are held together by the pairing of complementary nucleotide

bases on opposite DNA strands. The nucleotide bases, shown in different colours, meet in the middle of the helix [75].

DNA plays a fundamental role in cell division. When a cell divides into two daughter cells, its DNA and associated proteins are duplicated [2].
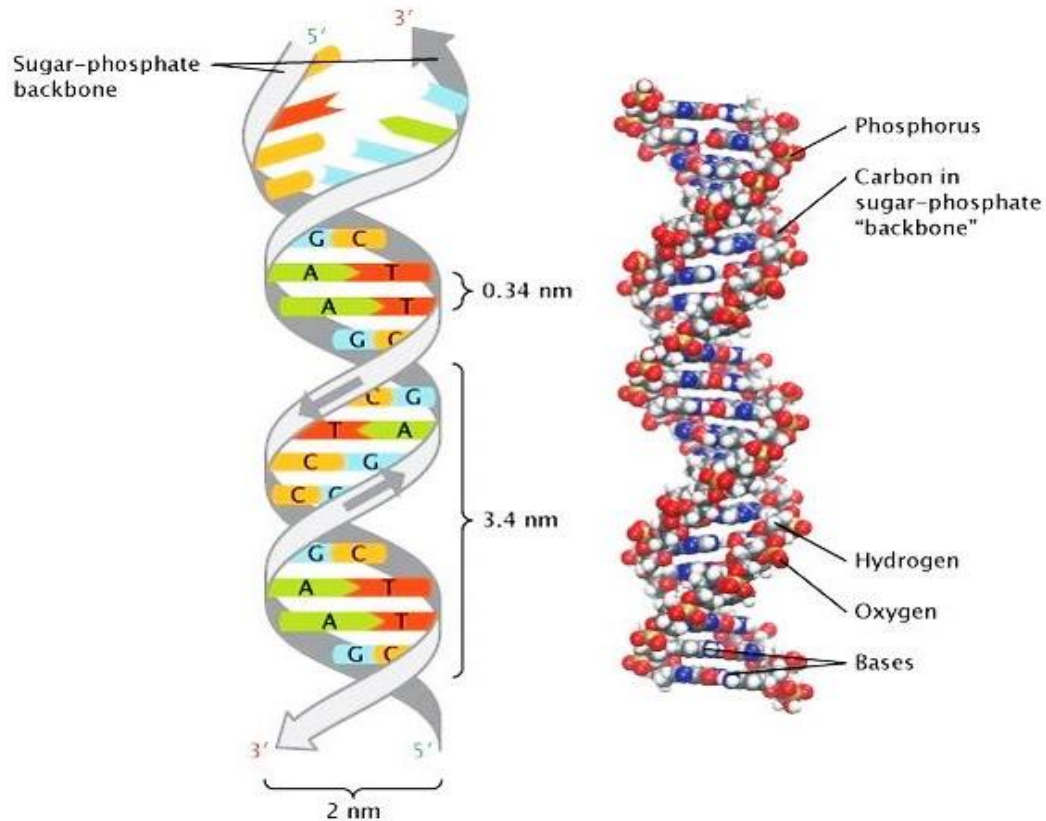
Figure 3.3: The double helix structure of DNA. The nucleotide guanine (G, shown in blue) binds with the nucleotide cytosine (C, shown in orange). The nucleotide adenine (A, shown in green) binds with the nucleotide thymine (T, shown in red) shown in the left figure. The distance between two base pairs is 0.34 nanometers. The length of one turn of the double-helix is 3.4 nanometers. The width of the DNA molecule is two nanometers. The right figure represents the space-filling molecular model, in which the bases, which contain hydrogen, oxygen, nitrogen, and carbon, connect the two sugar-phosphate backbone chains. (Image source: [75])

3.3 Genetic Endpoints

There are several genetic endpoints, which are generally examined in toxicological investigations, and these include DNA double-strand breaks (DSBs), DNA single strand break (SSB), chromosomal aberration (CA), Micronuclei (MN), free radical formation, cell proliferation, apoptosis, and antioxidants status. It is known that no single genotoxic endpoint, by itself, is capable of determining the genotoxic potential and the consequent cancer risk from occupational and environmental agents [76]. Therefore, it is relevant to examine more than one genotoxic endpoints for the overall assessment of genetic damage in MRI research investigations.

In general, any un-repaired or mis-repaired DNA damage is a key issue when assessing genetic risks. When an increase in the DNA primary damage in MRI-exposed cells is observed, it is imperative to examine the extent and the mechanism underlying such damage. Therefore, the main focus in the experimental studies (*in vitro* and *in vivo*) is placed on DNA DSBs. However, other endpoints including MN and proliferation were also assessed.

3.3.1 Double-strand Breaks

Since DNA is the repository of genetic information in each living cell, its integrity and stability is essential to life. DNA, however, is not inert; rather, it is a chemical entity subject to assault from the environment [77]. It is continuously damaged by endogenous and exogenous factors and then repaired by DNA repair enzymes. Any imperfect repair process or imbalance in damage and repair and mistakes in repair can lead to mutation, eventually disease, and cell death [78]. The best-known example of the link between environmental-induced DNA damage and disease is that of skin cancer, which can be caused by excessive exposure to ultraviolet radiation in the form of sunlight [78]. There are different types of DNA lesions. The common ones are DNA strand breaks either single strand break (SSB) or double-strand breaks (DSB). DNA DSBs are intrinsically more difficult to repair than other type of DNA damages. Due to its potential to lead to modification or loss of chromosomal material and genetic instability, it is considered to be particularly important with respect to

carcinogenesis [79]. The following section briefly describes one of the common methods for DNA DSBs detection, which was utilized in the experimental studies presented in this thesis.

3.3.2 Detection of DNA Double-strand Breaks

DNA DSB induction can result in post-translational modification of the histone tail, such as phosphorylation of the histone variant H2AX [80]. Phosphorylated histone H2AX (γ-H2AX) can be used as a biomarker of cellular response to DNA damage as it has the potential for monitoring DNA damage and repair mechanism in human cells [81]. Due to its sensitivity, efficiency and mechanistic relevance, it allows detection of individual cells and visualization of discrete γ-H2AX-foci [82-83]. This biomarker has a great potential, but is not limited to detecting DNA DSB damage.

Upon DSB formation, the core histone protein H2AX becomes rapidly phosphorylated. The phosphorylated form, γ-H2AX, accumulates at the site of damage and can be detected as foci by immunocytochemistry [84] (Figure 3.4). Cells with such specific sites are detected using specific antibodies with fluorescent tags and the discrete γ-H2AX foci are evaluated using different methods such as immunohistochemical and/or flow cytometry methods.
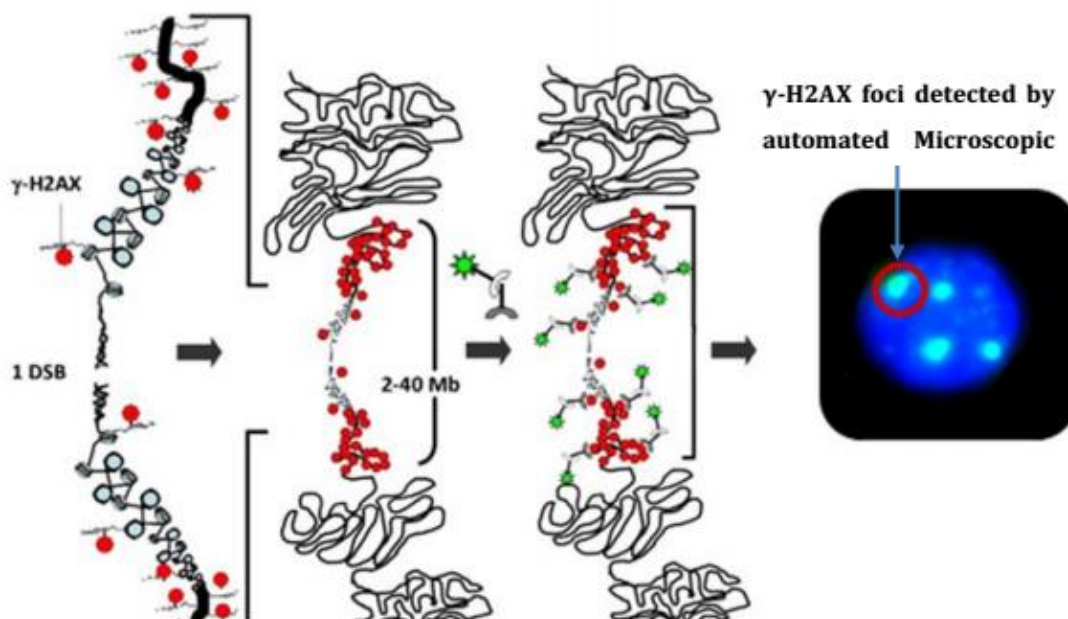
Figure 3.4: Schematic representation of γ-H2AX formation and detection. When DNA damage occurs, serine 139 of histone H2AX in the chromatin on both sides of the damaged site is phosphorylated. Phosphorylated histone H2AX is referred to as γ-H2AX foci, shown in a red ring. (Image source: [85])

Among different immunological γ-H2AX-tests, which are all based on the specific binding of an anti-γ-H2AX antibody, the microscopic immunofluorescence test is claimed to be the most sensitive method [84-85]. This method can be used in different cell types; however Peripheral blood mononuclear cells are very commonly used in genotoxicity.

A fully automated γ-H2AX foci technique (AKLIDES platform), which has been described in detail and evaluated elsewhere [86-88], was used in three experimental studies presented in this chapter. This method has some advantages over conventional manual counting, such as being less subjective and less time-consuming. In brief, a motorized inverse fluorescence microscope (Olympus IX81, Olympus, Hamburg, Germany), controlled by a software application provides a fully automated image acquisition, analysis, and evaluation of immunofluorescence. An objective with 60 x magnification, (Olympus, semi-apochromat LUCPLFLN 60X, 0.70 NA, W.D.1.5 – 2.2 mm); a multiband filter for the DAPI; and Alexa

488 dyes (DA/FI-A, Semrock, LakeForest, USA); 400 nm and 490 nm light emitting diodes (pE-2,Cool LED, Andover, UK); and a charge-coupled device, (CCD) gray level camera (DX4, Kappa Optronics, Gleichen, Germany); were used to acquire the image. The automated γ-H2AX AKLIDES system comprises a sequential process, including image acquisition, object identification and classification [86, 87], which are shown in Figure 3.5.
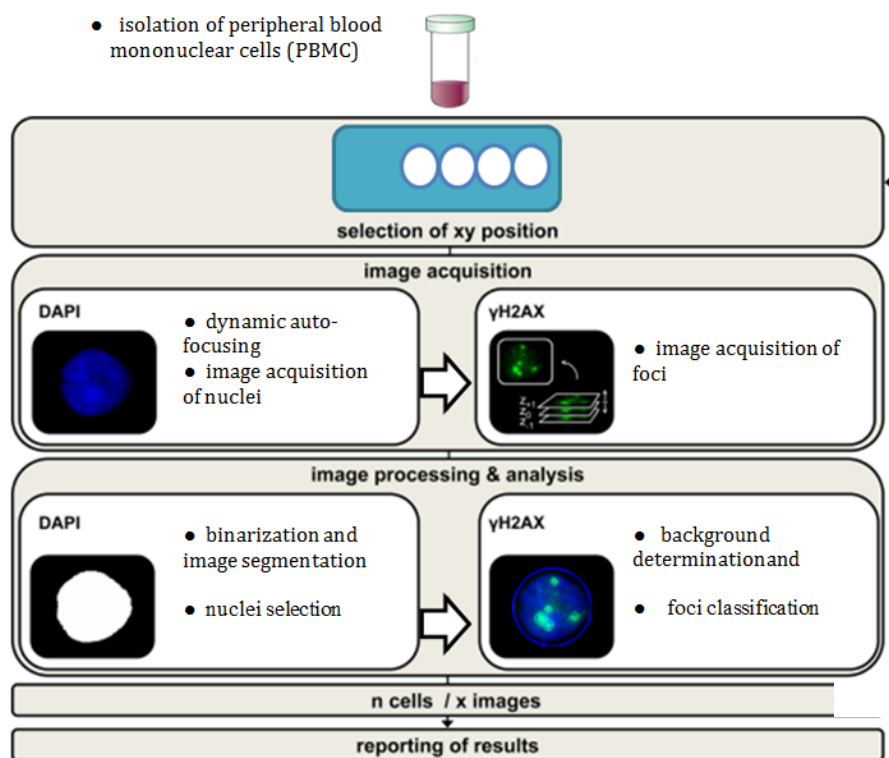
Figure 3.5: Flowchart of the main processes involved in automated γ-H2AX foci quantification. After insertion of slides into the system, using dynamic auto-focusing, the exact focal plane is automatically detected in DAPI channel and an image of the nuclei is acquired. For each nucleus, the corresponding three images in the γ-H2AX foci channel were analysed to identify the number of γ-H2AX foci per cell. (Image source: adapted and modified based on [87])

3.3.3 Micronuclei

Another genetic end-point which is normally assessed in genotoxicity studies is Micronuclei (MN). MN are small, extra-nuclear bodies originated from a chromosome or chromosome fragments that lag behind at anaphase, and are eventually excluded from the daughter nuclei during nuclear division [89-95].

Several different mechanisms can be involved in the formation of MN. A MN containing chromosome fragments may result from direct DNA DSB, conversion of DNA SSBs to DSBs after cell replication, or inhibition of DNA synthesis. Furthermore, a positive correlation is known to exist between MN and CA endpoints [71]. Some MN may have their origin in fragments derived from broken anaphase bridges [96, 97] formed due to chromosome rearrangements (dicentric chromatids, concatenated ring chromosomes or union of sister chromatids). Defects in the chromosome, such as damage to chromosomal substructures, mechanical disruption [98], and hypomethylation of centromeric DNA [99-101] are also hypothesized to be the essential events in micronucleus formation.

MN frequency in lymphocytes is known to be affected by gender, age, dietary factors, and lifestyle factors [102]. Also, biological factors such as genetic background can influence the baseline frequency of MN. It is known that MN frequencies are generally 1.2 to 1.6 times higher in females than in males. Furthermore, MN frequencies increase steadily and significantly with age in both sexes [103].

Figure 3.6 shows Micronuclei through a microscope. A micronucleus is visualized as an extra small nucleus beside the main nucleus. MN are expressed in cycling cells that have completed nuclear division, which makes the MN assay quantitatively unusable in non-dividing cell populations.
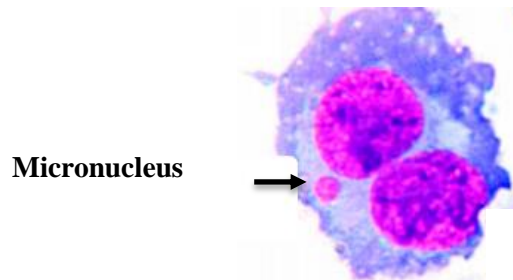
Micronucleus

Figure 3.6: Example of Micronuclei (black arrow) in a binucleated human lymphocyte. (Image source: [104])

The application of MN as an indicator of chromosomal damage has become a standard assay in both genetic toxicology and human biomonitoring studies [105]. Utilizing MN tests for human biomonitoring studies was first described by Meretoja et al. [106] and a few years later, Stich [107] proposed that MN could be used to study genotoxic effects in all human tissue. Since then, investigations with cells from the buccal and nasal mucosa, esophagus, bronchi, urinary bladder, and cervix, have been performed [108]. Due to the fact that cells from the haematopoietic system, especially peripheral blood cells, circulate everywhere in the body and are attainable easily, they are the most common cell types examined for MN. MN can be observed in almost any cells; therefore, in the last few years, there has been a strong increase in the employment of the MN assay as a tool for examining human genotoxic exposure and potential long term effects. It has also been used to quantify exposure to genotoxic chemicals and radiation in a large number of studies. A potential predictive role for this biomarker has been suggested on theoretical grounds [109]. However, the association between the frequency of MN and long-term biological consequences has not fully been elucidated yet. In many studies, preliminary evidence that MN frequency in peripheral blood lymphocytes is predictive of cancer risk, suggests that increased MN formation is associated with early events in carcinogenesis [110-111].

In particular, three research groups investigated the incidence of MN in cells exposed *in vitro* and *in vivo* to MRI. In *in vitro* studies, Lee et al. [10] reported MRI exposure duration-dependent increases in MN frequency, while Szerencsi et al. [13] reported no such increase.

An *in vivo* experiment by Simi et al. [9] reported a significant increase in MN frequency immediately after MRI exposure, but it returned to normal levels within 24-120 hours later. Thus, the induction or absence of MN induction remains controversial. However, evidence is emerging that elevated cancer risk in humans may be related to increased number of MN.

3.3.4 Detection of MN

The cytokinesis-block micronucleus (CBMN) assay is the standard method for measuring MN in cultured human and/or mammalian cells, because scoring is specifically restricted to once-divided bionuclated cells, which are the cells that can express MN [91-94, 112-115]. The CBMN assay was originally described for human lymphocytes by Fenech and Morley in 1985 [92]. Since then the method has widely been used as a sensitive and reliable technique for assessing chromosome damage in both *in vivo* and *in vitro*. The CBMN technique enables comparisons of chromosome damage between cell populations that may differ in their cell division kinetics [92].

Section II

3.4 Literature Review

Various attempts have been made to quantify the alleged carcinogenic risk possibly associated with exposure to magnetic fields. Numerous original, confirmation and replication studies have been conducted over the past several decades, to examine the potential adverse effects from exposure to SMF, GMF and RF respectively. Among the several biological/health effects examined, the genetic damage was the focus of research for many investigators, since excess damage in somatic cells can lead to carcinogenesis, while similar damage in germ cells can be transmitted to and affect future generations [71].

Several different genotoxicity endpoints, such as DNA SSB, DNA DSB, CA, MN and sister chromatid exchanges (SCE) and mutations (MUT) were tested to examine the extent of genetic damage and compared with that observed in un-exposed cells. Apart from a few comprehensive reviews on biological and health effects of MRI exposures published by

international organizations such as WHO, ICNIRP and SCENIHR, several other reviews have already been published on the specific frequency range of EMFs [116-135].

With respect to genetic damage investigations of MRI on human cells, there have been nine reports in peer-reviewed scientific literature. In these investigations, researchers have exposed the cells to SMF, GMF, RF, or MRI sequences, which are routinely used in clinics, and evaluated the extent of genetic damage using SSB, DSB, CA, MN and MUT as endpoints. The observations in these recent reports were contradictory. While many study groups fail to detect any genetic damage, others report significant increased genetic damage in cells from the MR-exposed group. The results from recent studies are critically reviewed and a summary is presented in Table 3.1.

Four studies investigated DSBs induction using γ-H2AX assay and the rest focused on other genetic end-points.

 Three of the studies showed no enhancement of DSBs, following either an *in vitro* exposure of human cancer cell lines (0h, 1h and 24h post exposure)[8], human lymphocytes (0h, 1h or 20 h post exposure)[4,14-15] or an *in vivo* exposure of human lymphocytes taken from patients 5 min after contrast-enhanced cardiac magnetic resonance imaging (CMR)[17]. In contrast, the following studies report a significant effect on the cells after exposure to MRI. In 2008, Simi et al. [9] reported a dose-dependent induction of micronuclei in human lymphocytes of 8 volunteers exposed *in vitro* to different MRI intensities, as well as *in vivo* after non-contrast enhanced cardiac MRI scans of the 8 subjects. After analysing one blood sample exposed to different exposure times of a routine 3 T MRI scan, Lee et al. [10] describe a dose-dependent increase of micronuclei, chromosome aberration and comet tail moment. In contrast, no induction of DNA damage was observed in an equal *in vitro* trial, repeated by Szerencsi et al. [13].

A significant increase in lymphocyte DNA damage, measured by alkaline comet assay, was reported by Yildiz et al. [11] in 2011, following analysing contrast-enhanced 1.5 T hyperphysical MRI of 28 subjects. Compared to baseline level non-contrast enhanced MRI

revealed a small, but not significant, rise in DNA damage, whereas the amount of DNA lesions increased significantly under gadolinium-treated conditions.

Recently, Fiechter et al. [12] reported a statistically significant increase in DSBs in human lymphocytes taken from patients immediately after a contrast-enhanced CMR. Whereas, Lancellotti et al. [16], reported no enhancement in T-lymphocytes taken from volunteers 1 hour and 2 hours post exposure to un-enhanced CMR. A significant enhancement was reported at day 2 and 1 month post exposure before returning to the baseline levels after 1 year (a significant increase was observed at 2 hours and on day 2 for NK cells, but not at other time points).

There are few concerns regarding the methodology in these two studies. In the study by Fiechter et al. [12], twenty subjects were included and the induction of DSBs in lymphocytes after 1.5 T cardiac MRI exposure was quantified by microscopy and flow cytometry analyses of immunofluorescence-stained γ-H2AX foci. However, the source of DNA damage could not be clearly distinguished between MRI-related effects, contrast agent effects and other effect, as sham exposed controls and patients receiving non-contrast enhanced MRI were not included.

In the study by Lancellotti et al. [16], the authors obtained the history of the subjects a week before the first blood drawing. Such information, i.e., whether the subjects were exposed to any agents/activity known to impact DNA integrity at later time-points, i.e. 2 days, 1 month and 1 year, is not mentioned. Also, the authors suggest that NK cells could be more sensitive markers than T lymphocytes for early CMR induced DNA damage. Although such cells are more abundant, they have a short-life of ~2 weeks; persistence of increased γ-H2AX at 1 month post-CMR needs to be viewed with caution, especially in the absence of alterations in apoptosis and necrosis during the entire period of study. There were reports indicating that phosphorylation of histone H2AX (γ-H2AX) occurs within minutes after induction of DSBs, accumulates within 20 to 30 minutes and subsequently, γ-H2AX becomes dephosphorylated over the next few hours [80-136]. In this context, the biological and mechanistic aspects in the persistence of γ-H2AX at 2 days and at 1 month post-CMR are not clear.

The overall information gained from these recent studies lacks consistency. Good laboratory protocols, such as blind examination of microscope slides to eliminate observer bias and inclusion of un-exposed as well as positive controls in the experiments for comparison of the observations in MRI-exposed cells, should be applied in all studies. Another intriguing question which has not been addressed is that of the cumulative effects of MR exposure from serial scanning. We addressed this question by conducting an *in vivo* study among frequently exposed volunteers to high and ultra-high field MRI. The results of this study are reported in section 3.10.

The importance of the studies with regard to health effects of exposure to MRI has been stressed as a high priority by the European Commission. The latest report by both, the International Agency for Research on Cancer (IARC) [131] and the Scientific Committee on Emerging and Newly Identified Health Risks (SCENIHR) [132] suggest the need for large scale and carefully designed, well-coordinated, multi-centred collaborative *in vitro* and *in vivo* investigations with validated dosimetry, multiple genotoxicity endpoints, blind evaluations with adequate statistical power, and appropriate analytical methods. Such studies probably would require exposures from MRI scanners in different centres.

Table 3.1: Summary of recent studies on genetic damage in cells following *in vitro* and *in vivo* exposure to MRI, adapted from [71]

	Schreiber et al. 2001 [7]	Schwenzer et al. 2007 [8]	Simi et al. 2008 [9]	Lee et al. 2011[10]	Yildiz et al. 2011[11]	Fiechter et al.2013 [12]	Szerencsi et al. 2013 [13]	Lancellotti et al. 2015[16]	Brand et al.2015 [17]	Studies presented in this thesis [4, 14, 15]
Study	In vitro	In vitro	In vitro and in vivo	In vitro	In vivo	In vivo	In vitro	In vivo	In vivo	In vitro- frequently exposed- In vivo
Flux (T)	1.5 T and 7.2 T	3 T	1.5 T	3 T	1.5 T	1.5 T	3 T	1.5 T	1.5 T	7 T, 3 T, 1.5 T
Cell origin	Salmonella typhimurium bacteria	Humancancer Cells	Humanblood Lymphocytes	Humanblood lymphocytes	Humanblood Lymphocytes	Humanblood Lymphocytes	Humanblood lymphocytes	Human (T lymphocytes and NK cells)	Humanblood lymphocytes	Humanblood lymphocytes
Endpoint	Mutation	DSB	MN	CA, MN, SSB/DSB	SSB/DSB	DSB	SSB/DSB, MN	DSB	DSB	DSB, MN
Expts Donors	≥2 expts 3 platesper exposure	-	In vitro: 8 healthy donors. In vivo: 8 donors	1 donor (3 repeats)	28 patients	20 patients	2 healthy donors 3 repeats	20 healthy donors	45 patients	16 and 22 healthy donors, 53 patients
Contrast agent	-	-	No contrast	-	With and without gadolinium	Gadolinium	-	No contrast agent	Gadolinium	With and without
Positive control	Chemical mutagens	4 Gy 6MV x-rays	-	SSB: cisplatin MN, CA: bleomycin	Chemical mutagens	-	4 Gy γ-rays	-	-	120 kV CT scan and 0.2 Gyγ-rays
Result	No significant effect	No significant effect	In vitro and in vitro Significant	SSB, MN, CA: significant	Significant increase	Significant increase	No significant effect	Significant increase	No significant effect	No significant effect

3.5 Hypothesized Mechanisms for MRI-Induced Genetic Damage

For a damage to occur following an MRI exposure, signals need to be perceived or transduced in biological molecules in such a way as to alter their size, shape, charge, chemical state or energy. When the signal is amplified, a cascade of sequential events at the molecular, cellular, and tissue level would be required without interruption to the final outcome. The induced changes can be transient, reversible, or repaired. However, the final outcome or 'disease' requires successful completion of many more intermediate steps which are shown in Figure 3.7. It is also possible that the signal produced by the preceding step might be within normal variations and therefore, would have no further functional consequences beyond that point in the causal chain. Since the health of human bodies depends on the normal structure and function of a large number of molecules (e.g., proteins, nucleic acids, carbohydrates, and lipids), any mechanism proposed must predict how MRI could interfere with or modify the normal synthesis, function, or degradation of these molecules [71]. The interaction mechanisms would then predict thresholds in terms of safety of exposure amplitudes, frequencies, homogeneity, and exposure duration, etc.
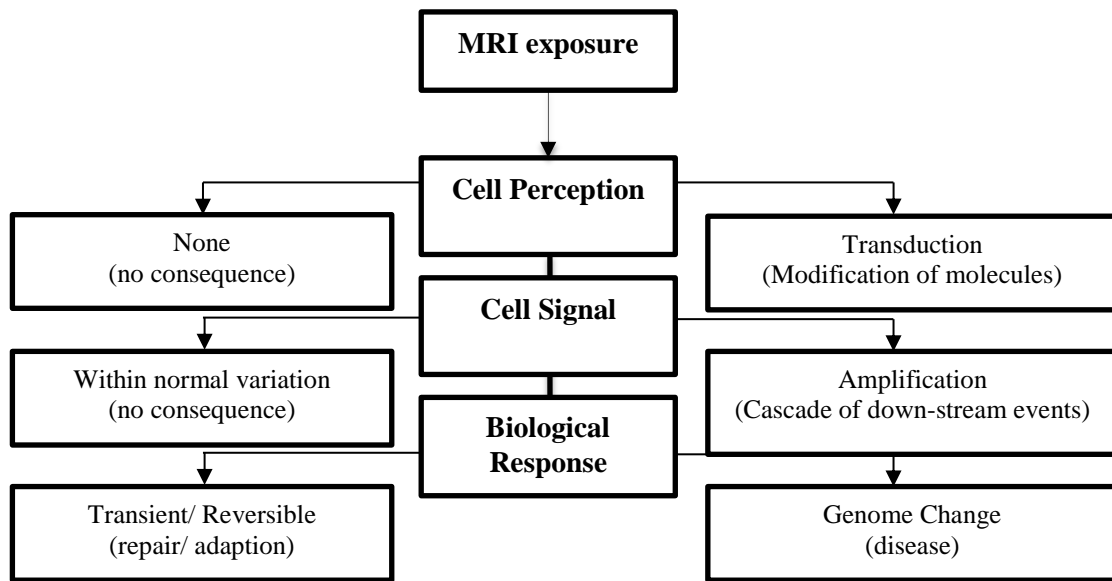
Figure 3.7: Potential cascades of sequential events for MRI-generated EMFs interaction with a human body. (Image source: [71])

Furthermore, indirect effects cannot be excluded. EMF generated by MRI possibly may affect the cells by changing cellular architecture and metabolic processes within cells that might lead to DNA damage.

The energy levels used in MRI are extremely low, below 1micro electronvolt (1 eV = 1.6×10^{-19} J). This energy level is directly related to the precessional frequency through the following equation: $\Delta E = hf$, where h is Planck's Constant and f is the precessional frequency, and can be calculated from the Larmor frequency (ω), through: ω $= 2\pi f$. This energy is about 1.75×10^{-7} eV for a proton in a 1 T field, i.e. an extremely small amount of energy compared with electron binding energies [137]. Such energy is very unlikely to cause damage and currently, no direct damage mechanism is elucidated for MRI. Nevertheless, it is important to examine and understand potential mechanisms if any.

A possible scenario for an effect on DNA is suggested by a few studies [2, 138-144]. The two chains of DNA are held together by relatively weak H-bonds joining the complementary bases of DNA. H-bonds are hydrogen (protons) that are bonded to both chains by electron pairs. If EMFs forces displace electrons in H-bonds, this may lead to local charging and generate forces that overcome the H-bonds and initiate disaggregation of the chains. Recent progress in these fields reveals that low energy electrons can attach to DNA or DNA fragments in any one of the components such as (i) nucleobase [138], (ii) sugar [139] (iii) phosphate group [140] or, as a dipole bound state (DBS) [141] outside the molecular framework [142]. The low energy electron attachment to the target may lead to the formation of a metastable state (also known as a temporary negative ion) or an electronically stable anionic species. The metastable state, which is often referred to as ''resonance'' and exists only for a very short period of time [142-144]. However, the temporary negative ion can play a prominent role in induced damage to bio-molecules like DNA by causing mutagenesis to the organisms which is described in details in the study by Bhaskaran et al [142].

Section III: Empirical Evidences

This section of the thesis refers to the series of experiments (*in vitro* and *in vivo*) which were carried out to quantitatively determine the potential genotoxic and cytotoxic impact of 7 T

MRI on human peripheral blood mononuclear cells under controlled conditions. The experiments were planned in a stepwise approach (*in vitro* to *in vivo*) to cover some of the current gaps and uncertainties regarding genetic damage induced by 7 T MRI. Flowchart 3.8 illustrates the experimental design. In all the experiments, to assess genotoxicity potential of MRI, γ-H2AX focus evaluation, as described in section 3.3.2, was carried out by automated fluorescence microscopy and flow cytometry.

The MRI sequence used in the *in vitro* and *in vivo* experiments was Echo Planar Imaging (EPI) sequences, which is a common fast imaging acquisition technique in cardiac, abdominal, diffusion, perfusion and functional imaging. In order to enhance the potential degree of damage and unlike *in vivo* protocols, EPI sequence was adjusted to reach the maximum permissible gradient effect and 100% of permissible SAR in the *in vitro* experiment. All the experiments presented in this chapter were carried out in collaboration with the immunology and the radiology department of the Otto-von-Guericke University Magdeburg, Germany and approved by the local ethics committee (RAD 244 and RAD 265), and the volunteers gave written consent.
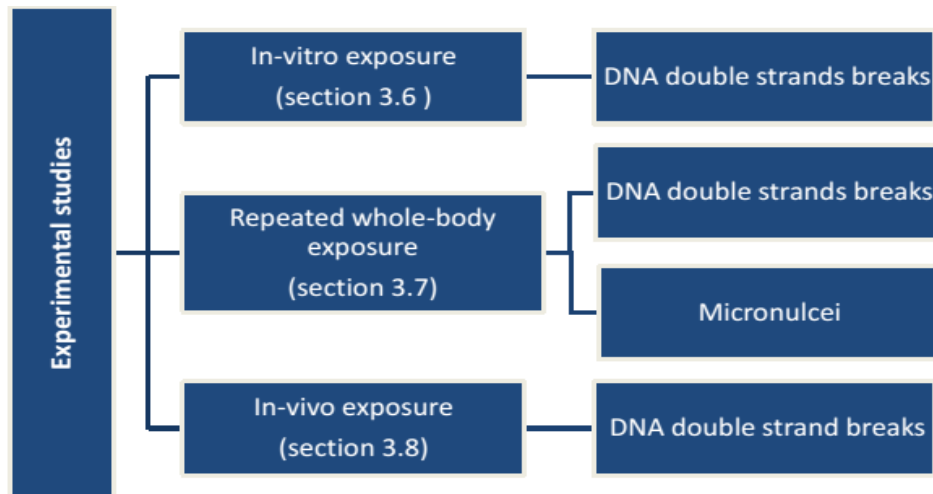
Figure 3.8: Flowchart of experimental design in three levels, *in vitro*, repeated whole-body exposure and *in vivo* exposure

3.6 *In vitro* Analysis of DNA DSB in Human Lymphocytes

The first experiment aimed to investigate the genotoxic and cytotoxic potential of 7 T MRI on isolated human peripheral blood mononuclear cells with the hypothesis that there is no or little effect.

3.6.1 Methods

Sixteen healthy volunteers (8 male; 8 female; age 25-58 years, mean age 36 years) were recruited for this experiment. Heparinized venous blood was obtained from each donor and peripheral blood mononuclear cells (PBMCs) were isolated by density gradient centrifugation according to the manufacturer's instructions using Biocoll separating solution (Biochrom, Berlin, Germany). After isolation, PBMCs were washed and resuspended to a final density of 1 x 10^6 cells/ml in RPMI 1640 medium (Biochrom) containing 10% fetal calf serum (FCS, Pan Biotech, Aidenbach, Germany), 100 U/ml penicillin and 100 µg/ml streptomycin (both Life Technologies GmbH, Darmstadt, Germany). Blood drawing was performed on the day of experiments and cells were kept at 37°C in a humidified atmosphere with 7% CO_2 prior to exposure.

The PBMC suspension of each donor was divided into five sample tubes according to the investigated exposure conditions, as it is shown schematically in Figure 3.9. Cells were either i) left untreated, ii) exposed to 7 T SMF alone (7 T-B_0), or iii) exposed to EPI sequences (7 T-EPI). Additionally the cells were irradiated by iv) X-ray-based CT scans and by v) γ-rays at a dose of 0.2 Gy served as a positive control group.
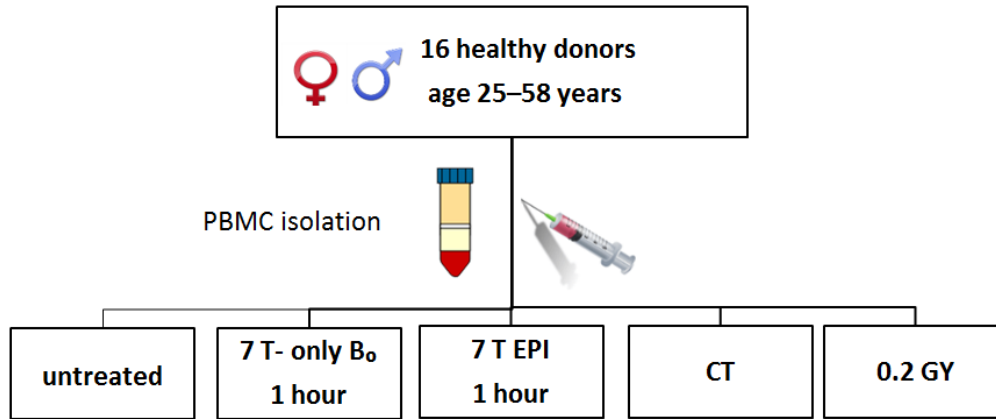
Figure 3.9: Experimental design for the *in vitro* experiment

Duration of the MRI exposure was 60 min in a 7 T whole-body MR scanner (Siemens AG, Healthcare Sector, Erlangen, Germany). 7 T-EPI sequences used with the maximum permissible switched gradient and a SAR in research mode for 1 hour scan procedure. All exposures were performed at room temperature. The tubes were placed inside the scanner bore in close proximity (about 7 cm) to the iso-centre within the exposure period (Figure 3.10).
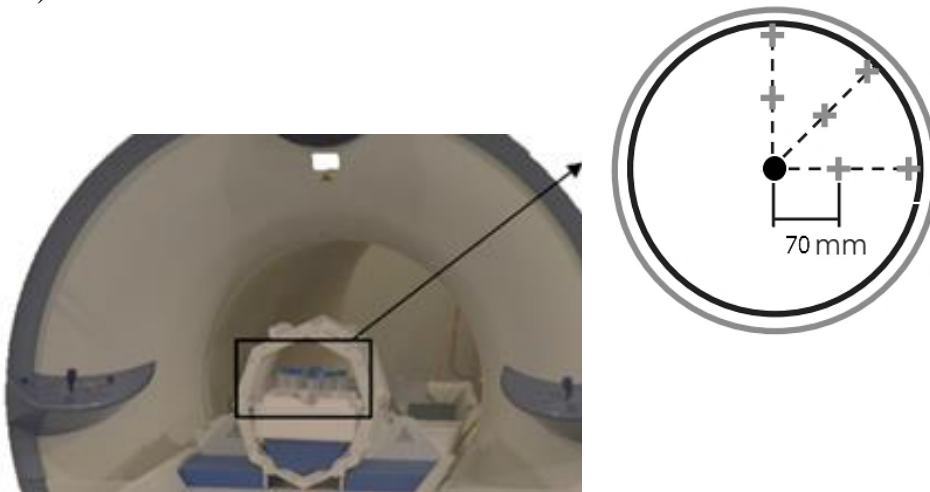
Figure 3.10: Exposure setup for *in vitro* experiment. The samples from each donor, containing 10 ml cell solution, were arranged in a test tube rack within a radial distance of approximately 7 cm from the iso-centre. Gradient: 65 mT/m, slew rate: 180 mT/m/ms, read out gradient: 35 mT/m, TR: 7900 ms, TE:22 ms, flip angle: 80, SAR: 10 W/kg for an average of 5 kg head.

Right after the exposure, tubes were put on ice to slow down metabolic activities and prevent potential biochemical or molecular changes that may affect cytometric or downstream results. They were kept on ice for a maximum of 1.5 hours until the treatment for the remaining samples was completed.

Positive control cells were exposed to X-rays by conducting a spiral CT-scan (Aquilion Prime, Toshiba Medical Systems, Tustin, California, USA or Siemens Somatom Definition AS, Siemens Medical Systems, Erlangen, Germany, respectively) with a constant potential of $120\,kV$ and a current of $200\,mA$ with an aluminum filter of $3\,mm$ (Toshiba) or $6.8\,mm$ (Siemens) and a rotation time of 0.5 seconds. They were radiated by γ-rays at a dose of 0.2 Gy (Biobeam 8000, Cs 137, Gamma-Service Medical GmbH, Leipzig, Germany). Initial DNA DSBs were measured in PBMCs, by means of γ-H2AX analysis, immediately after exposure. In order to allow phosphorylation process to happen at 37°C and 7% CO_2, γ-H2AX foci were determined after a 1 h incubation period. The residual γ-H2AX foci were determined 20 hours after exposure. DNA DSBs were quantified by flow cytometry and automated microscopy analysis of immunofluorescence stained γ-H2AX.

For microscopy analysis, immunofluorescence staining was performed at all of the experiments, as described in section 3.3.2, using a γ-H2AX-immunofluorescence staining kit (Medipan, Berlin/Dahlewitz, Germany). For flow cytometry measurements, cells were stained in round bottomed falcon tube analog to the protocol for immunohistochemistry preparation according to the protocol of Redon et al. [82]. In brief, cells were stained in a round bottomed falcon tube. An additional fixation after PFA-treatment with 70% ethanol was included, and cells harvested immediately or 1 hour after exposure were stored in 70% ethanol overnight at 4°C. In contrast, cells fixed 20 hours post exposure on the next day, were treated with 70% ethanol for 20 minutes at room temperature. After permeabilization, cells were either stained with anti-γ-H2AX antibody or IgG-isotype control. In order to enhance the intensity signal, the dilution of the secondary antibody was reduced from 1:2000 for microscopy to 1:500 for flow cytometry analysis. Stained samples were kept on ice in the dark for the measurement. PBMCs were identified by forward and side scattered light signals and by an additional fluorescence signal originating from 0.5μM DAPI (Sigma-Aldrich, St.

Louis, MO, USA) staining. For flow cytometry measurements, a minimum of 20,000 gated events was analysed for each sample. The level of γ-H2AX was quantified by the median fluorescence intensity (MFI) in arbitrary units (AU) using a BD LSR Fortessa cell analyser (BD Biosciences, Mountain View, CA, USA) and FlowJo analysing software (Treestar Inc., Ashland, OR, USA). For harmonization, MFI data was adjusted by subtraction of the corresponding IgG-isotype control of each donor, which was fixed together with the samples at time point 1 (0 h) [14].

The mean γ-H2AX foci/cell, MFI of the nucleus in γ-H2AX channel, as well as the percentage of γ-H2AX focus-positive cells, and classification of cells according to their individual focus number, were assessed from at least 200 cells per sample.

Viability assay, which is an assay to determine the ability of organs, cells or tissues to maintain or recover viability, was carried out according to the manufacturer's instructions (CellTiter-Blue assay, Promega, Madison, WI, USA), in order to monitor the metabolic activity of unstimulated PBMCs. In brief, 5×10^4 cells/well were seeded as triplicates into flat bottomed 96-well plates. Cell Titer-Blue reagent resazurin was added to the wells either 24 hours, 48 hours or 84 hours after exposure, and plates were allowed to incubate in the dark for an additional 2 hours at 37°C and 7% CO_2. The fluorescent signal was measured at an excitation of 560 nm and an emission of 590 nm by a Tecan Safire plate reader equipped with appropriate Magellan data analysis software (Tecan Austria GmbH, Salzburg, Austria). Cell viability was normalized to corresponding control samples [14].

DNA synthesis of exposed cells was assessed by a standard [^{3}H]-thymidine incorporation assay. PBMCs were seeded at 1×10^5 cells/well into a flat bottomed 96-well plate as quadruplicates and stimulated with 2 µg/ml phytohemagglutinin (PHA, life technologies/Gibco, UK). After 84 h, cells were pulsed with [^{3}H]-thymidine at a dose of 0.2 µCi/well for additional 6 h. Cells were harvested after the incubation period and [^{3}H]-thymidine incorporation was quantified using the microplate liquid scintillation counter Wallac MicroBeta TriLux from Perkin Elmer (Waltham, MA, USA). The detailed results are presented in section 3.10.

3.7 Repeated Whole-body Exposure to 7 T MRI and Analysis of DNA DSB and MN in human Lymphocytes

A question, which has not being addressed so far, is about the potential cumulative effects of MRI exposure from serial scanning. This question is addressed in this section of the thesis by reporting an experiment which was conducted among frequently exposed 7 T MRI volunteers.

The other aspect taken into account in this experiment is assessing more than one genetic endpoint. As previously discussed (section 3.3), it is known that no single genotoxic endpoint, by itself, is capable of determining the genotoxic potential of an agent [71] and it is necessary to examine several genotoxic endpoints for the overall assessment of genetic damage in MRI research investigations. Thus, two different genetic endpoints (DNA DSB and MN) were assessed in this experiment.

The following objectives are reflected in this section:

- To determine the level of damage (DNA DSB and MN frequency) in PBMCs obtained from healthy individuals who routinely work with 7 T UHF MRI and participate frequently in 7 T research investigations, and compare the baseline level in this group with the non-exposed group.
- To assess potential different sensitivities in two groups of cells (cells from the frequently exposed individuals and from the control group) by exposing both cell groups to 7 T.
- To determine whether 7 T MRI exposures alter the genotoxic effect of a genotoxic agent, such as a chemotherapeutic drug, Etoposide (ETP) and to assess the kinetics of DNA damage repair.

3.7.1 Methods

Twenty two healthy male individuals, who were non-smoking, non-alcohol drinking and had never undergone radio-/chemo-therapy, or scintigraphy, and had not had an X-ray examination for at least one year prior to participating in this study, recruited. Participants

were divided in two groups as schematically represented in Figure 3.11. The first group comprise of healthy individuals who have been repeatedly exposed to UHF MRI (Rep). They were selected either from MRI staff or volunteers of MRI research. Therefore, they have been exposed to 7 T and 3 T MRI while working with and around MRI scanners and/or frequently participating as 7 T and 3 T research subjects. The second group of 11 subjects served as a control group (Ctl), who had never been exposed to 7 T MRI. Only one subject in this group was examined by MRI at 1.5 T within one year of this study (spinal MRI, 6 months before blood withdrawal).
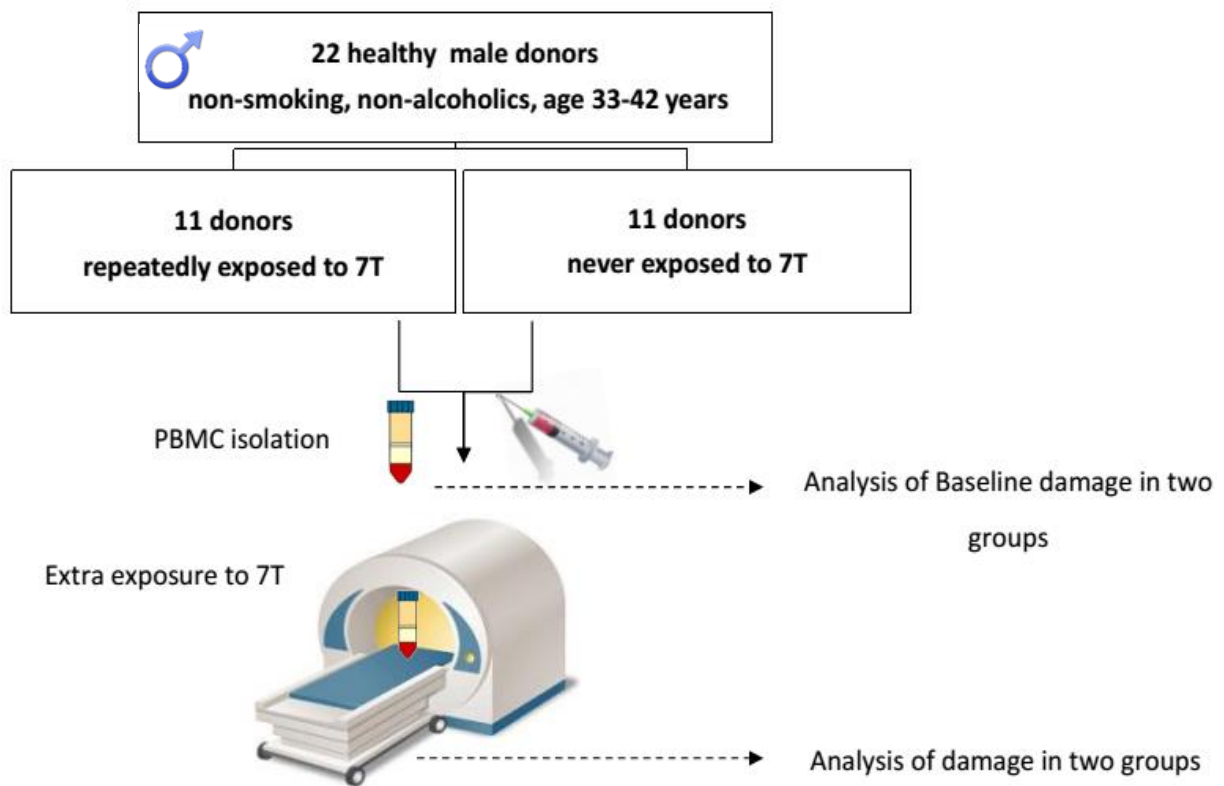
Figure 3.11: Experimental design for the repeated whole-body exposure to 7 T

The period between the last MR exposure and blood withdrawal was very different among individuals. Detailed information on repeated exposures to 7 T MRI is presented in Table3.2. On average the blood was taken between 1-4 weeks after the last *in vivo*7 T MRI exposure.

Only one participant (Rep 9) was excluded from this average, as he has not been exposed to 7 T MRI as a subject in the last year, however, due to his routine tasks, he has been exposed to the fringe field frequently.

Table 3.2: 7 T UHF MRI repeated exposures in participants of the study, adapted from [15]

Rep 1-11	Age	Experience with 7 T MRI (years)	Average exposure to 7 T MRI fringe field (h/week) *	Exposure to combined EMFs as subject inside 7 T MRI scanner (hours in the last year)
Rep 01	32	4	3	100
Rep 02	38	8	4	75
Rep 03	40	8	6	80
Rep 04	35	8	4	160
Rep 05	31	3	3	175
Rep 06	25	4	4	40
Rep 07	49	8	6	65
Rep 08	28	2.5	0.5	12
Rep 09	32	3	3	0
Rep 10	35	7	4	2
Rep 11	29	2.5	1	10

*: average

A blood sample was drawn from each participant. Heparinized peripheral blood was collected and PBMCs were separated, washed and re-suspended at the final concentration of 2×10^6 cells/ml. Similar to the procedures explained earlier for the *in vitro* study, for each participant, five aliquots were distributed into separate tubes for different exposure conditions.

In order to assess the potential difference in genotoxic sensitivity in two groups of cells, they were additionally exposed to 7 T. The whole body 7 T MR scanner was equipped to provide the maximum gradient strength of ~70 mT/m and maximum gradient slew rate of ~200 mT/m/ms. An 8-channel head coil was used in normal operating mode and EPI pulse

sequences were adjusted to simulate a worst case exposure scenario in terms of maximum switched gradient within the peripheral nerve stimulation threshold and permissible SAR. The sequences used in this experiment, created an average RF power of 50 W. The parameters were set as follows for the exposure: 65.43 mT/m maximum gradient strength, 186 mT/m/ms maximum slew rate, 35.33 mT/m maximum readout gradient strength, 7900 ms repetition time (TR), 22 ms echo time (TE), 80° flip angle, 0.8 mm × 0.8 mm × 1.5 mm voxel size and 100 slice. The TR and flip angle were adjusted to reach the maximum permissible SAR level for the head, i.e., 10 W/kg with an average human head weight of 5 kg. For MR exposure, tubes were placed inside the scanner bore in close proximity (2-7 cm) to the iso-centre for 1 hour.

The unexposed control samples from each participant were also handled virtually in the same way as their corresponding 7 T samples, but placed in a different room in the MR building at the same temperature (20 ± 2°C). Furthermore, a sample of cells from each participant was exposed to 0.2 Gy γ-radiation (^{137}Cs source, Biobeam 8000, Gamma-Service Medical GmbH, Leipzig, Germany) at a dose rate of 2.8 Gy/min as a positive control. After different exposures, the cells in all tubes were kept on ice for a maximum of 20 min while transporting to the laboratory. Moreover, to determine if 7 T MRI exposures can alter the genotoxic effect of a DNA damaging chemotherapeutic drug, cells from both groups were challenged with etoposide (ETP). For each participant, a sample of cells was treated with 10 µM ETP (Sigma, St. Louis, MO) 15 minutes prior to exposure. The ETP-treated cells were exposed to 7 T MRI for 1 hour, whereas, the other sample was left outside the scanner room. The induced number of γ-H2AX foci was determined 1 hour after additional incubation at 37 °C. The remaining cells were washed, suspended in fresh medium and DNA repair kinetics were analysed 1 h, 4 h and 20 h after ETP-removal [15].

Similar to the *in vitro* study, number of DSBs was assessed by γH2AX-immunofluorescence staining as described in detail above. The initial γ-H2AX analysis was performed after 1 hour and the residual DSBs were determined after 20 hours and 72 hours.

For MN assessment cells were treated according to the protocol stimulated with 1% phytohemagglutinin (PHA, Gibco, Waltham, MA) after exposure and cytochalasin-B

(4 µg/ml; Sigma) was added at 44 hours. The cells were harvested after a total culture period of 72 hours, treated with 100 mM KCl for 3 minutes, centrifuged and the cell pellet was re-suspended in ice cold methanol: acetic acid (5:1) fixative. Fixed cells were dropped onto microscope slides, air-dried and stained with 5% Giemsa. Finally, the cells were covered with DPX (Sigma). All slides were coded in Magdeburg, Germany and duplicates were mailed to San Antonio where they were blindly examined using a light microscope (Carl Zeiss MicroIma-ging GmbH, Jena, Germany) at 1000× magnification. For each sample, 2000 consecutive cells (1000 cells per slide) were examined. The frequency of cells with 1, 2 and $\geq$3 nuclei (1N, 2N and $\geq$3N, respectively) were recorded and number of binucleated cells (BN) were obtained. The proliferative index (PI) was derived from [(1xN1 + 2xN2 + 3xN3)/N] where N is the total number of cells examined [15]. The incidence of BN cells with 1, 2 and $\geq$3 MN was recorded and the sum of MN/2000 cells calculated.

The detailed results are presented in section 3.10.

3.8 *In vivo* Analysis of DNA DSBs in Human Lymphocytes

This section further investigates the impact of different magnetic field strengths on DNA DSB formation in peripheral blood mononuclear cells by covering the most common SMF used in clinics (1 T, 1.5 T, and 3 T) and 7 T. The 7 T MR systems, which are currently only allowed for research purposes, are included for *in vivo* genotoxicity analysis for the first time.

3.8.1 Methods

Patients receiving either an MRI (n = 43) or CT (n = 10) scan were recruited for this study between April 2014 and October 2015. Eligible participants were adults aged 18– 80. Patients were excluded if they received X-ray-based or nuclear imaging within the last three days, had undergone radiation therapy- or chemotherapy, or if they were previously diagnosed with lymphoma or leukemia. Patients were assigned to the nine following groups according to the scan procedure:

- 1 T MRI without contrast agent (n = 5)

- 1 T MRI with contrast agent (n = 5)

- 1.5 T MRI without contrast agent (n = 5)

- 1.5 T MRI with contrast agent (n = 5)

- 3 T MRI without contrast agent (n = 5)

- 3 T MRI with contrast agent (n = 5)

- 7 T MRI without contrast agent (n = 13)

- CT without contrast agent (n = 5)

- CT with contrast agent (n = 5)

In each group a minimum of 5 subjects (7 T: n = 13) were involved. Subjects examined by contrast-enhanced MRI were included when Gadolinium-based contrast agent (GBCA) Gadovist® was administered to keep the groups as homogenous as possible. Gadobutrol (Gd-DO3A-butrol) 0.1 mmol//kg body weight - Gadovist, Bayer Healthcare, Leverkusen, Germany) was used for 1, 1.5 and 3 T MRI.

43 patients (mean age 46.1 years [range: 20–77 years]; 22 women: mean age 44.5 years [range: 26–71 years]; 21 men: mean age 47.7 years [range: 20–77 years]) were examined by MRI. Demographic characteristics of patients assigned to the different MRI subgroups, the type of scan and the mean RF exposure are displayed in Table 3.3. For estimation and quantification of the exposed RF in different MR protocols, the mean applied whole body specific absorption rate (SAR) for each protocol employed is listed, as is a standardised energy dose in J/kg (whole body SAR multiplied by total exposure time). Further, 10 patients were examined by CT scan (mean age 64.6 years [range: 48–80 years]; 3 women: mean age 63.0 years [range: 51–77 years]; 7 men: mean age 65.3 years [range: 48–80 years]) served as positive controls. Depending on the additional injection of iodinated CA, CT patients were also classified in unenhanced and enhanced group (2 thorax and 3 abdominal CTs per CT subgroup).

Different scanners were used for the diagnostic MRI, including: 1 T (Philips Panorama, Philips Healthcare, Best, Netherlands), 1.5 T (Philips Intera), 3 T (Philips Achieva), and 7 T (Siemens Healthcare, Erlangen, Germany) MR system. Serving as positive controls for

ionizing radiation-induced γ-H2AX foci, patients receiving either an unenhanced or iodine-based contrast-enhanced (80-120 ml Imeron 300, Bracco Imaging, Milan, Italy) CT scan (Aquilion Prime, Toshiba Medical Systems, Tustin, California, USA or Siemens Somatom Definition AS, Siemens Healthcare, Erlangen, Germany, respectively) were enrolled.

Table 3.3: Calculated whole body SAR and standardised energy dose (SED) in J/kg (SAR multiplied by the exposure time) for each used MR protocol as well as patient's demographic characterization, taken from [4].

Protocol	SAR Wb_{mean} [W/kg]	Exp.time [s]	SED [J/kg]	n	female	male	Age [year] Mean ± SD
1 Tesla MRI - without contrast agent							
Shoulder	0.4	2070	840	5	3	2	32.8 ± 11.7
1 Tesla MRI - with contrast agent							
Cardiac	0.3	605	193	5	3	2	39.8 ± 17.2
1.5 Tesla MRI - without contrast agent							
Abdominal	1.4	755	1065	3	5	0	44.2 ± 11.9
Knee	2.1	1345	2808	1			
Thorax	2.4	679	1149	1			
1.5 Tesla MRI - with contrast agent							
Lumbar spine	2.6	1656	4379	1	1	4	54.2 ± 19.8
Lung	2.0	679	1369	1			
Pancreas	2.0	1409	2818	2			
Pelvis	1.4	761	1027	1			
3 Tesla MRI - without contrast agent							
Ankle	0.9	1439	1295	1	3	2	45.0 ± 8.9
Cervical spine	1.3	2038	2726	1			
Knee	1.1	1227	1350	3			
3 Tesla MRI - with contrast agent							
Lumbar spine	1.3	1188	1511	1	1	4	67.8 ± 10.3
Pelvis	1.1	1673	1757	2			
Prostate	1.2	1432	1718	1			
Rectum	1.2	1861	2311	1			
7 Tesla MRI - without contrast agent							
Knee	0.2	1982	312	13	6	7	43.2 ± 13.5

Venous peripheral blood was drawn from each patient into heparinized vacuum tubes directly before the scan (t_1) as well as five minutes (t_2) and 30 minutes (t_3) after examination. This is schematically presented in Figure 3.12.
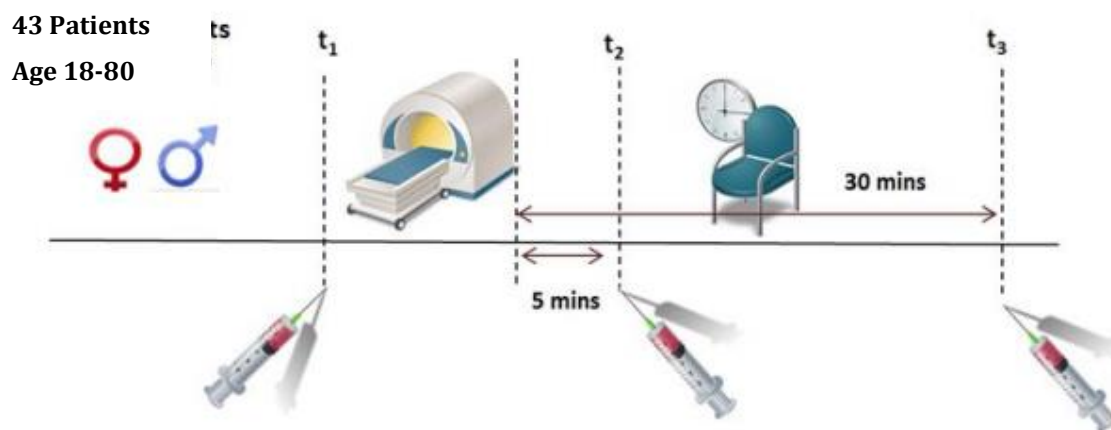
Figure 3.12: Experimental design for the *in vivo* experiment

3.9 Statistical Analysis

GraphPad Prism software version 5.01 (Graph Pad Software, La Jolla, CA, USA) was used for the statistical analysis. Significance levels were calculated by repeated measures ANOVA with a 95% confidence interval ($\alpha = 0.05$), followed by Dunnett's post-hoc test. A *P*-value of <0.05 was considered as significant difference, and data in text and figures are displayed as mean ± standard error of the mean (SEM). For the *in vitro* study, pairwise comparisons of the interaction between groups were done using Fisher's least significant difference test.

Significance levels were calculated by Friedman tests with a 95% confidence interval ($\alpha = 0.05$) followed by Dunns post-hoc tests. Comparison was only performed within the same group between initial values and corresponding values at different times post exposure. In the figures, significances are indicated by asterisks (**: $P \leq 0.01$, *: $P \leq 0.05$).

In the *in vivo* study, no mathematical correction for multiple comparisons was made, increasing the probability to falsely detect a DSB-inducing effect that is not present. To compare differences between MR and CT exposure, normalized data was analysed by a Mann-Whitney-Test at t_2 and t_3 after exposure. Minimal detectable effect size was calculated according to Cohen's *d*, by performing a power analysis for nonparametric tests for the given

α = 0.05, standard deviation, number of patients and power of 0.8, using *XLSTAT for MS Excel* (version 2015, Microsoft, Redmond, WA).

3.10 Results

In this section the results of three experiments (*in vitro*, repeated whole-body exposure and *in vivo*) are reported respectively in section 3.10.1- 3.10.3.

3.10.1 *In vitro* Analysis

The results from *in vitro* analysis using two different detection methods: flow cytometry analysis and automated microscopy, are presented in Figures 3.13 and 3.14.

In the flow cytometry method no significant changes were detected in the 7 T SMF group (MFI = 412 AU; range 12-927 AU) and the EPI sequence group (MFI = 414 AU; range 80-899 AU) at time point 0 h in comparison to the control (MFI = 414 AU; range 38-807 AU). A minor increase in γ-H2AX level directly after CT scan (MFI = 442 AU; range 65-996 AU) and a significant rise (MFI = 765 AU; range 184-1744 AU) after 0.2 Gy γ radiation was found. An enhanced intensity was detected in all the groups after a 1h incubation period at 37°C, but this increase was not significant among any of the MRI groups, whereas samples exposed to ionizing-radiation (CT: MFI = 834; range 155-1458 AU and 0.2 Gy: MFI= 2130 AU; range 1151-3378 AU) showed a significant increase.

Due to DSB repair 20 h post exposure, the determined γ-H2AX levels in cells after 7 T and CT exposure did not differ significantly from the control (MFI = 1042 AU; range 81-1807 AU) and even samples previously treated with 0.2 Gy γ-radiation only showed a slight increase in MFI (MFI = 1256 AU; range 103-1963 AU).
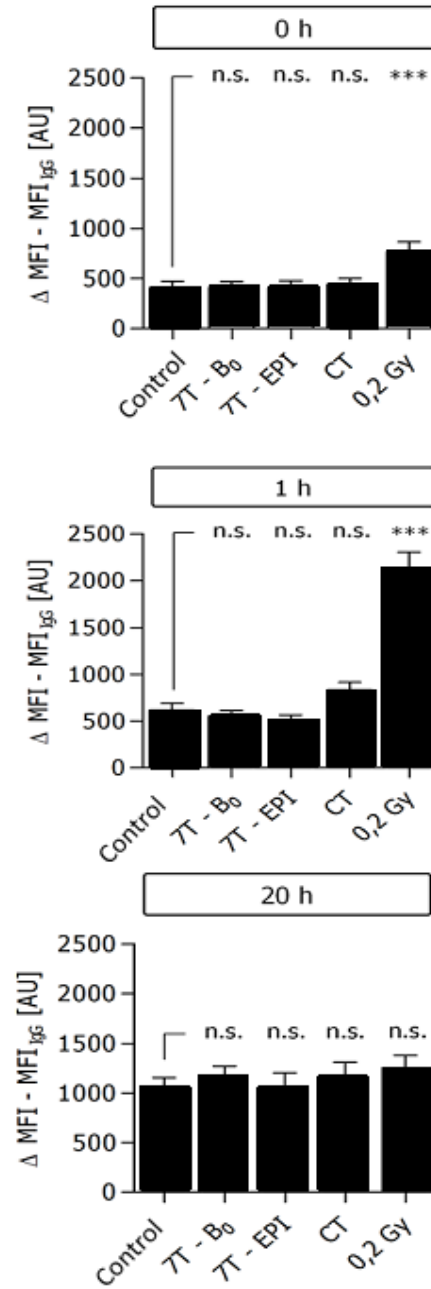
Figure 3.13: Analysis of γ-H2AX-stained DNA DSB using flow cytometry. Mean γ-H2AX intensity was assessed in PBMCs immediately, 1 h and 20 h after the indicated exposure conditions. Difference of mean fluorescence intensity (MFI) of γ-H2AX and IgG-isotype control staining from 16 independent experiments at three different time points after exposure as mean ± SEM (***: $P \leq 0.001$, ns: non-significant) [14].

Analysis of γ-H2AX-stained DNA DSB was also performed by automated microscopy (Fig. 3.14). Intensity data (Fig. 2b) was similar to the results obtained by flow cytometry and confirmed those results. In this method, no differences in the mean number of γ-H2AX foci/cell between cells harvested immediately or 1 hour after exposure were determined. Cells exposed to 7 T SMF (1 h - mean: 0.065 γ-H2AX foci/cell; range: 0.005-0.137) or EPI sequences (1 h - mean: 0.057 γ-H2AX foci/cell; range: 0.004-0.169) revealed no changes in the number of DSB compared to baseline level of unexposed cells (1 h - mean: 0.058 γ-H2AX foci/cell; range: 0.009-0.196) (Fig. 2c).

In contrast, a significant ($P < 0.01$) rise in γ-H2AX foci formation was detected for all samples irradiated with CT scan (1 h - mean: 0.377 γ-H2AX foci/cell; range: 0.183-0.730) and 0.2 Gy (mean: 2.101 γ-H2AX foci/cell; range: 1.063-3.123). Following 20 h, 0.2 Gy treated cells still showed a statistically relevant increase in γ-H2AX foci (mean: 0.267 γ-H2AX foci/cell; range: 0.101-0.542), compared to the unexposed control (mean: 0.088 γ-H2AX foci/cell; range: 0.021-0.225) [14].
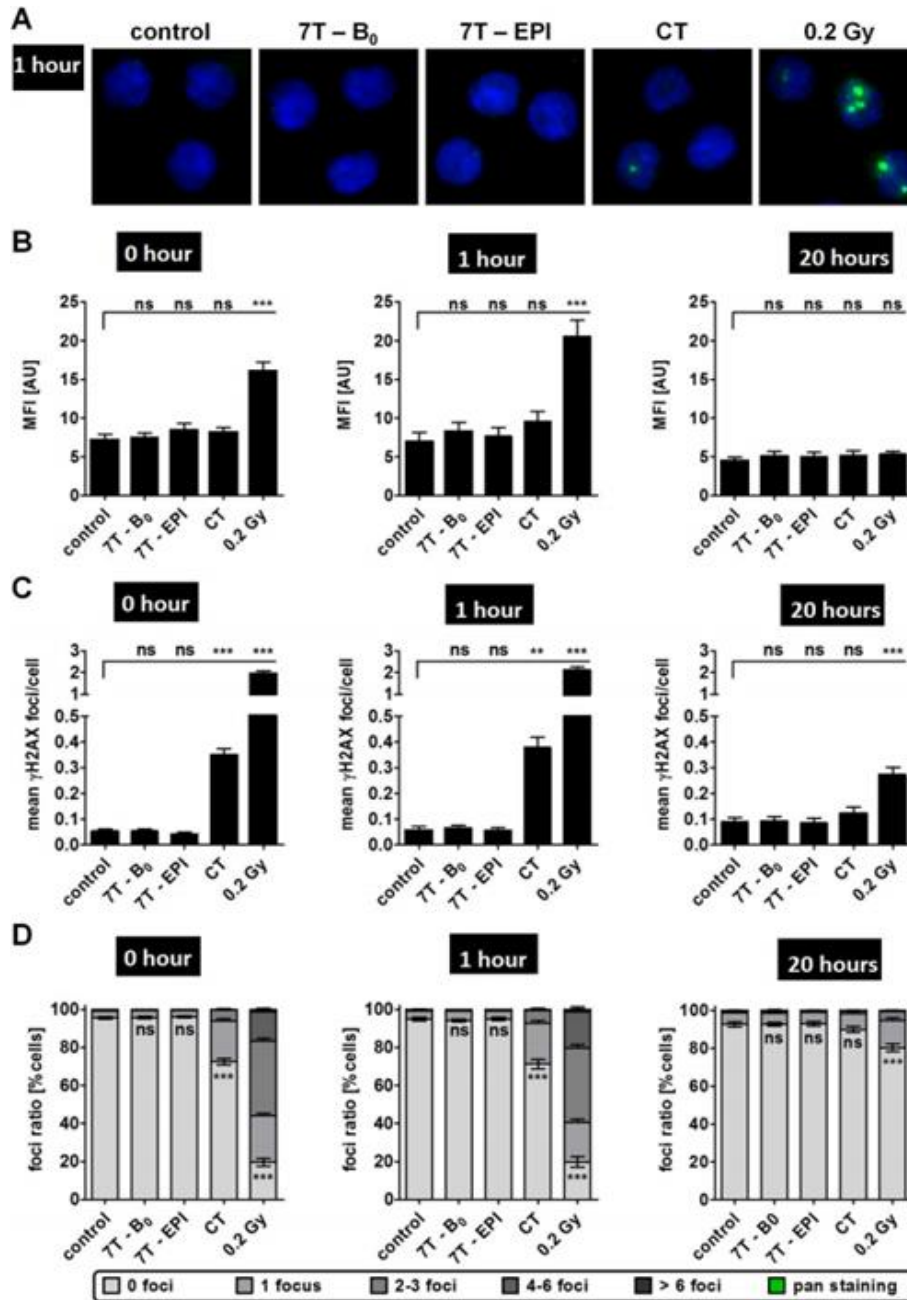
Figure 3.14: Analysis of γ-H2AX-stained DNA DSBs by automated microscopy [14]. **(A)** Representative images of DAPI (blue) and γ-H2AX-stained (green) PBMCs measured 1 h after indicated exposure. **(B)** Mean fluorescence intensity of γ-H2AX-level, **(C)** amount of mean γ-H2AX foci/cell and **(D)** mean foci ratio from 16 independent experiments at three different time points. Mean ± SEM (***: $P \leq 0.001$; **: $P \leq 0.01$; *: $P \leq 0.05$; ns: $P > 0.05$). Cells with nuclei exhibiting the maximum γ-H2AX fluorescence signal throughout the whole

nucleus were classified as pan-stained. These cells were recorded separately and not included into γ-H2AX focus and intensity analysis. (Image source: [14])

For cytotoxicity analysis, cell viability of unstimulated PBMCs was determined 24 hours, 48 hours and 84 hours after exposure. The detailed values are presented in Table 3.3. No significant changes in viability could be detected at any of the analysed time points for PBMCs exposed to 7 T magnetic field or CT. The only significant decrease in cell viability compared to normalized control (100%) was detected after 48 hours (90.1% ± 11.8%) at a dose of 0.2 Gy radiations. After 84 h viability decreased further to 84.4% ± 11.6% in this group.

Table 3.4: Individual data depicted in Figure 2b: Mean fluorescence intensity (MFI) of γ-H2AX staining determined by automated microscopy as arbitrary units [AU].

Donor No.	24 h					48 h					84 h				
	control	7 T-SMF	7 T-EPI	CT	0.2 Gy	control	7 T-SMF	7 T-EPI	CT	0.2 Gy	control	7 T-SMF	7 T-EPI	CT	0.2 Gy
01	100	100	100	88	86	100	108	94	81	82	100	100	103	72	68
02	100	95	101	106	95	100	111	104	111	92	100	107	100	103	79
03	100	105	105	100	100	100	112	104	99	98	100	114	107	93	89
04	100	108	109	104	97	100	110	103	93	83	100	121	114	87	69
05	100	113	105	109	108	100	110	117	122	122	100	103	102	96	91
06	100	111	107	113	113	100	112	112	105	101	100	117	116	110	102
07	100	104	120	119	127	100	102	102	99	101	100	105	99	96	95
08	100	96	96	90	98	100	93	92	92	95	100	113	109	104	99
09	100	93	99	108	91	100	85	93	101	80	100	89	97	107	86
10	100	93	92	91	89	100	85	86	86	79	100	98	96	102	87
11	100	86	78	89	87	100	84	68	78	77	100	79	61	73	67
12	100	100	104	106	103	100	96	96	97	95	100	106	108	107	97
13	100	95	91	92	87	100	93	89	89	79	100	98	98	96	72
14	100	93	97	99	96	100	94	93	97	89	100	97	100	103	88
15	100	92	97	101	93	100	92	99	102	86	100	100	111	110	88
16	100	94	98	100	91	100	90	100	99	83	100	91	106	103	73
mean	100.0	98.6	99.9	100.9	97.6	100.0	98.6	97.0	96.9	90.1**	100.0	102.4	101.7	97.6	84.4 ***
std	0.0	7.6	9.2	9.2	10.9	0.0	10.5	11.2	10.9	11.8	0.0	10.9	12.4	11.6	11.6
min	100.0	86.0	78.0	88.0	86.0	100.0	84.0	68.0	78.0	77.0	100.0	79.0	61.0	72.0	67.0
max	100.0	113.0	120.0	119.0	127.0	100.0	112.0	117.0	122.0	122.0	100.0	121.0	116.0	110.0	102.0

Cell viability analysis of unstimulated PBMCs by CellTiter-Blue assay [14]. Metabolic activity was measured 24 h, 48 h and 84 h after indicated exposure conditions. Diagrams display mean ± SEM of 16 independent experiments (***: P ≤ 0.001; **: P ≤ 0.01)
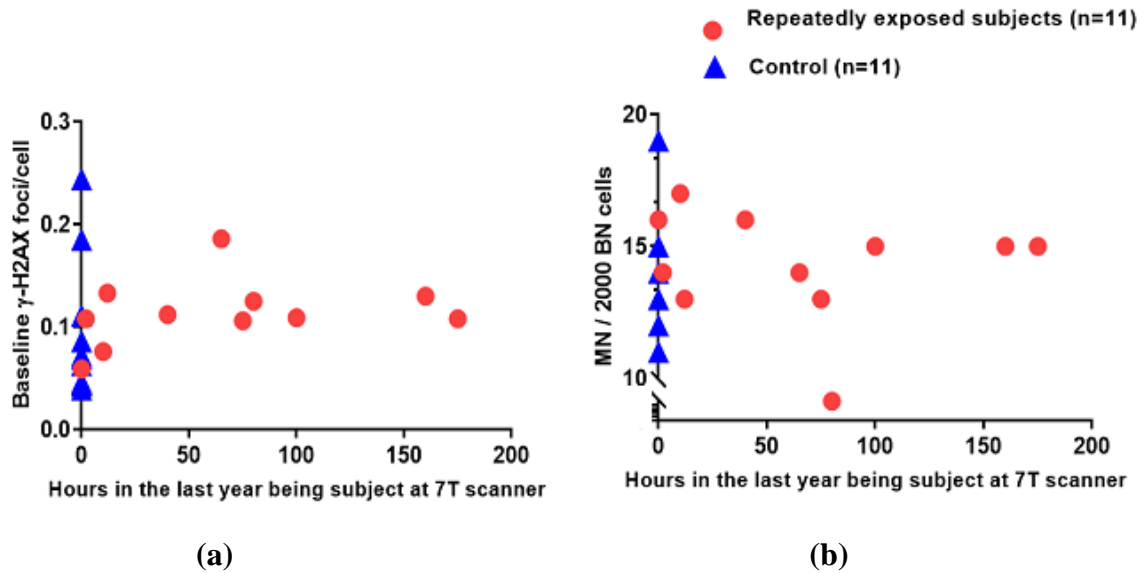
Proliferation response was investigated 84 hours after exposed PBMCs were subsequently stimulated with PHA (Figure 3.15). Compared to unstimulated cells (497 ± 172 cpm), PHA-induced proliferation lead to a mean [³H]-thymidine incorporation of 12,362 ± 4,220 cpm in unexposed control samples. No significant changes in proliferation response were detected for cells exposed to 7 T SMF field alone (11,630 ± 3,849 cpm) or to 7 T SMF combined with GMF and RF in EPI sequence (10,967 ± 3,827 cpm). PBMCs exposed to lower doses of ionizing radiation, CT (11,386 ± 3,765 cpm) and 0.2 Gy (12,924 ± 3,895 cpm), did not differ significantly from the control.
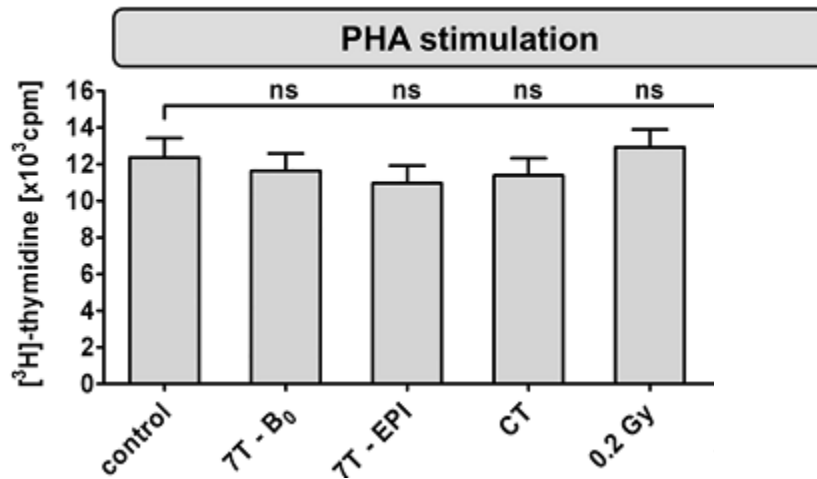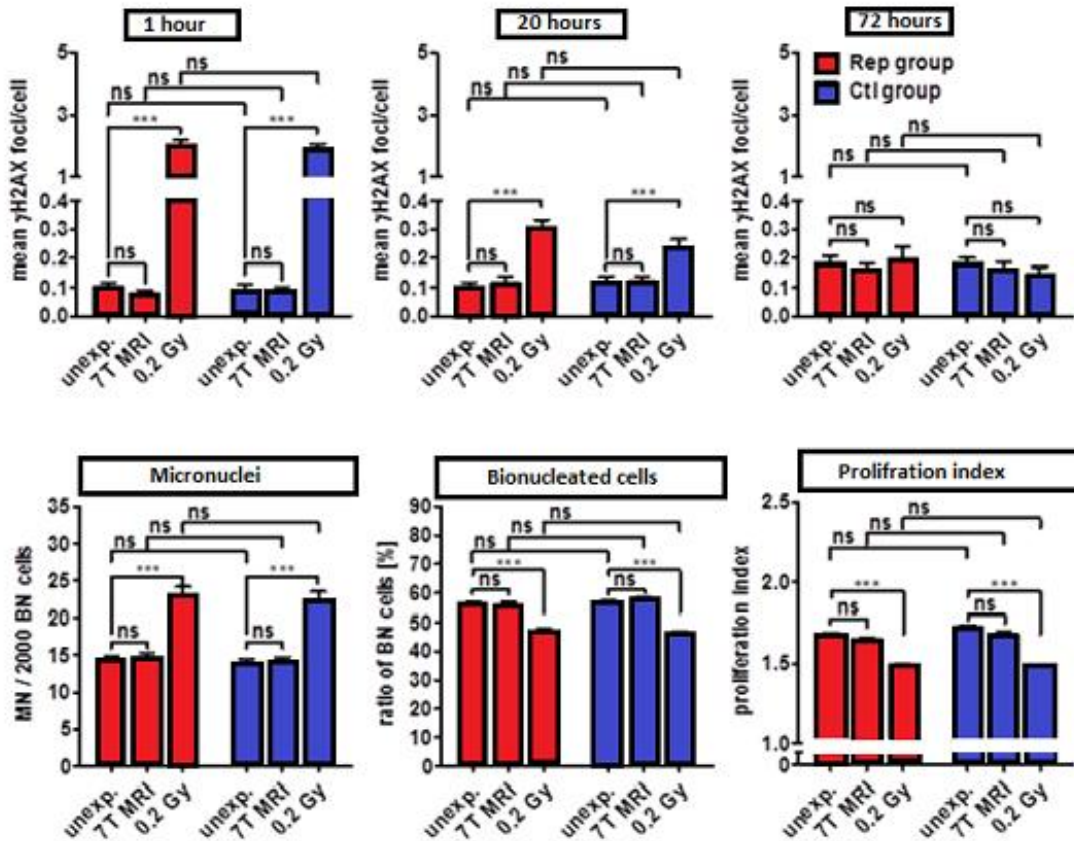

Figure 3.15: Proliferation assay of subsequently PHA-stimulated PBMCs [14]. [³H]-thymidine incorporation was determined 84 h after different exposure conditions. Diagram displays mean ± SEM of 16 independent experiments.

3.10.2 Repeated Whole-body Exposure Analysis

DNA DSBs were determined in the repeatedly exposed (Rep) group (mean age 34 ± 7 years) and age-matched control (Ctl) group (mean age 33 ± 9 years). The mean base-level of γ-H2AX foci/cell and MN/2000BN in two groups of cells, Rep (0.10 ± 0.01) and Ctl (0.09 ± 0.02) are shown in Figure 3.16. No significant difference, neither in γ-H2AX foci/cell nor in frequency of MN was detected in the baseline levels of the two groups.

Figure 3.16: **(a)** The mean base-level of γ-H2AX foci/cell in two groups of cells. **(b)** The baseline incidence of MN/2000 BN cells in two groups of Rep in red and Ctl in blue.

After additional *in vitro* exposure to 7 T MRI, analysis at 1, 20 and 72 hours post-exposure also did not present any significant difference between the two groups. In contrast, exposure to 0.2 Gy γ-radiation resulted in a ~20-fold significant increase in γ-H2AX foci in both Rep (2.01 ± 0.1) and Ctl (1.92 ± 0.16) cells at 1 h after irradiation (Figure 3.17). The spontaneous incidence of MN/2000 BN cells, without additional 7 T MRI, were not significantly different between Rep (14.4 ± 0.6) and Ctl (13.8 ± 0.6) cells. Figure 3.16 and 3.17 illustrate these results.

No significant changes in MN frequencies were detected in Rep (14.6 ± 0.6) and Ctl (14.1 ± 0.7) cells after an additional *in vitro* 7 T MRI exposure. In contrast, exposure to 0.2 Gy γ-radiation resulted in a similar and significant increase in MN in Rep and Ctl cells (22.9 ± 1.2 and 22.2 ± 1.3, respectively).

Figure 3.17: Isolated PBMCs of 11 healthy individuals repeatedly exposed to 7 T MRI (Rep; red bars) and 11 unexposed control subjects (Ctl; blue bars) were treated either unexposed, exposed *in vitro* for 1 h to 7 T MR or irradiated with 0.2 Gy γ-radiation. (Image source: [15])

The mean number of γ-H2AX foci/cell was determined (top row) 1 hour, 20 hours and 72 hours after exposure. The bottom row shows the micronucleus frequency in 2000 binucleated (BN) cells determined 72 h after additional PHA-stimulation and cytokinesis-block, differences in cell division determined by the ratio of BN cells and calculation of proliferation index. Bars display the mean ± SEM of 11 experiments (***: P ≤0.001; ns: P >0.05) [15].

In addition to incidence of MN/2000 BN cells, figure 3.17 contains the information on the percentage of BN cells and proliferation index (PI), which were assessed in two groups, before and after additional *in vitro* exposure to 7 T. The percentage BN were similar in Rep (56.3 ± 0.70%) and Ctl (57.0 ± 0.64) cells and, additional *in vitro* exposure to 7 T MRI had no significant effect in either of the two groups: 55.9 ± 0.87 Rep and 57.6 ± 0.67 Ctl (Figure

3.17). The PI was essentially the same in Rep (1.68 ± 0.01) and Ctl (1.72 ± 0.01) cells and, additional *in vitro* exposure to 7 T MRI had no significant impact: 1.64 ± 0.01 Rep and 1.68 ± 0.02 Ctl (Figure 3.17). Positive control samples exposed to 0.2 Gy radiation showed a significant decrease in percentage BN cells (Rep: 47.05 ± 0.86; Ctl: 46.05 ± 0.86) and PI (Rep: 1.49 ± 0.01; Ctl: 1.48 ± 0.01). Detailed data are presented in Appendix A.

The result of repair kinetics in cells exposed to ETP with and without 7 T MRI exposure indicated that the both Rep and Ctl cells treated with ETP showed a significant increase in γ-H2AX foci/cell, however, no significant difference between the two groups of cells was found (Figure 3.18). The numbers of γ-H2AX foci induced by ETP were significantly reduced in both Rep and Ctl cells 4 h after ETP removal. However, the residual damage in Rep and Ctl cells at 20 hours was higher than in those that were not treated with ETP.
Treatment with ETP of Rep and Ctl cells with or without additional 7 T MRI exposure showed no significant impact: (Rep- ETP: 2.80 ± 1.23; Rep- ETP+7 T: 2.87 ± 1.14; Ctl- ETP: 2.54 ± 1.26, Ctl- ETP+7 T: 2.60 ± 1.27 foci/cell).
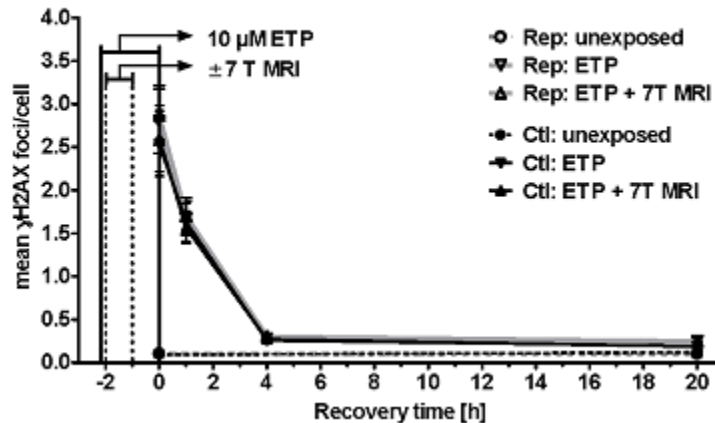

Figure 3.18: The initial γ-H2AX foci in isolated PBMCs of 11 healthy individuals repeatedly exposed to 7 T MR (Rep, gray lines) and 11 unexposed control subjects (Ctl, black lines) was analysed in different condition: unexposed (dotted line) or treated with 10μM ETP either alone (▼) or combined with a 1 hour 7 T MR examination (▲). DSB repair was analysed 1 hour, 4 hours and 20 hours after the ETP was removed and mean γ-H2AX foci/cells are plotted against recovery time. (Image source: [15])

3.10.3 *In vivo* Analysis

The mean level of initial γ-H2AX foci (t_1) in lymphocytes from all 53 patients was 0.13 ± 0.02 foci/cell. No significant difference (P = 0.699) in basal DSB level was observed between male and female subjects. The combined results of all 43 subjects within the MR groups revealed a mean baseline level of 0.13 ± 0.02 foci/cell (t_1). No significant changes were determined after MR exposure (t_2: 0.12 ± 0.02; t_3: 0.11 ± 0.02 foci/cell), as shown in Figure 3.19. In contrast, CT examination led to a significant induction of DNA DSBs, increasing from a mean γ-H2AX baseline level of 0.14 ± 0.05 foci/cell (t_1) to 0.26 ± 0.07 foci/cell (t_2) and 0.24 ± 0.07 foci/cell (t_3) after CT scan.

Unlike two experiments presented previously, where only healthy volunteers were enrolled, heterogeneity of initial γ-H2AX values increased in this *in vivo* study, ranging from 0.01–0.58 foci/cell. This spread in individual baseline DSBs led to high standard deviations. To account for individual differences and not to underestimate the personal risk, we normalized the results from t_2 and t_3 to the individual DSB values at $t_1 = 1$ (figure 3.19). Thereby the coefficient of variation for the MR group was reduced by more than 50%. Again, relative results revealed no changes within the MR group (t_2: 0.94 ± 0.07; t_3: 0.96 ± 0.06 fold), whereas γ-H2AX foci increased significantly (P $\leq$ 0.05) after CT examination (t_2: 4.00 ± 1.13; t_3: 2.52 ± 0.49 fold). In comparison to absolute values, CT results exhibited even stronger differences in relative γ-H2AX levels, due to the high range of individual baseline levels.
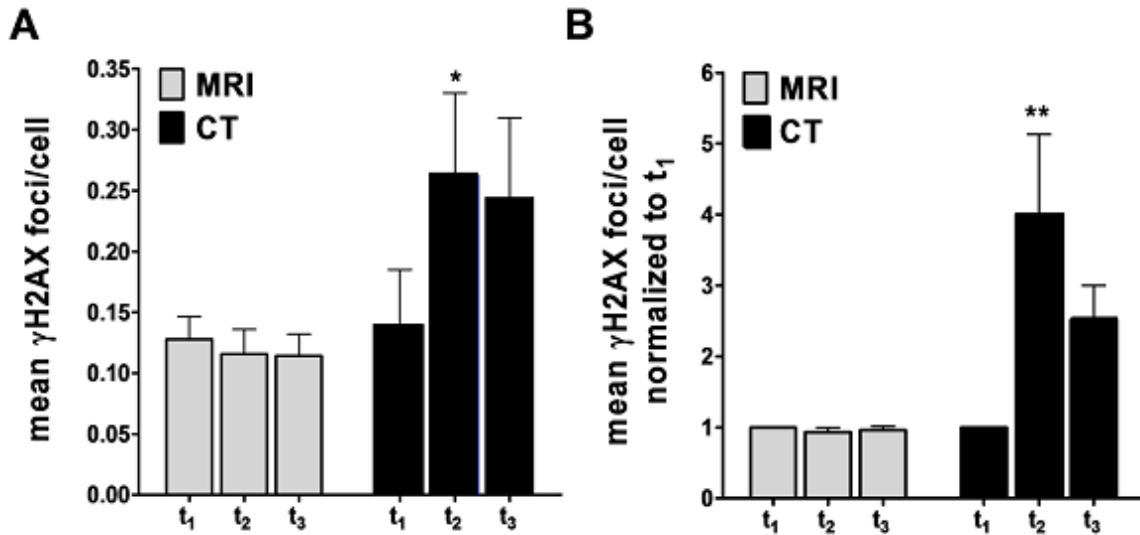
Figure 3.19: γ-H2AX analysis in lymphocytes from patients isolated before (t_1) as well as 5 minutes (t_2) and 30 minutes (t_3) after *in vivo* MRI or CT exposure. **A)** Mean γ-H2AX foci/cell of all 43 patients receiving MRI (light bars) and all 10 patients receiving a CT (dark bars) scan. **B)** Data depicted in (A) normalized to the individual γ-H2AX value at t_1. Bars display mean ± SEM (**: $P \leq 0.01$; *: $P \leq 0.05$). (Image source: [4]).

Differentiated analysis of subgroups, classified according to the applied SMF and the administration of GBCA, shown in Figure 3.20 (A), also showed no significant change in the amounts of DSBs before and after the MR scan. Compared to unenhanced high-field (1 T, 1.5 T, 3 T) MRI (t_1: 0.11 ± 0.02 foci/cell; t_2: 0.10 ± 0.02 foci/cell; t_3: 0.10 ± 0.02 foci/cell) there was no evidence that GBCA-enhanced high-field MRI (t_1: 0.15 ± 0.04 foci/cell; t_2: 0.13 ± 0.04 foci/cell; t_3: 0.13 ± 0.04 foci/cell) or unenhanced ultra-high-field 7 T MRI (t_1: 0.12 ± 0.04 foci/cell; t_2: 0.11 ± 0.04 foci/cell; t_3: 0.11 ± 0.04 foci/cell) lead to an increase of γ-H2AX foci. In the unenhanced CT group the level of DSBs increased from initially 0.18 ± 0.08 foci/cell to 0.21 ± 0.10 foci/cell (t_2), and 0.27 ± 0.12 foci/cell ($P \leq 0.05$) (t_3) and after CT examination combined with iodinated CA, from initially 0.10 ± 0.05 foci/cell (t_1) to 0.32 ± 0.10 foci/cell ($P \leq 0.05$) (t_2), and 0.21 ± 0.08 foci/cell (t_3). Diagrams displaying the normalized data (Figure 3.20.B) revealed again, no changes in relative DSB levels after MRI, but an increase after unenhanced CT (t_2: 2.22 ± 0.88 fold; t_3: 2.27 ± 0.51 fold, $P \leq 0.05$) and contrast-enhanced CT (t_2: 5.79 ± 1.83 fold, $P \leq 0.05$; t_3: 2.77 ± 0.88 fold).

64

In order to exclude heterogeneity among different MRI groups, stratified analyses of normalized data were conducted. The results showed that neither the applied field strength (P = 0.392) nor administration of gadolinium-based contrast agent (P = 0.317) affected the γ-H2AX value determined at t_2 and t_3 significantly. Although the total number of subjects is high, each subgroup for this analysis contained only 5 patients potentially limiting the sensitivity of the study. Comparison of normalized data between the MRI and CT group revealed significant differences in the level of induced γ-H2AX foci at t_2 (P < 0.0001) and t_3 (P = 0.0002) after exposure.
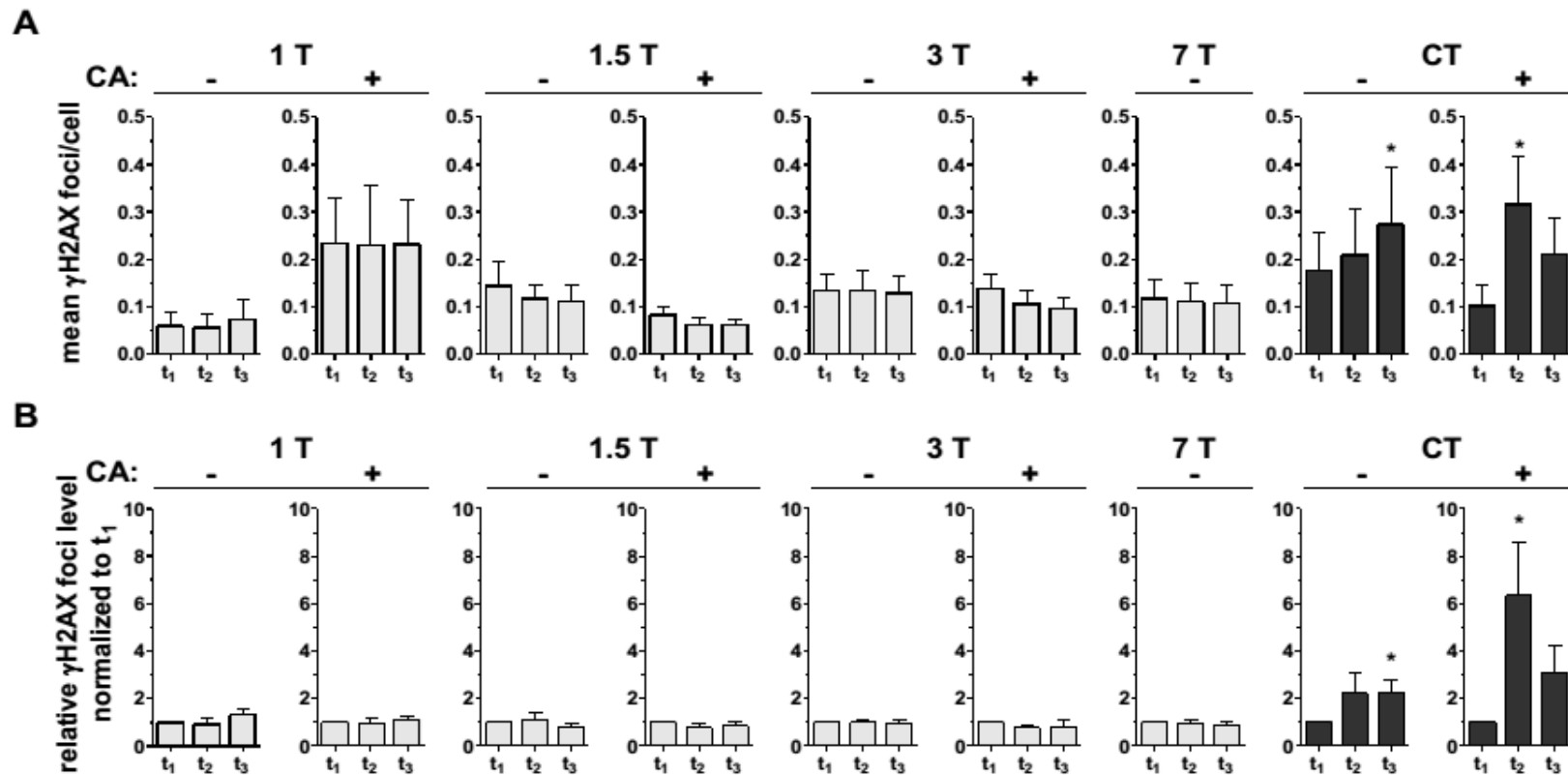
Figure 3.20: Mean results of γ-H2AX analysis in lymphocytes before (t₁) as well as 5 minutes (t₂) and 30 minutes (t₃) after *in vivo* MRI or CT exposure. Groups were divided according to SMF of the MR scanner applied (1 T, 1.5 T, 3 T, 7 T) and further subdivided, whether or not gadolinium-based contrast agent (CA) was injected. For comparison with imaging using ionizing-radiation patients receiving CT with and without iodine-based contrast agent were enrolled. The mean ± SEM (**: $P \leq 0.01$; *: $P \leq 0.05$) of five patients per condition (7 T = 13 patients) is displayed for each time point, depicting **(A)** the mean number of γ-H2AX foci/cell and **(B)** the relative increase in γ-H2AX-level, normalized to individual baseline value determined before the scan (t₁ = 1) (Image source: [4]).

66

Since no significant changes in γ-H2AX foci values after MRI were found, we additionally performed a reverse power analysis to state how high a potentially undetected effect of induced γ-H2AX foci may be. Reverse power analysis from all normalized MR data revealed a minimal detectable effect size of 0.396, i.e. changes of more than 39.6% should have been detected. This equals a change of more than 0.05 foci referred to the mean at t_1.

3.11 Conclusions and Discussion

This chapter reported a set of experiments that helped to resolve some of the current uncertainties in the field. In the first experiment, the un-stimulated human PBMCs were exposed to 7 T SMF alone or 7 T EPI sequences (SMF combined with imaging gradients and pulsed radio frequency). For comparison, cells radiated by routine CT scan as well as γ-rays at doses of 0.2 Gy were included. Genotoxicity assessment of γ-H2AX-stained cells did not reveal any differences in levels of DSB after 7 T exposures compared to untreated samples.

In the second experiment, the control group was compared with frequently exposed participants, who were exposed inside a 7 T MRI for up to 175 hours within one year. This study revealed no differences in DNA integrity (γ-H2AX foci, micronuclei) supporting the hypothesis that no long term or delayed effects are induced.

The results from the third experiment (*in vivo*) indicated that neither MR examination alone (1 T, 1.5 T, 3 T, or 7 T) nor addition of GBCA led to a detectable induction of DNA DSBs in PBMCs. For standardised assessment of γ-H2AX foci nuclei were evaluated by automated image analysis.

Despite the fact that the energy levels associated with electromagnetic fields used in MRI unlike ionizing radiation, which is known to induce DNA DSB even at very low doses, are not sufficient to induce any direct breaking of chemical bonds [145], a few recent *in vitro* and *in vivo* studies reported contradictory results.

The study by Fiechter et al. in 2013 [12] raised attention due to reporting of an increased level of DNA DSBs in 20 patients before and after contrast-enhanced 1.5 T CMR using γ-

H2AX microscopy and flow cytometry analysis of lymphocytes. In 2015 two additional reports were published to determine the level of damage in DNA by evaluating γ-H2AX formation in lymphocytes isolated before and after 1.5 T CMR. Brand et al. [13] investigated the effects of three different CMR protocols, all combined with GBCA. Microscopy analysis of lymphocytes from 45 patients showed no significant changes in DSB levels before and 5 minutes after MR scan. Lancellotti et al. [10], enrolling 20 healthy male participants for non-contrast enhanced CMR, studied the DSB induction as well as blood cell counts and activation. Whereas flow cytometric measurements of different T cell subsets and the whole T cell population showed no changes in γ-H2AX level one and two hours after MR exposure, the authors reported a significant rise in the amount of DSBs within the whole T cell population, two days and one month post CMR. However, the described increase in γ-H2AX level two days after CMR only occurred in a few subjects and a high inter-individual variation was observed in subjects one month after CMR.

The results of the presented study do not confirm the results from Lancellotti's study [10]. Despite using a higher B0 and SAR than those used in Lancellotti's study [10], no similar increase in γH2AX foci was detected at any of the time points (1, 20 and 72 hours after exposure).

The time period used in Lancellotti's study [10] study was also covered in the presented *in vivo* study, as half of the participants were either MRI staff or active research participants, and therefore they were repeatedly exposed to UHF strengths for months (or years). Yet, no significant effect of 7 T MRI exposures was detected compared to the unexposed controls. The reported correlation between the γ-H2AX values one month after exposure and the initial SAR in Lancellotti's study [10], is intriguing, however this correlation cannot be extrapolated, e.g., to no exposure, where a negative number of γ-H2AX is predicted.

Moreover, sufficient controls were not included in this study and thus it is difficult to judge whether the observed increase in γ-H2AX fluorescence intensity reflects a specific MR-related effect [94].

In the *in vitro* experiment presented in this thesis, the impact of exposure to static field alone, as well as combined exposure of all three electromagnetic fields, was considered and assessed. There were no differences found in DSB formation between the unexposed samples and both 7 T MR conditions. In the *in vivo* study, the main focus of the experiment was placed in the realistic and common exposure scenarios for the staff and volunteers. If differences between unexposed and 7 T MR-exposed samples were found, investigations with specific exposure (B0, B0 + GMF and B0 + RF) could have been added to separate potential effects of the different frequency ranges [15].

Moreover, the incidence of spontaneous MN was determined in the study on repeatedly exposed participants. The incidence of MN detected was similar in Rep and Ctl cells and also after additional *in vitro* 7 T MRI exposure (~14 MN in 2000 BN cells). All these indices confirmed those reported in a large database such as the study by Vijayalaxmi et.al, (n = 14,888; mean MN 8.6/1000 BN cells ± 7.78 s.d.) [146]. In contrast, 0.2 Gy irradiation resulted in a significant increase in MN in both Rep and Ctl cells, as well as after *in vitro* 7 T MRI exposure (~23 MN in 2000 BN cells).

In a study by Tucker et al. [147], it is reported that the lowest detectable γ-radiation dose that could induce significantly increased MN was different among individuals: 0.18 to 0.26 Gy for 20 to 70 year-old individuals, respectively. In the *in vivo* experiment of this thesis, a significant increase in MN in both Rep and Ctl cells exposed to 0.2 Gy γ- radiation was detectable. However, the extent of increase in MN was not similar in all participants: in one participant, it was an increase of only 2 MN in 2000 BN cells. It is also interesting to note that while 0.2 Gy γ-radiation caused a significant increase in γH2AX foci in all 22 participants, such increase in MN was not observed in all subjects. This could be due to differences between sensitivities of genotoxicity assays used to evaluate DNA damage [15].

Part II

Exposure Assessment in (ultra)-high Field MRI Environments

4 Evaluation of Exposure to (Ultra) High Static Magnetic Field during Research Activities with MRI Scanners

The work presented in this chapter has been partly presented in the following published article:

4.1 Introduction and Objectives

Recent advances and emerging applications in high and UHF MRI have inevitably led to the increased occupational exposure to EMFs generated by MRI systems. It is known and well-documented that a human body moving in the stray field of MRI scanners induces electric currents inside the body as discussed in Chapter 2. Such currents may cause transient sensory effects experienced by MRI workers, such as vertigo, metallic taste, nausea and headaches [30], which are explored and discussed more in Chapter 5.

Data on individual exposure of UHF MRI personnel to SMF and motion-induced time-varying magnetic fields (TVMF) is scarce. Currently, no standardised assessment procedure dealing with SMF and movements in SMF is available in the literature. Such a procedure, however, is a prerequisite for determining compliance with the proposed restrictions and guidelines regarding B and dB/dt, in particular, for motion around the MRI magnet.

Only limited data is currently available on occupational exposure to high and UHF SMF, and most of them are focused on the occupational exposure levels among personnel in clinical MRI facilities, but not research facilities [9, 18, 148-152]. However, such assessment in research environments is also relevant.

In research as well as clinical practice, workers may lean into the MRI magnet to attach accessories such as coils to the patients or volunteers, or to communicate with or comfort them. The fringe fields from radio-frequency excitation (B_1) and gradients (G_x, G_y, G_z) decrease very rapidly with distance from the bore, and are only active during the image acquisition [154]. However, the SMF is continuously present and extends beyond the scanner bore, so most of the personnel who enter the area around the scanner are subject to a strong and inhomogeneous SMF. Therefore, in extreme cases, MRI personnel may be exposed to almost the same extent as patients and volunteers. Due to the fact that they usually move faster close to the MRI scanner than the patients who are lying down on the patient table, they may even be exposed to a larger TVMF.

A proper assessment of exposure to UHF MRI scanners requires a broad research on workers' exposure patterns, local safety regulations, average duration of the task performed close to the scanner, construction of the scanner and individual sensitivity to the EMFs generated by an MRI scanner.

There are many studies in which occupational exposure to MRI-generated SMF and TVMF are estimated using different methods, including measurements of simulated movements of MRI personnel [1,155-160], measurement of the fields at various points around the scanner [160] or numerical calculations in anatomical models [162-163]. These studies provided an estimation of MRI workers' exposure. However, they are more focused on the job titles and have not been able to provide exposure variability either among different individuals with the same job title, or in different movement patterns around the scanner. Therefore, it is difficult to directly compare the results of those studies, since different strategies and measuring equipment were used [157].

In the chapter, individual exposure to high ($B_0 = 3$ T) and ultra-high ($B_0 = 7$ T) magnetic fields during research activities close to the MRI scanners was measured, both to assess compliance with exposure restrictions proposed by the current guidelines and for future epidemiological studies on the potential adverse effects (if any) of SMF.

The focus of the current chapter is on MRI research-related activities, which can also be relevant for the clinical use of scanners. However, due to the fact that medical personnel have a relatively standardised shift length, work protocol, and consequently a similar pattern of exposure [155], which is not the case for the work of MRI researchers, which varies a lot, ranging from scanning patients and volunteers to test coils and phantoms at different locations around the magnet: the levels of exposure in these two groups could be different.

4.2 Methods

Before starting with the measurements, a questionnaire was completed by the participants (n = 5). The questionnaire included questions regarding age, height, weight, current job title and

incidence of MRI-related symptoms and their perceptions of safety. In addition to the questionnaire, we conducted a short interview with the participants to obtain information on their typical activities, tasks and movements around the scanner. Based on the interview results, three simplified trajectories, including lateral motions and rotation around the body axes (leaning forward and bending over), were chosen as the most common elements of movements by the MRI research personnel around the scanner.

Five researches who routinely work with both 3 T and 7 T (Siemens Healthcare, Erlangen, Germany) were recruited for the measurement of individual exposure to the SMF and TVMF (dB/dt). The 7 T MRI scanner used in this study was passively shielded whereas the 3 T scanner was actively shielded. The measurement of the SMF was carried out using a three-axis Hall magnetometer (THM1176-HF, Metrolab, Geneva, Switzerland) with a resolution of ±0.5 mT and a sampling frequency of up to 6.5 Hz. The absolute values of B and dB/dt were calculated according to Equations. 1–3. Taking into account that the international guidelines [30] do not specify the formula to analyse the rate of time variability of the magnetic flux density vector, dB/dt can be evaluated using two different equations (Eqs. 2, 3), which may result in slightly different values. Eq. 2 was used to calculate the dB/dt throughout the experiment.

$$B(t) = \sqrt{(B_x)^2 + (B_y)^2 + (B_y)^2} \tag{1}$$

$$\frac{dB_V}{dt} = \left| \frac{B(t_2) - B(t_1)}{t_2 - t_1} \right| \tag{2}$$

$$\frac{dB_{xyz}}{dt} = \sqrt{(dB_x/dt)^2 + (dB_y/dt)^2 + (dB_z/dt)^2} \tag{3}$$

Participants were asked to follow the pre-defined paths, which were a selection of motions covering a range of normal human gait and typical exposure scenarios for researchers in close proximity to MRI scanners.

The subjects, three males and two females with an average height of 169 ± 13 cm were asked to wear an elastic strap to fix the Hall sensor on their head or chest. The sensor was connected to the data logger (Figure 4.1.A). A zero-field adjustment of the sensor was carried out before starting the experiment. All three orthogonal components of B (B_x, B_y, B_z) were recorded as a function of time (Figure 4.1.B).
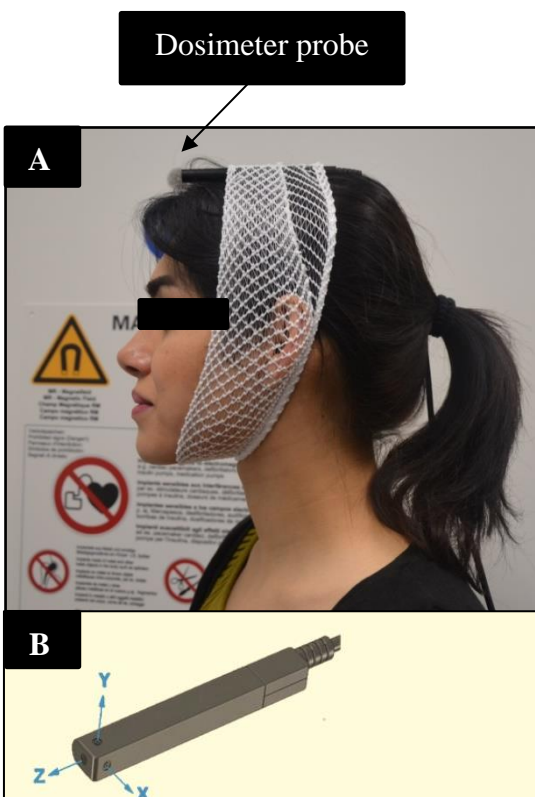
Figure 4.1: **A**: Three-axis Hall probe of the magnetometer attached to the subject's head. **B**: The top schematic view of the Hall sensor probe

To assess the exposure variability among the individuals, according to the coordinate system (Figure 4.2), the three paths (a, b, c) shown schematically in Figure 4.3, were followed by five participants of different heights, weights and walking pace, while having the Hall probe

attached to two different positions, on the head and chest, at two different scanners (3 and 7 T). Overall, 60 scenarios were analysed.
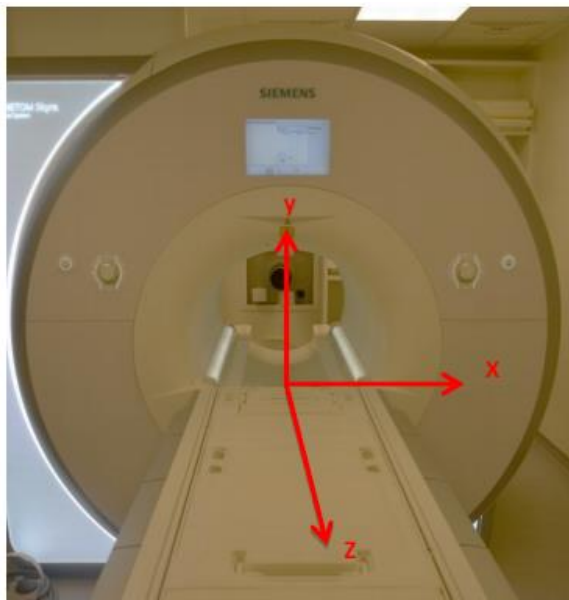
Figure 4.2: Coordinate system used in all the measurements and analysis

Path a (1-7) comprised seven different movements. It was designed to mimic activities related to the patient/volunteer positioning inside the bore and adjustment of the coil. It included movements along the bed and the long axis of the magnet (Z axis) while facing the scanner bore. It was started from one corner of the scanner room, followed by a 180° rotation around the Y axis, a movement along the Z axis, 90° rotation around the Y axis, followed by a movement along X axis, 90° rotation around the Y axis and another movement along the Z axis. Finally, the participants were asked to follow an orthogonal path in the X–Z plane toward the coil shelves and to end the path by walking outside of the scanner room.
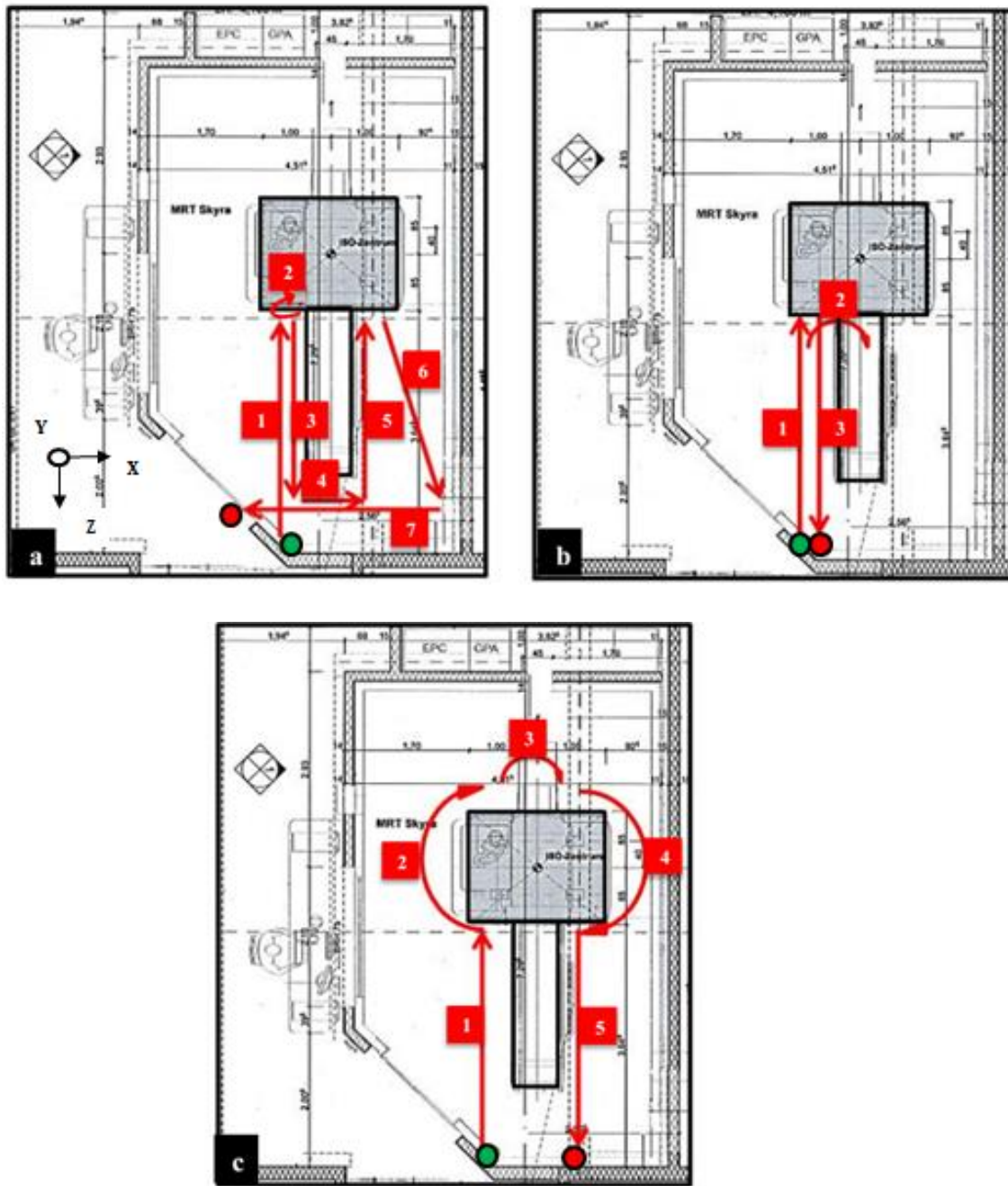
Figure 4.3: Schematic top view of the trajectories (path: a, b, c) considered in the assessment of the typical exposure scenarios around the MRI scanner

Path b (1–3) mimicked activities related to an experimental setup and positioning of a phantom at the entrance or partially inside the scanner bore. This path covered movement along the Z axis; 90° rotation around the Y axis and bending of the upper body about 90° around the Z (leaning towards the table), followed by a bending in X–Z plane (leaning towards the inside of the magnet bore). It was completed by a 90° rotation around the Y axis and the subject walking back along the Z axis.

Path c (1–5) mimicked some unusual movements around the scanner, e.g. accessing the MRI patient or volunteer from the end of the bore, adjusting the peripherals, such as a camera, mirror or cable by bending toward the inside from the end of the bore. It included movement along the Z axis, followed by a semi-circular path toward the end of the magnet, rotation of the upper body around the Z axis and a similar path in the opposite direction to get to the endpoint.

In order to conduct a realistic measurement of the fields, participants were asked to follow the paths at the same speed they usually walk near the scanner during their daily work. The spot measurement of the SMF was also carried out along the patient table to characterize the spatial distribution of the field for both scanners. Participants were asked about the incidence of MRI-related symptoms and potential discomfort during and right after the completion of the movement along the paths.

Magnetic flux density (B) was recorded at the head and chest, during the movements, expressed in mili-Tesla (mT). The metrics of exposure, including the actual value [B(t)], the actual value of the time derivative (dB/dt and the changes of B over any 3-s motion ($\Delta B_{3\,s}$) have been taken into consideration to be compliant with the restrictions for workers' exposure provided by ICNIRP guidelines [18, 30].

According to ICNIRP there are two sets of exposure guidelines, for the controlled and uncontrolled working environments. Guidelines for a controlled environment accept higher levels of exposure for workers. There are applied only when appropriate work practices are implemented to control movement-induced sensory effects [30].

In the event of exposure in an uncontrolled environment, the following exposure restrictions are provided: 2000 mT as the limit of the spatial peak magnetic flux density in exposure of the head and trunk to protect against vertigo due to movement in the SMF [156], and 2000 mT to be the maximum change of B over any 3-s motion to protect against vertigo due to TVMF exposure, with a frequency not exceeding 1 Hz [1]. In extremities and controlled exposure of the head and trunk, the limit goes up to 8 T [156] but this case was not evaluated in this study, as neither scanners exceed 8 T. Additional basic restrictions have been provided with regard to the electric field induced in the body due to movement in SMF or exposure to time-varying B fields at frequencies of 0–25 Hz. They are set to protect against potential adverse effects in the peripheral nervous system (in a controlled environment) or to protect against magnetophosphenes (in an uncontrolled environment) [18, 30].

Generally, the basic restrictions are not easily measurable at the workplace, therefore, compliance can be assessed based on the reference levels expressed by dB/dt, at a fixed level 2700 mT/s (with respect to the controlled environment), or a frequency-dependent level: 2700 mT/s up to 0.66 Hz and 1800/f mT/s at higher frequencies (with respect to the uncontrolled environment).

Based on this structure of ICNIRP restrictions, the following standardised parameters characterizing the exposure over the recorded exposimetric samples were analysed. $L_1 = B(t)/2000$;　$L_2 = |dB/dt|/2700$;　$L_3 = |dB/dt|/(1800 \times 2 \times \Delta t)$;　$L_4 = |\Delta B_{3\,s}|/2000$.　Each metric ($L_1$, L_2, L_3, L_4) was standardised based on the particular ICNIRP limits, i.e. exceeding the value of one, when overexposure was detected. Metrics were analysed with respect to their maximum value over particular subsets of data, as well as the statistical distribution (median and 95th percentile in the set of samples) in the subsets of results spread between the head (H) and chest (C), between paths (a, b, c, over a group of all five subjects), between subjects (1, 2, 3, 4, 5 over a group of all three paths) and at 3- and 7 T scanners separately.

Since an MRI environment is considered as a controlled environment, parameters L_2 and L_4 were the most relevant metrics to assess compliance with the exposure restrictions.

4.3 Results

Maximum SMF values recorded for all five subjects at both field strengths are shown in Table 4.1. At 3 T, a max B of 2057 mT was recorded, which is about 68% of the B_0, and at 7 T, a max B of 2890 mT, which is about 41% of the B_0 was recorded.

Table 4.1: The SMF exposure in 60 scenarios. B measurements (five subjects, three paths, two scanners and two locations for the Hall sensor), adapted from [157].

|	*Height (cm)*	*SMF strength (T)*	*Max B on head (mT)*			*Max B on chest (mT)*		
			path a	*Path b*	*path c*	*path a*	*path b*	*path c*
Subject 1	183	3	140	1246	759	282	548	313
		7	698	1977	1317	1018	1127	939
Subject 2	175	3	246	2057	1671	282	1098	878
		7	900	2890	2672	1113	1439	1279
Subject 3	171	3	126	1909	2000	388	651	732
		7	680	2505	1894	1102	1105	1000
Subject 4	169	3	195	1600	1138	465	642	537
		7	806	1942	834	1188	1247	982
Subject 5	147	3	512	550	673	176	1464	1440
		7	983	2026	2265	1387	1200	126
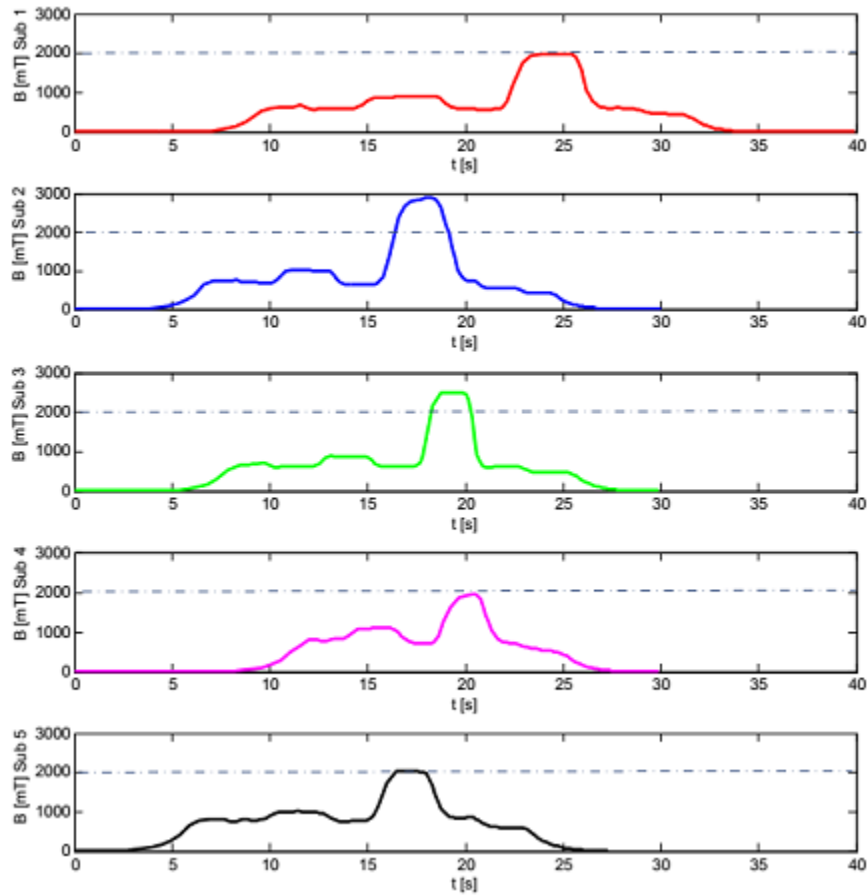
Figure 4.4: SMF exposure measurement for five subjects recorded from the starting point to the end point during path **b** in close proximity to the 7 T MRI scanner. (Image source: [157])

Figure 4.4. summarizes the SMF exposure level recorded on the head of five participants along path b, at the 7 T MRI scanner. The figure shows a similar pattern of exposure for all the participants; however, the exposure level is different among them.

Since this study only included 3 and 7 T scanners, the 8 T limit for exposure of the extremities and head or trunk under controlled conditions was never exceeded.

Figures 4.5 and 4.6 present statistical distributions of standardised metrics L_1–L_4 of exposure near 3- and 7 T scanners, in the subsets of results spread between the head (H) and chest (C), between paths (a, b, c; over a group of all five subjects) and between subjects (1, 2, 3, 4, 5; over a group of all three paths).
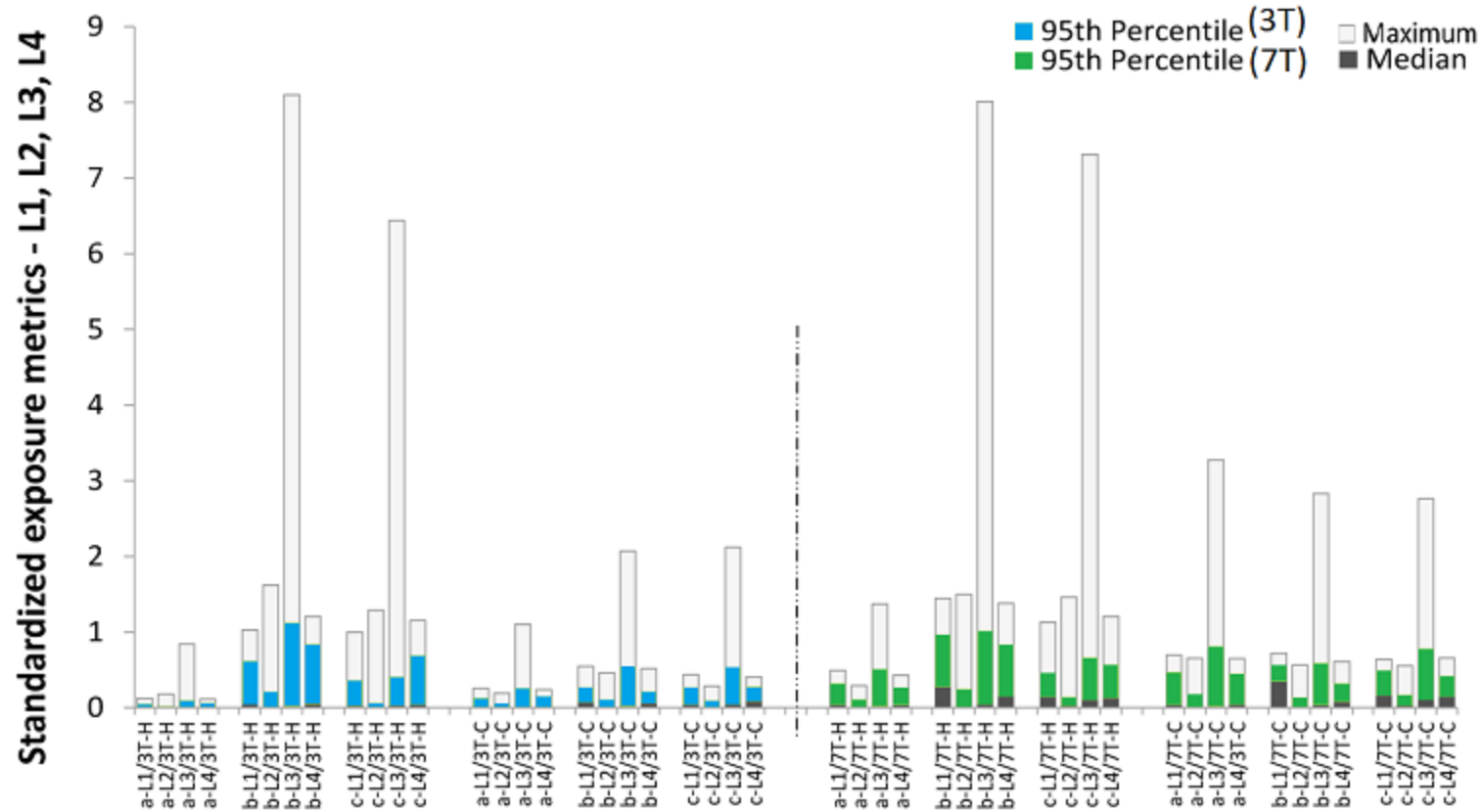
Figure 4.5: Distribution of standardised values of exposure metrics (L_1–L_4) in sub-sets covering exposure of all subjects (S_1–S_5), during particular movements (a, b, c), at the head (H) and at the chest (C), near 3- and 7 T scanners. Black areas show medians, green and blue bars show the 95th percentile. Adapted from [157].
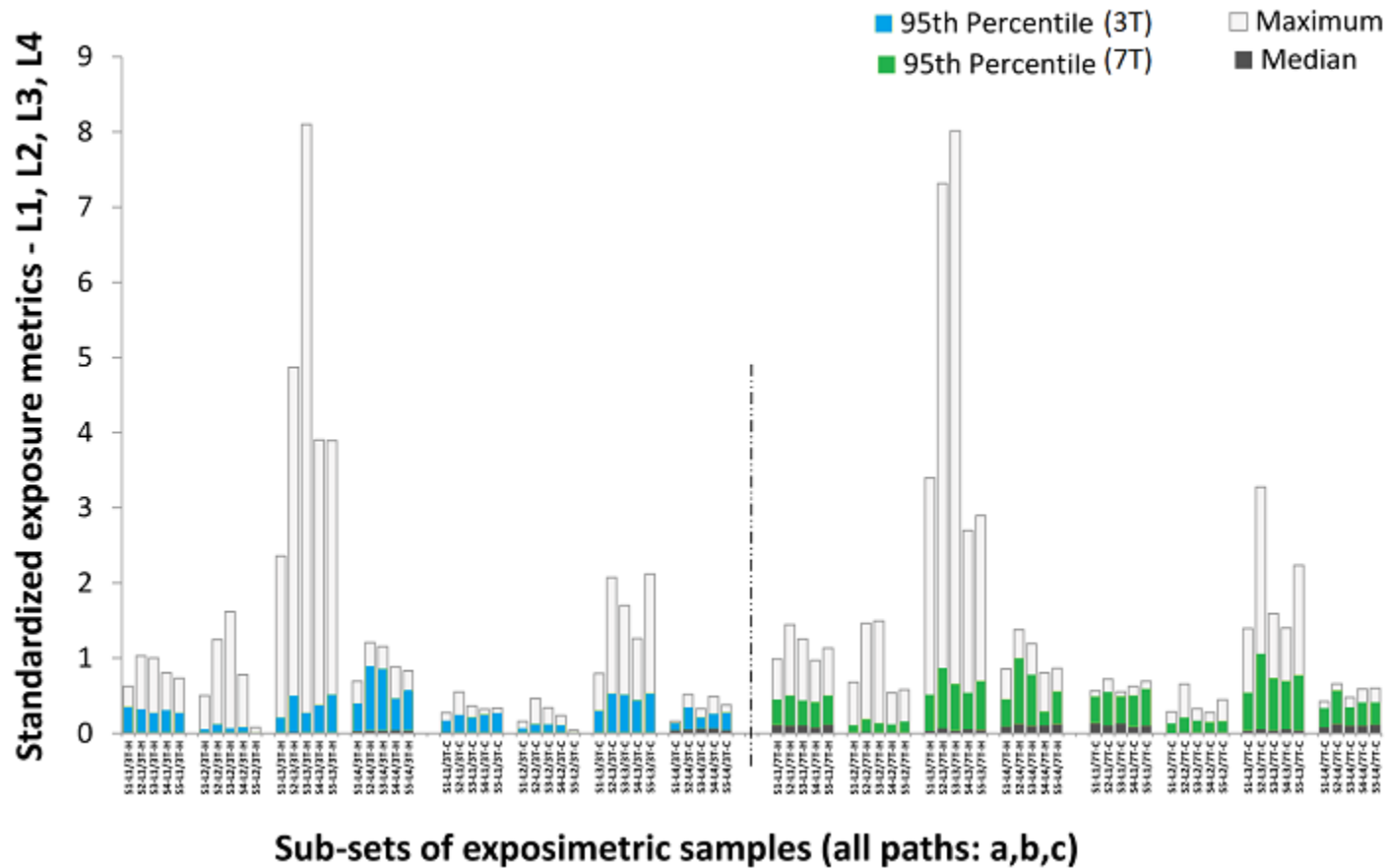
Figure 4.6: Distribution of standardised values of exposure metrics (L$_1$–L$_4$) in sub-sets covering exposure during all movements (a, b, c), performed by particular subjects (S$_1$–S$_5$), at the head (H) and at the chest (C), near 3- and 7 T scanners. Black areas show medians, green and blue bars show the 95th percentile. Adapted from [157].

Exposure to time-varying fields arising from movement within the B fringe field resulted in a max dB/dt of 4347 mT/s for the head and 1200 mT/s for the chest at 3 T. For 7 T, the measured max dB/dt values were 3900 and 1700 mT/s for the head and the chest, respectively.

The repeatability of the measurement result for path c was tested at the 3 T scanner using nine recordings of head exposure. The metric of intra-subject variability for maximum exposures was defined as $VR_H = [(\text{maximum value} - \text{minimum value})/\text{average value}] \times 100\%$. Parameter VR_H showed a higher value in dB/dt than in B values (in maximum values of B at the head, the repeatability was $VR_H = 39\%$, while in maximum value of dB/dt, the repeatability was $VR_H = 57\%$). The VR_H parameters for the 95th percentiles of exposure levels for B and dB/dt were 35 and 46%, respectively. On average, max B values over nine recordings at the head during movements of the same subjects in path c was 756 mT (with an average 95th percentile value of 490 mT and an average value of 105 mT). In this set of samples, the average value for max dB/dt was 2220 mT/s (with the average 95th percentile value of 543 mT/s and an average value of 105 mT/s).

The results indicate that the exposure to the SMF as well as the TVMF was highly variable among individuals, although they worked with the same scanner in the same manner and they followed the same paths near the scanner. The metric of inter-subject variability for maximum exposure was defined as $VS = [(\text{maximum value} - \text{minimum value})/\text{average value}] \times 100\%$. The parameter VS_H for maximum values in head exposure at the 3 T scanner was 32 and 169%, for B and dB/dt, respectively. In chest exposure, $VS_C = 74\%$ for B and 170% for dB/dt.

At the 7 T scanner, $VS_C = 19$ and 68%, $VSH = 20$ and 116%, for B and dB/dt, respectively. In general, VS showed a higher variability at the 3 T scanner than at the 7 T scanner. It was also higher in the head exposures than in the chest exposures. In the head exposures, the VS_H parameter for the 95th percentiles of exposure level has similar values to the mentioned values for maximum levels, whereas in the chest exposures, variability in values of the 95th percentiles is roughly twice as low.

On average, maximum B values over subjects and paths were approximately twice as high when working with a 7 T scanner (1300 mT) compared to working with a 3 T scanner (820 mT). However, this average for max dB/dt was not much higher for the 7 T scanner (1822 mT/s) than for the 3 T scanner (1475 mT/s). More detailed distributions of particular metrics of exposure near both scanners are shown in figures 4.5 and 4.6. The plots indicate that the parameter which exceeded the ICNIRP restrictions, the most at both scanners is $L_3 = |dB/dt|/(1800 \times 2 \times \Delta t)$, which is more relevant for an uncontrolled environment, whereas exceeding the restrictions for a controlled environment (L_2 and L_4) happened only in a few cases during path b and c, where rotation and bending were included in the movement. In general, overexposures were not found up to the 95th percentiles. They happened in an extremely small percentage of recorded samples, i.e. less than 5% of exposure duration was related to exposures exceeding the recommendations for workers' exposure in a controlled environment.

Considering the incidence of sensory effects during and after the experiment, only one of the participants (subject #5) reported feelings of vertigo and headaches right after completing each path (a, b, c). Other participants did not report any adverse feeling or discomfort related to the magnetic fields, regardless of their exposure level covered by the range of movements in this study. In the results of the exposimetric measurements of SMF exposure, no significant difference between the exposure pattern of subject #5 and the other subjects was found. All the participants stated that they feel safe while working with the scanner.

4.4 Conclusions and Discussion

Chapter 4 characterises the most common exposure scenarios to high and ultra-high field MRI in research activities. Maximum exposure values of B = 2057 mT and dB/dt = 4347 mT/s for a 3 T scanner and B = 2890 mT and dB/dt = 3900 mT/s for a 7 T scanner were determined. It should be noted that the movements near the MRI scanners in this study were not randomly sampled, but were identified using a questionnaire and chosen

to include the typical movements of MRI researchers in the vicinity of MRI scanners, including translations and rotations.

Considering the average over subjects and paths, the maximum B value was approximately twice as high when working with a 7 T scanner compared to a 3 T scanner. However, the average for max dB/dt was not much higher for a 7 T scanner than a 3 T scanner, and even 95th percentiles are comparable in these two cases. Variability of the results, observed between and within subjects shows that the inter-subject variability is larger than the intra-subject variability. The high inter-subject variability can be easily explained by many parameters, such as the spatial distribution of the field at different individuals' heights and differences in personal behavior (i.e. walking velocity and bending angle) [162]. This may explain why dB/dt recorded near the actively shielded 3 T scanners, where stronger dB/dx inhomogeneity normally exists, was higher than dB/dt around the 7 T scanner.

In passive shielding, tons of iron is used to effectively reduce the extent of the fringe field, whereas the concept of active shielding is to include two reverse polarity coils in the coil array, which reduces the field immediately at the entrance of the bore. This design commonly results in smaller fringe fields and, consequently, stronger spatial gradients of the magnetic field close to the magnet. The maximum dB/dt recorded close to the magnet cover at 7 T in the current study was about 1.5 times lower than that in a similar, but actively shielded scanner. This difference was smaller between actively and passively shielded 3 T scanners. All measurements were conducted at a Siemens scanner (Siemens Healthcare, Erlangen, Germany). As scanner from other manufacturers may use different designs for the magnet, they may lead to different outcomes. Regarding the incident of MR-related sensory effects and the perception of safety, the perception of safety of healthy individuals working with human 7 T MRI is retrospectively assessed [164] and the result is reported in chapter 5.

The results from that study indicated the average perception of a moderately safe work environment, which is confirmed in the current study. In the current study, only one subject (20% of subjects involved) reported vertigo and headaches right after completing the experiment which is similar to the previous results [165]. Since this particular subject was

expecting sensory effects prior to the experiment, due to her previous experience, along with the fact that she was reluctant to bend over the bed completely in path b, we hypothesize that this subject appeared to be more sensitive and susceptible to MR-related symptoms than the others. Considering the height (Table 4.1) and the walking velocity of the subject (Figure 4.3), we also hypothesise that both height and walking velocity were significant determinants in exposing that particular subject to higher B and dB/dt, which resulted in experiencing more sensory effects. This may also explain the small value of B and dB/dt in all paths, recorded for subject #1, who was the tallest among the participants and spent more time to complete the paths (i.e. path b, shown in Figure 4.3). This result could be due to the fact that the head and chest of the taller workers are further away from the strong B.

Considering the answers from all participants, no correlation was found between reporting the MRI-related sensory effects and exceeding the reference values.

Previous personal exposure data are available, in which the 3-axis Hall sensor was worn on the hip or chest [166]. It is generally accepted that the exposure measured at the head is usually higher than exposure measured at the chest and lower body; however, this is highly dependent on the individual's height and there is no data available that directly compares the impact of various positions for the Hall probe.

A limitation of the methodology in the current study was that, due to the long cable used for data transmission, the participants had to be more attentive while walking around the scanner. This might possibly affect (reduce) their walking velocity, though this should not affect their speed of rotation and bending.

The present results from available data indicate that violation of the ICNIRP restrictions for max B during workers' exposure in the controlled environment at 3- and 7 T MRI scanners was unlikely to happen, which is in accordance with the previous studies [150, 167,168]. Exceeding of the dB/dt reference level at 3 and 7 T were almost similar (30% of 60 exposure samples).

Analysis of the max B revealed a large variability between participants, even though the paths, and therefore the chance of approaching the bore, were identical for all the participants. This result accords well with the study by Schaap et al. [155]. The relatively large variability between subjects may suggest the importance of performing personal exposure measurements instead of relying solely on mathematical calculations. By using a simply designed personal exposure measurement probe for MRI researchers, it will be possible to gather a wide and reliable pool of data on exposure levels during research activities in the proximity of MRI scanners. Such data would assist studies on the possible bio-effects of MRI-generated electromagnetic fields. However, further multi-centred, comprehensive studies assessing exposure levels at different positions around high and ultra-high field MRI scanners, which research personnel encounter during their routine research activities, deserve consideration. This study seeks to provide a realistic overview of what level of exposure can be expected in typical research activities. The inter-subject variability of exposure levels found in this study may be considered in future instructions for workers in a controlled high and ultra-high field MRI environment.

This result can also be used as a starting point and may help to develop guidelines for the adoption of some simple precautionary rules for researchers' behavior around MRI scanners to avoid exceeding the limits.

Part III

Transient and Sensory Effects

5 Transient and Sensory Effects of Exposure to Ultra-high Field MRI

The work presented in this chapter is partly published in the following article:

5.1 Introduction and Objective

Currently, more than 70 UHF MRI human research sites are in operation worldwide [169,170]. The rapid growth in the number of UHF MRI sites has quickly led to the development of active research areas, such as: neuroscience, brain, cardiac, body and breasts [68,172-174]. This expansion in the use of UHF MRI inevitably increases the exposed groups and possibly can multiply the already existed safety concerns.

It is known that the exposing of a human body to MRI scanners may cause transient sensory effects, including but not limited to vertigo, metallic taste, nausea and headaches [30]. As discussed in Chapter 2, safety guidelines are published by international organizations to minimize the unwanted effects of EMFs used in MRI systems. Apart from those, many research groups have assessed the transient effects induced by MRI scanners. However, most of the works carried out in this domain have focused on prevention and reduction of "objective" risks. Only limited attention has been directed toward subjective perceptions of safety in MRI environments. With regards to UHF MRI even fewer publications are available. Only a few studies have assessed the acceptance of UHF MRI among volunteers and subjects [155,175-176].

Subjective perceptions of safety and risk at work are shown to be linked to objective risks and therefore can affect safety outcomes in organizations [177]. Thus, it is essential to evaluate how workers perceive the safety in UHF MRI environments and what adverse side effects, if any, are reported by them.

In this chapter, the focus is on retrospective, self-reported perceptions of safety and the prevalence of UHF MR-related sensory effects. The results of a comprehensive survey among healthy individuals who occupationally work with and around 7 T MRI scanners is reported and discussed.

5.2 Methods

A total of 118 UHF MRI personnel from 8 different locations across Europe, where 7 T MRI scanners are used for human research: Magdeburg, Leipzig, Heidelberg, Essen in Germany; Oxford and Nottingham in the United Kingdom; Utrecht in The Netherlands; and Pisa in Italy, were identified and given the opportunity either to agree or refuse participation in the study. Finally, 66 individuals, 23 females and 43 males with the mean age of 31 ± 7 years agreed to participate in the study. An overview of the study population can be found in Table 5.1.

The study was approved by the ethics committee of the Otto-von-Guericke-University Magdeburg, Germany. The participants who agreed to participate in the study completed either a paper-based or web-based questionnaire (depending on their physical location), during two consecutive months. There were variations in participants' job titles and usual physical locations during the work in the 7 T MRI suites. The majority of the participants were students performing UHF MR research (n = 33). The second group were scientific researchers at UHF MR centres (n = 28) followed by (n = 2) physicians and (n = 2) MRI technicians.

Participant in Magdeburg and Heidelberg completed a paper-based questionnaire and other participants completed a web-based question, which they received via their email. Participants were asked to answer some questions on demographics; years of experience working with 7 T MRI scanners; how often and for how long they usually stay in the 7 T MRI scanner suite; their physical location with respect to the 7 T MRI scanner during image acquisition (inside or outside the scanner room); average working hours per week; number of months they had been working; and their perceptions of safety in their working environment. The other questions related to the 7 T MRI exposure-related symptoms, including sensory and transient symptoms. The questionnaire contained 19 different symptoms, which were commonly reported by previous studies [155, 178-179].

Table 5.1: Overview of the study population for the retrospective survey, taken from [164]

7 T Ultra-high Field MRI site	MRI Scanner vendor	Shielding method	N	%
Magdeburg	Siemens	Passive	24	36.2
Heidelberg	Siemens	Passive	22	33.3
Leipzig	Siemens	Passive	4	6.1
Oxford	Siemens	Active	2	3.1
Nottingham	Philips	Active	6	9
Utrecht	Philips	Active	2	3.1
Essen	Siemens	Passive	2	3.1
Pisa	GE	Active	4	6.1
Total			66	100
Characteristics			**N**	**Mean ± SD**
Female			23	
Male			43	
Age (years)				31 ± 7.4
Hours/week working with 7 T MRI				3.2 ± 3.6
Work experience with 7 T MRI (months)				47 ± 32

Apart from two of symptoms which were related to switched GMFs, i.e., tingling sensation in the body and involuntary muscle contraction, the other symptoms were SMF-related symptoms, i.e., vertigo, nausea, seeing light flashes, feeling of instability, metallic taste, ringing in the head or ear, tachycardia, sweat attacks, depression, fear, headaches, feeling faint, changes in appetite, fatigue, and loss of concentration. Two unrelated symptoms, including irritated and red skin and blurred or double vision, were used to control for potential over-reporting of symptoms. All of the above symptoms were rated on a five-point Likert scale from "never" to "always" referring to the frequency of occurrence.

Participants were also asked whether their work practice had been adversely affected by the symptoms they experienced and if yes how.

The perception of safety level was assessed with the question "How safe do you feel while working with 7 T MRI?" Response options ranged on a seven-point Likert scale from "very unsafe" = 1 to "very safe" = 7.

The questionnaire ended with an open question, with a direction to record any other regularly experienced symptoms during their work, which were not included in the questionnaire.

The data was subjected to the Mann-Whitney U-test to identify significant differences in the response of the participants to the questions on the paper-based questionnaire with those on the web-based questionnaire: no significant differences were observed between the two methods (P => 0.05), and hence, all data was pooled. The response rate for the paper-based questionnaire in Magdeburg was 74% and in Heidelberg was 55%. The response rate for the web-based questionnaire, which was used in other 7 T MR centres, was 47%.

Testing for potential relationships between different factors, as presented below, was conducted using non-parametric bivariate Spearman correlation (r_s). The correlation was calculated between the number of symptoms experienced by the participants, their perception of safety and (i) the location of work with respect to the scanner (inside/ outside of the scanner room); (ii) the number of hours spent in the scanner suite; (iii) participants' gender; and (iv) self-reported workload.

The answers that related to working with or around an actively or passively shielded scanner were examined using a non-parametric independent test, between n = 3 samples from actively shielded scanners and n = 3 randomly selected samples from the rest of the scanners (passively shielded). The test showed no significant differences (P> 0.05) between both shielding methods, and thus answers from both scanner types were combined.

In order to test the potential effects of different centres on the results, a stratifying analysis was conducted. The following samples were chosen out of the total samples: Magdeburg (n = 2), Leipzig (n = 2), Oxford (n = 2), Nottingham (n = 2), Utrecht (n = 2), Pisa (n = 2), Essen (n = 2) and Heidelberg (n = 2). We conducted a non-parametric test for independent samples to check if any centre showed any significant differences in the number of reported

symptoms or the level of perceived safety. A similar test was performed between participants from Magdeburg (n = 24) and Heidelberg (n = 22) which were comparable in numbers. The results showed that the factor "centre" did not have any effect either on the number of reported symptoms or on the perception of safety (P > 0.05) and therefore the answers from all centres were combined. Values with 95% confidence interval (CI) were calculated and *p*-values of less than 0.05 were considered as significant differences.

5.3 Results

5.3.1 Prevalence of Sensory Effects

The detailed prevalence of different symptoms reported by the participants is presented in Figure 5.1. The results indicate that, among the 19 symptoms, vertigo (62%) and metallic taste (51%) followed by headaches (36%) and fatigue (33%) were by far the most frequently reported sensory symptoms. The least prevalent symptoms were irritated or red skin and blurred or double vision, which were added as assumed EMFs unrelated symptoms to control for potential over-reporting of symptoms. Both symptoms were reported by one male participant.

The results indicate that 7.6% (5/66) of the participant who routinely work with and around 7 T MRI did not report any MR-related transient symptoms during their work with MRI.

The most frequently experienced symptom in this study was vertigo, which is believed to be due to an interaction between the magnetic field and the vestibular system of the inner ear responsible for balance [180].
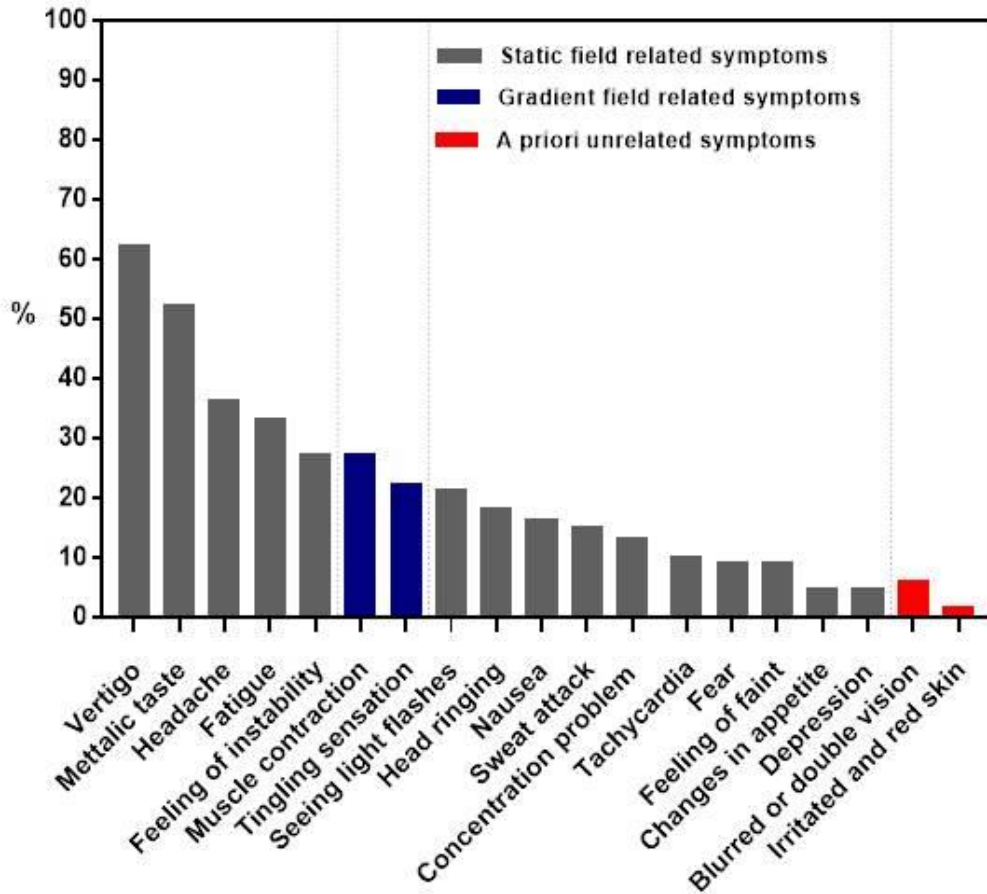
Figure 5.1: Prevalence of different symptoms reported by participants (n = 66). SMF-related symptoms are shown in gray, GMF-related in blue and a priori unrelated symptoms are shown in red.

5.3.2 Sensory Effects and Work Locations around the Scanner

Since there were some variations in the physical location of work among the participants,

in order to control the potential effects of physical location on the number of reported symptoms, participants were asked about their physical location with respect to the 7 T MRI scanners during image acquisition (inside or outside the scanner room). A significant effect of location on the number of reported symptoms (P = 0.001) was found. Those participants, who frequently attended inside the scanner room due to the nature of their work, reported significantly higher number of sensory symptoms. There were no significant differences in

the number of reported symptoms (p > 0.05, 95% CI [−2.23 to 1.52]) between males and females.

There was also no significant correlation (1) between the number of reported symptoms and the number of hours spent in the vicinity of the 7 T MR scanner (rs = − 0.069, 95% CI [−0.55 to 0.58]), and (2) between the number of reported symptoms and the self-reported workload level (rs = − 0.37, 95% CI [−3.27 to 0.002]).

None of the participants added any more information regarding additional sensations that were not mentioned in the questionnaire.

Participants were asked whether their work practice has been adversely affected by the symptoms they experienced. Sixty-five (98.5%) reported that their work practice is not adversely affected by any of the symptoms mentioned in the questionnaire. Only one participant (female, 1.5%) reported that her work practice is slightly affected by regularly experiencing headaches and vertigo during her work, which resulted in her terminating the experiment as an investigator.

Moreover, in the other section of the questionnaire, participants were asked about their medical condition, if any, and whether they need to take medication, and what medication. No case was found to have any medical condition triggered by or related to working with 7 T MRI.

5/66 (7.6 %) of the participants did not report any MR-related symptoms while working with 7 T MRI scanner.

5.3.3 Perception of Safety

Safety refers to the state of being "safe", the condition of being protected from harm or non-desirable outcomes. However, perceived or subjective safety refers to the users' levels of comfort and perceptions of risk, without consideration of standards or safety history.

Participants in this study were asked about the subjective perception of safety at the 7 T MRI environments.

45.5% participants (30/66) reported that they feel very safe; 39.4% (26/66) moderately safe; 4.5% (3/66) slightly safe; 9.1% (6/66) neutral; and 1.5% (1/66) reported a slightly unsafe feeling while working with UHF MR. None of the participants stated that they feel moderately or very unsafe.

No significant difference in the perception of safety was found between males and females ($p > 0.05$, 95% CI [−0.56 to 0.41]).
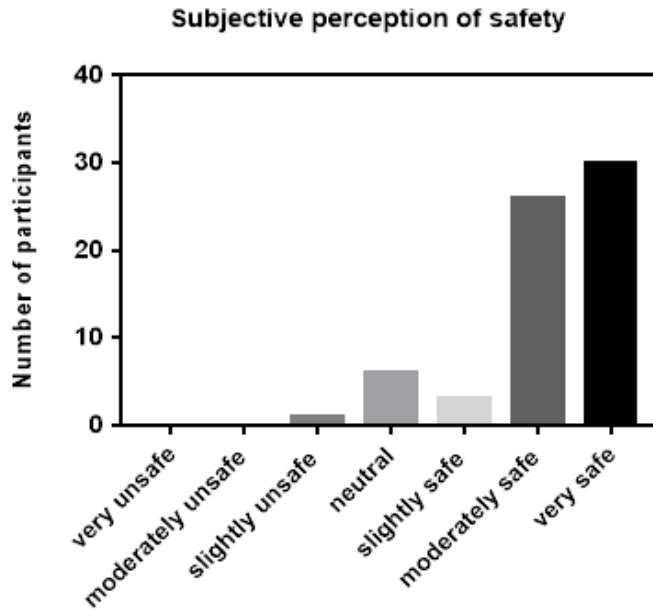
Figure 5.2: The perceived level of safety reported by n = 66 UHF workers, on a seven-point Likert scale: "very unsafe"; "moderately unsafe"; "slightly unsafe"; "neutral"; "slightly safe"; "moderately safe" and "very safe". Adapted from [164]

5.4 Conclusions and Discussion

A fair number of studies have examined the possible transient effects of UHF MRI on human subjects and volunteers, but most of them are based solely on damage thresholds established mainly for heating effects of UHF MRI and generally try to quantify the associated objective

risk. Despite that subjective and objective assessment of hazards being strongly related, they are distinct phenomena. Both are relevant in risk assessment in a working environment [181], as employee's perception of safety is directly linked to safety outcome in an organization [182].

Workers do not use quantitative risk analysis when evaluating their subjective occupational risks [183-184]. A number of factors can contribute to how we view the safety and risks at our work environment. Williams et al. [177] observed internal factors such as memory, experience, and stress, as well as external factors such as the work environment, exposure, and sensory information that may contribute to the workers' perception of risks and safety.

In this chapter subjective safety perceptions among 7 T MRI workers retrospectively was assessed. The most important finding of this retrospective survey is those participants routinely working with 7 T MRI scanners on average viewed their work as a safe environment, despite a clear experience of UHF MR-related symptoms.

This could be due to their prior knowledge about MRI and knowing the transient nature of MR-related symptoms. The most frequently reported high-field sensation in this survey was vertigo, followed by metallic taste and headaches. This result confirms findings from previous studies [169, 175, 185]. Moreover, this accords very well with the study by Schaap et al. [155], in that MR-related symptoms other than vertigo and metallic taste are shown to be manageable and not so common among the staff [155].

Perceptions of safety were not affected by the number of hours per week the staff spent in the vicinity of the 7 T MR scanner, or the number of months they worked with 7 T MR. We, therefore, conclude that staff working around 7 T scanners do not initially have major concerns regarding safety, and that their concerns reduce with more experience. This may be due to their prior experience with lower-field systems.

There are few studies in which the risk perception is assessed in a different working population [155]. However, we believe that as the risk factors to which they are exposed in their work environment are not similar to MRI environments, the result of those studies may

or may not be comparable to the MR environment. In the study by Dongen et al. [178], perception of health risks of EMFs by MRI radiographers and airport security officers was compared to the general working population. It is shown that MRI radiographers had a lower perceived risk, felt less negative, and more positive towards different sources of EMFs than the general working population and the security officers at airports. The authors concluded that MRI radiographers have more education and training in their occupational EMF sources (MRI) than the security officers, and are probably more technology-orientated than security officers and the general working population. However, we believe that MR workers do not have entirely different risk perceptions from the other working populations, partly because of their prior knowledge regarding the transient nature of the sensory effects, and also because the research may be more than "only a job". Hence, they may have a relatively positive view about working with 7 T MRI scanners. This could have a profound effect on their perception of safety and potential risks of 7 T MR scanners.

SMFs extend beyond the limits of the scanner bore and, consequently, most of the staff who stay in the area around the scanner are subject to a strong magnetic field. Whereas all the fringe fields from B1 and Gx, y, z decrease very rapidly with distance from the bore entrance [154]. As it was expected, only staff who remain very close to the scanner within the scanner room during the image acquisition reported switched gradient field target symptoms; a tingling sensation in the body and involuntary muscle contraction. These symptoms were rarely reported by the other staff. Overall, MR workers may only be exposed to B1 or switched gradient fringe fields when they stay very close to or even inside or partially inside the bore during scanning, which is unlikely to happen. Therefore, the strong magnetic field seems to be the main contributing factor to evoke most of the acute transient symptoms. This may suggest that vertigo can potentially be stimulated by the SMF which is present all around the scanner and, more importantly, by the speed of motion within the field, e.g., during subject positioning. This hypothesis is supported by some recent studies [185-186]. Schaap et al. [179] reported that at almost all of the MRI departments that performed scans on human subjects for research purposes, which is the case in 7 T MRI facilities, workers regularly volunteered to be scanned. This exposes them to all three types of MRI-generated fields. In the questionnaire, workers were asked about MR-related effects and perceived

safety while working with 7 T MRI. They were not asked to ignore their experiences as a volunteer. This may overestimate the frequency and intensity of the effects, and may consequently affect the results. Since volunteering as a research subject seems to be common for many workers in almost all 7 T MR research centres, it should be taken into account when assessing the perceptions of safety. It should also be noted that due to a lack of reference data from lower-field strength, the assignment of symptoms as UHF-related effects need to be confirmed by future studies.

In this research, due to the large variability between subjects and the fact that subjects who report side effects usually reported many of them, it is hypothesized that some participants appeared to be more sensitive and susceptible to the MR-related symptoms than others.

This finding suggests a possible underlying trait of personal sensitivity to MR-related symptoms consistent with the findings of the study by Schaap et al. [155].

Given the fact that only a few hundred personnel work in and around UHF MRI scanners in Europe, the number of participants investigated (n = 66) is a good representation of the research personnel associated with 7 T MRI scanners.

The number of limitations regarding this work merits discussion. Due to the descriptive nature of the study, a control population which was not associated with UHF MRI facilities was not recruited and their perceptions of safety and the prevalence of symptoms were not assessed. Given the fact that very specific experience and expertise was required to answer most of the questionnaire items, such as MR-related effects, it is not straightforward to include a proper control group with similar knowledge about MRI, but without respective experience. Even when assuming willingness and honesty of the participants in the survey, a control group would also not have been able to deal with potential different individual interpretations of the wording chosen in the Likert scales (very/moderately/slightly [un]safe), including language-related issues in this multicentre study. Although we believe that MR workers do not have entirely different risk perceptions in different 7 T MRI centres, as the safety regulations are identical, an individual's perception of safety is very subjective, and can be different to others due to factors such as: previous experience, levels of education,

training, and personal factors such as confidence, attitudes, interests, and motives. Therefore, by definition, an individual's perceptions are neither right nor wrong.

The next limitation of this study lies in its retrospective nature. The retrospective design allows immediate access to the data, but at the cost of limited control over data collection and recording of covariates. Thus, the inclusion of a scientific metric, such as physically measured subject exposure levels, was not possible by design and it calls for further study.

6 General Discussion, Conclusions and Future Research

6.1 General Discussion

MRI has established itself as a routine technique in medical diagnostics. The absence of ionizing radiation as well as the excellent soft-tissue contrast and flexibility, are the major advantages of MR systems compared to ionizing techniques such as computer tomography (CT). It has been used for clinical and research purposes for about three decades with an apparently good safety record and few or no serious side effects aside from well-documented acute injuries resulting from acceleration of ferromagnetic materials or RF-induced burns due to poor positioning of the patient in the scanner [187]. However, the legal status of UHF MRI, as well as official documentation, is currently lagging well behind the lower field strengths. It is not yet approved for clinical use and it is labeled as ''investigational devices'' by the regulatory authorities.

The concern of the general public has mainly been centred on the possibility of long-term effects of EMFs used in MRI scanners, with particular reference to a possible association with the incidence of genetic damage. Questions about possible genotoxic effects from MRI go back for many years. This issue has recently reemerged, with an inconsistent and even contradictory set of reports.

The results from the available literatures show, with few exceptions, that animal and human cell exposed *in vitro* and *in vivo* to SMF, GMF or RF (i.e., each one independent of the other) at different frequencies, modulations, flux densities, SAR, at or below the international recommended guidelines, do not exhibit significantly increased genetic damage compared with that in un-exposed cells. Moreover, despite the numbers of known and scientifically documented interaction mechanism for each of the fields used in MRI, the interaction mechanisms of combined sources of exposure in MRI with living materials remains unexplained. This absence of a plausible biophysical mechanism in MRI remains a significant component in the weight of the evidence against health effects. It is, however, not practically possible to prove "a negative", i. e., that no effect exists. It is best discussed in terms of a very low probability.

One prerequisite to pave the way for transferring UHF MRI scanning to clinical use is to assure that the risk is minimal for both subjects and workers. An important step in this direction is presented within this thesis.

This thesis has exhibited a multidisciplinary approach to evaluate the UHF MRI safety concerns in different aspects (biological, technical, subjective) that are relevant for patients, subjects, staff and therefore, it is crucial for policy makers. Such multidisciplinary approach, helped to provide a broad insight on the topics which are usually investigated separately.

In the context of genotoxicity potential of UHF MRI, impacts of 7 T MRI on human lymphocytes were assessed through a set of experiments. In the *in vitro* study, human

PBMCs were exposed to the SMF of a 7 T MRI alone or combined with imaging gradients, and a pulsed radiofrequency in EPI sequences.

To mimic the worst case scenario and enhance the potential degree of damage, the power deposited in the samples was maximized by using the maximum permissible SAR level and switched gradient. Genotoxicity assessment of γ-H2AX-stained cells did not reveal any differences in levels of DSB after 7 T exposures compared to untreated samples.

The uncertainties about the impacts of repeated 7 T MRI expositions were also addressed in this thesis. It is to be noted that some study participants have been exposed to 7 T MRI as research subjects for hundreds of hours, i.e., much longer than most patients or other subjects. These "frequent flyers" may be among the most exposed individuals. The result reflected no significant impact on genetic damage and cytotoxicity indices from their lymphocytes.

For the first time, 7 T MRI, which is currently only allowed for research purposes, was included for *in vivo* experimental study in this thesis. In the *in vivo* study impacts of different field strengths on DNA DSB formation were investigated and it was attempted to reveal a potential hazardous effect of contrast material. The results revealed no induction of DSBs by MR imaging irrespective of the field strength and contrast material enhancement. The results of all experimental studies are based on γ-H2AX analysis, one of the most sensitive assays for detecting DSBs.

6.2 Conclusions

As far as we can ascertain from the results presented in this thesis and the previous available literature, the balance of scientific evidence does not indicate that harmful effects occur in MRI. The risks, if any, should be very small and its impact on public health substantially negligible compared to other risks. The absence of increased γ-H2AX foci and MN indices in

cells after exposure to 7 T indicates that *in vitro*, *in vivo* and even repeated exposure to 7 T can be considered a safer alternative to ionizing based imaging techniques.

Nonetheless, further investigation on potential genotoxic effects may shed light on the mechanism of interaction (if any), and should be considered.

Uncertainties about the actual exposures and the perceived risks and safety of 7 T MRI during routine MRI research procedures was investigated by evaluating a number of scan scenarios and various exposure schemes in (ultra) high field MRI environments. In this thesis it is shown that the guidelines are compliant, i.e. the EMF reference levels are sufficient to keep the dose under the permitted basic restrictions for UHF MRI research activities.

With regard to the perceived safety and sensory effects experienced by the MRI occupational group, the 7 T scanner is shown, to be similar to 3 T, except for limited transitory physiologic effects. Among the most frequently reported are vertigo and metallic taste.

6.3 Future Research

Further advances in the research field of UHF MRI safety are subject to progress in the following areas:

- establishing new hypotheses on interaction of EMFs used in MRI with the human bodies and *in vitro*, *in vivo* analysis of the hypotheses.
- blinded evaluations of multiple genotoxicity endpoints (including appropriate positive and concurrent unexposed controls) with adequate statistical power
- evaluation of UHF MRI impact on formation of oxidative stress and free radicals in living materials.
- implementation of broader analysis methods that search for different genotoxicity and cytotoxicity markers to highlight potential hazardous biologic effects of MR in large cohorts.

The analysis in this thesis was restricted to human blood lymphocytes. However, the extent of genetic damage in other tissues needs to be examined, as the impacts of MRI focused on different organs, such as the brain and the heart, may be different. For instance, little is known about a potential genotoxic effect on e.g. highly proliferative human haematopoietic stem/progenitor cells or on cells from individuals carrying deficiencies in DNA damage repair mechanisms.

- implementation of appropriate and straightforward methods for the measurement of real exposure in UHF MRI environments.
- verification of previous studies

An additional issue to be addressed would be to determine the critical component of exposure (SMF, GMF, RF) if any. To address this issue, experiments with animals can be useful. Small and larger animals can be exposed to very high magnetic fields with immunologic different markers for potential defects, including endpoints, which are generally examined in toxicological investigations, such as; free radical formation, cell proliferation, apoptosis, single/double-strand breaks, chromosomal aberrations, micronuclei, sister chromatid exchanges and mutations.

In the context of transient and sensory effect and its relationship with the actual exposure, the presented studies in chapter 4 and 5 of the thesis suggested that some participants appeared to be more sensitive and susceptible to the MR-related symptoms than others. Therefore, differences in magnetic field susceptibility between individuals should be studied in the future. It is also recommended that studies are conducted to assess the relationship between "subjective" perceptions and "objective" assessment of MR-related sensory effects.

Future research could also focus on assessing potential neuro-behavioral and cognitive effects of exposure to UHF MRI scanners. Potential effect modifiers, such as the psychological factors, personality and character traits, and depression, stress, and anxiety levels should be considered. The applicability of a standard questionnaire to assess the transient effects and its correlation with individuals' susceptibility for magnetic field exposure should be considered for future research.

Appendix A

Isolated PBMCs of 11 healthy blood donors (CTR group) and 11 highly exposed MR volunteers (MR group). Micronucleus frequency in 2000 binucleated (BN) cells was determined 72 h after additional PHA-stimulation and cytokinesis-block and differences in cell division were determined by the ratio of BN cells and calculation of proliferation index. All data are displayed as the mean ± std of 11 experiments and significance levels between the untreated sample and the exposed samples among the same group are indicated behind (***: $P \leq 0.001$; ns: $P > 0.05$). P-values between the two groups, comparing only identical treatment conditions are displayed in the column CTL< >MR.

Table 1. Micronucleus analysis of PBMCs after 7 T MRI and 0.2 Gy exposure

MN / 2000 BN lymphocytes			
treatment	CTL group	MR group	CTL< >MR
unexp.	13.8 ± 2.1	14.4 ± 1.9	$P > 0.05$
7T MRI	14.1 ± 2.2^{ns}	14.6 ± 2.0^{ns}	$P > 0.05$
0.2 Gy	$22.2 \pm 4.4^{***}$	$22.9 \pm 4.0^{***}$	$P > 0.05$

Binucleated lymphocyte %			
treatment	CTL group	MR group	CTL< >MR
unexp.	57.0 ± 2.1	56.3 ± 2.3	$P > 0.05$
7T MRI	57.6 ± 2.2^{ns}	56.0 ± 2.9^{ns}	$P > 0.05$
0.2 Gy	$46.1 \pm 2.9^{***}$	$47.1 \pm 2.9^{***}$	$P > 0.05$

Proliferation Index			
treatment	CTL group	MR group	CTL< >MR
unexp.	1.72 ± 0.05	1.68 ± 0.05	$P > 0.05$
7T MRI	1.68 ± 0.05^{ns}	1.65 ± 0.05^{ns}	$P > 0.05$
0.2 Gy	$1.48 \pm 0.04^{***}$	$1.49 \pm 0.03^{***}$	$P > 0.05$

Isolated PBMCs of 11 healthy blood donors (CTR group) and 11 highly exposed MR volunteers (MR group) were either left untreated, exposed for 1 h to 7 T MR combined with strong gradient and radiofrequency fields or were irradiated with 0.2 Gy γ-radiation. Mean number of γH2AX foci/cell was determined 1 h, 20 h, and 72 h after exposure. All data are displayed as the mean ± std of 11 experiments and significance levels between the untreated sample and the exposed samples among the same group are indicated behind (***: $P \leq 0.001$; ns: $P > 0.05$). P-values between the two groups, comparing only identical treatment conditions are displayed in the column CTL< >MRV.

Table 2. Analysis of γH2AX foci in PBMCs after 7 T MRI and 0.2 Gy exposure

mean γH2AX foci / cell - 1 h after exposure			
treatment	CTL group	MR group	CTL< >MR
unexp.	0.09 ± 0.07	0.10 ± 0.04	$P > 0.05$
7T MRI	0.09 ± 0.05^{ns}	0.08 ± 0.04^{ns}	$P > 0.05$
0.2 Gy	$1.92 \pm 0.52^{***}$	$2.01 \pm 0.55^{***}$	$P > 0.05$

mean γH2AX foci / cell - 20 h after exposure			
treatment	CTL group	MR group	CTL< >MR
unexp.	0.12 ± 0.06	0.10 ± 0.05	$P > 0.05$
7T MRI	0.12 ± 0.07^{ns}	0.12 ± 0.08^{ns}	$P > 0.05$
0.2 Gy	$0.24 \pm 0.10^{***}$	$0.31 \pm 0.09^{***}$	$P > 0.05$

mean γH2AX foci / cell - 72 h after exposure			
treatment	CTL group	MR group	CTL< >MR
unexp.	0.17 ± 0.09	0.18 ± 0.11	$P > 0.05$
7T MRI	0.16 ± 0.08^{ns}	0.16 ± 0.08^{ns}	$P > 0.05$
0.2 Gy	0.15 ± 0.09^{ns}	0.20 ± 0.14^{ns}	$P > 0.05$

Appendix B

List of Acronyms

ALARA	As Low As Reasonably Achievable
CA	Chromosomal Aberrations
CA	Contrast Agent
CBMN	The cytokinesis-block micronucleus
CI	Confidence Interval
CT	Computed Tomography
CMR	Cardiac Magnetic Resonance
DNA	Deoxyribonucleic Acid
DSB	Double Strand Break
ELF	Extremely Low Frequencies Magnetic Fields
EPI	Echo-Planar Imaging
ETP	Etoposide
FDA	Food and Drung Adminstration
GBCA	Gadolinium-based Contrast Agent
GMF	Gradient Magnetic Field
IRB	Institutional Review Board

MFI	Mean Fluorescence Intensity
MN	Micronuclei
MRI	Magnetic Resonance Imaging
MU	Mutation
NMR	Nuclear Magnetic Resonance
RF	Radio Frequency
PBMC	Peripheral Blood Mononuclear Cells
SAR	Specific Absorption Rate
SCE	Chromatid Exchanges
SCENIHR	Scientific Committee for the Emerging and Newly Identified Health Risk
SMF	Static Magnetic Field
SSB	Single Strand Breaks
T	Tesla
TR/TE	Repetition Time/Echo Time
TVMF	Time-Varying Magnetic Field
UHF	Ultra-high Field
UV	Ultraviolet
VIS	Visible Light
WHO	World Health Organization

Appendix C

List of Figures

114

Appendix D

List of Tables

Appendix E

List of Publications

Journal Articles

1. **Fatahi M**, Reddig A, Friebe B, Reinhold D, Speck O. MRI and Genetic Damage: An Update. Current Radiology Reports. 2017 Apr 8;6(5):1-7.

2. **Fatahi M**, Karpowicz J, Gryz K, Fattahi A, Rose G, Speck O. Evaluation of exposure to (ultra) high static magnetic fields during activities around human MRI scanners. Magnetic Resonance Materials in Physics, Biology and Medicine. 2016 Dec 16:1-0, DOI: 10.1007/s10334-016-0602-z.

3. Reddig A, **Fatahi M**, Roggenbuck D, Ricke J, Reinhold D, Speck O, Friebe B. Impact of in Vivo High-Field-Strength and Ultra-High-Field-Strength MR Imaging on DNA Double-Strand-Break Formation in Human Lymphocytes. Radiology. 2016 Sep 30:160794.

4. **Fatahi M**, Reddig A, Friebe B, Hartig R, Prihoda TJ, Ricke J, Roggenbuck D, Reinhold D, Speck O. DNA double-strand breaks and micronuclei in human blood lymphocytes after repeated whole body exposures to 7 T Magnetic Resonance Imaging. NeuroImage. 2016 Jun 30;133:288-93.

5. **Fatahi M**, Demenescu LR, Speck O. Subjective perception of safety in healthy individuals working with 7 T MRI scanners: a retrospective multicentre survey. Magnetic Resonance Materials in Physics, Biology and Medicine. 2016 Jun 1;29(3):379-87.

6. Reddig A, **Fatahi M**, Friebe B, Guttek K, Hartig R, Godenschweger F, Roggenbuck D, Ricke J, Reinhold D, Speck O. Analysis of DNA double-strand breaks and cytotoxicity after 7 Tesla magnetic resonance imaging of isolated human lymphocytes. PloS one. 2015 Jul 15;10(7):e0132702.

7. Vijayalaxmi, **Fatahi M**, Speck O. Magnetic resonance imaging (MRI): A review of genetic damage investigations. Mutation Research/reviews in Mutation Research. 2015 Jun 30;764:51-63.72.

8. Vijayalaxmi, Scarfi M.R, **Fatahi M**, Reddig A, Reinhold D and Speck O, 2015. Letter by Vijayalaxmi et al Regarding Article, "Biological Effects of Cardiac Magnetic Resonance on Human Blood Cells" by Lancellotti et al. Circulation Cardiovascular Imaging; 8:e003697.

Conference Publications

1. **Fatahi M**, Karpowicz J, Gryz K, Speck O. Occupational exposure to (ultra) high static magnetic field during research activities around 7 T and 3 T MRI scanners, BioEM 2016, Ghent, Belgium. (Poster presentation)

2. **Fatahi M**, Demenescu L, Fattahi A, Speck O. Prevalence of sensory symptoms associated from ultra-high field magnetic resonance scanners, BioEM2016, June 2016, Ghent, Belgium. (Poster presentation)

3. **Fatahi M**, Reddig A, Friebe B, Roggenbuck D, Reinhold D and Speck O. Genetic damage investigations after repeated exposures to 7 T Magnetic Resonance Imaging. 24th Annual Meeting of International Society of Magnetic Resonance in Medicine, ISMRM 2016, Singapore. (Electronic poster)

4. **Fatahi M**, Redding A, Friebe B, Reinhold D, Speck O. Analysis of DNA Double-Strand Breaks in human Peripheral Blood Mononuclear Cells after exposure to 7 T MRI. 23rd Annual Meeting of International Society of Magnetic Resonance in Medicine. ISMRM, Toronto, Canada. (Oral presentation)

5. **Fatahi M**, Redding A, Reinhold D, Hartig R, Speck O. 7 Tesla MRI Does Not Induce DNA-Double-strand breaks in Isolated Human Lymphocytes. The 36th, Progresses in Electromagnetics Research Symposium, PIERS 2015, Prague, Czech Republic. (Poster presentation)

Bibliography

bibliography
1. Hartwig V, Giovannetti G, Vanello N, Lombardi M, Landini L, Simi S. Biological effects and safety in magnetic resonance imaging: a review. International journal of environmental research and public health. 2009 Jun 10;6(6):1778-98.

2. Habash R. Bioeffects and therapeutic applications of electromagnetic energy. CRC press; 2007 Nov 19.

3. Blank M, Goodman R. Comment: a biological guide for electromagnetic safety: the stress response. Bioelectromagnetics. 2004 Dec 1;25(8):642-6.

4. Reddig A, Fatahi M, Roggenbuck D, Ricke J, Reinhold D, Speck O, Friebe B. Impact of in Vivo High-Field-Strength and Ultra-High-Field-Strength MR Imaging on DNA Double-Strand-Break Formation in Human Lymphocytes. Radiology. 2016 Sep 30:160794.

5. Marshall J, Martin T, Downie J, Malisza K. A comprehensive analysis of MRI research risks: in support of full disclosure. The Canadian Journal of Neurological Sciences. 2007 Feb 1;34(01):11-7.

6. McRobbie D.W, Moore E, Graves M, Prince M, MRI: From picture to proton, second ed vol. 232. Cambridge: Cambridge University Press, Aug. 2007.

7. Schreiber WG, Teichmann EM, Schiffer I, Hast J, Akbari W, Georgi H, Graf R, Hehn M, Spieβ HW, Thelen M, Oesch F. Lack of mutagenic and co-mutagenic effects of magnetic fields during magnetic resonance imaging. Journal of Magnetic Resonance Imaging. 2001 Dec 1;14(6):779-88.

8. Schwenzer NF, Bantleon R, Maurer B, Kehlbach R, Schraml C, Claussen CD, Rodegerdts E. Detection of DNA double-strand breaks using γh2AX after MRI exposure at 3 Tesla: An in vitro study. Journal of Magnetic Resonance Imaging. 2007 Nov 1;26(5):1308-14.

9. Simi S, Ballardin M, Casella M, De Marchi D, Hartwig V, Giovannetti G, Vanello N, Gabbriellini S, Landini L, Lombardi M. Is the genotoxic effect of magnetic resonance negligible? Low persistence of micronucleus frequency in lymphocytes of individuals after cardiac scan. Mutation Research/Fundamental and Molecular Mechanisms of Mutagenesis. 2008 Oct 14;645(1):39-43.

10. Lee JW, Kim MS, Kim YJ, Choi YJ, Lee Y, Chung HW. Genotoxic effects of 3 T magnetic resonance imaging in cultured human lymphocytes. Bioelectromagnetics. 2011 Oct 1;32(7):535-42.

11. Yildiz S, Cece H, Kaya I, Celik H, Taskin A, Aksoy N, Kocyigit A, Eren MA. Impact of contrast enhanced MRI on lymphocyte DNA damage and serum visfatin level. Clinical biochemistry. 2011 Aug 31;44(12):975-9.

12. Fiechter M, Stehli J, Fuchs TA, Dougoud S, Gaemperli O, Kaufmann PA. Impact of cardiac magnetic resonance imaging on human lymphocyte DNA integrity. European heart journal. 2013 Jun 21:eht184.

13. Szerencsi Á, Kubinyi G, Váliczkó É, Juhász P, Rudas G, Mester Á, Jánossy G, Bakos J, Thuróczy G. DNA integrity of human leukocytes after magnetic resonance imaging. International journal of radiation biology. 2013 Oct 1;89(10):870-6.

14. Reddig A, Fatahi M, Friebe B, Guttek K, Hartig R, Godenschweger F, Roggenbuck D, Ricke J, Reinhold D, Speck O. Analysis of DNA double-strand breaks and cytotoxicity after 7 Tesla magnetic resonance imaging of isolated human lymphocytes. PloS one. 2015 Jul 15;10(7):e0132702.

15. Fatahi M, Reddig A, Friebe B, Hartig R, Prihoda TJ, Ricke J, Roggenbuck D, Reinhold D, Speck O. DNA double-strand breaks and micronuclei in human blood lymphocytes after

repeated whole body exposures to 7 T Magnetic Resonance Imaging. NeuroImage. 2016 Jun 30;133:288-93.

16. Lancellotti P, Nchimi A, Delierneux C, Hego A, Gosset C, Gothot A, Tshibanda LJ, Oury C. Biological Effects of Cardiac Magnetic Resonance on Human Blood CellsCLINICAL PERSPECTIVE. Circulation: Cardiovascular Imaging. 2015 Sep 1;8(9):e003697.

17. Brand M, Ellmann S, Sommer M, May MS, Eller A, Wuest W, Engert C, Achenbach S, Kuefner MA, Baeuerle T, Lell M. Influence of cardiac MR imaging on DNA double-strand breaks in human blood lymphocytes. Radiology. 2015 Jul 30;277(2):406-12.

18. International Commission on Non-Ionizing Radiation Protection. Guidelines on limits of exposure to static magnetic fields. Health Physics. 2009 Apr 1;96(4):504-14.

19. Formica D, Silvestri S. Biological effects of exposure to magnetic resonance imaging: an overview. Biomedical engineering online. 2004 Apr 22;3(1):11.

20. Kangarlu A, Pierre-Marie L. Biological effects and health implications in magnetic resonance imaging. Concepts in magnetic resonance. 2000 March 28;12.5: 321-359.

21. Schenck JF. Safety of strong, static magnetic fields. Journal of magnetic resonance imaging. 2000 Jul 1;12(1):2-19.

22. Holden AV. The sensitivity of the heart to static magnetic fields. Progress in biophysics and molecular biology. 2005 Apr 30;87(2):289-320.

23. Perrin A. MRI and Static Electric and Magnetic Fields. InElectromagnetic Fields, Environment and Health 2012 (pp. 11-24). Springer Paris.

24. Crozier S, Liu F. Numerical evaluation of the fields induced by body motion in or near high-field MRI scanners. Progress in biophysics and molecular biology. 2005 Apr 30;87(2):267-78.

25. Chakeres DW, de Vocht F. Static magnetic field effects on human subjects related to magnetic resonance imaging systems. Progress in biophysics and molecular biology. 2005 Apr 30;87(2):255-65.

26. Schenck JF. Health and Physiological Effects of Human Exposure to Whole-Body Four-Tesla Magnetic Fields during MRI. Annals of the New York Academy of Sciences. 1992 Mar 1;649(1):285-301.

27. de Vocht F, van Drooge H, Engels H, Kromhout H. Exposure, health complaints and cognitive performance among employees of an MRI scanners manufacturing department. Journal of Magnetic Resonance Imaging. 2006 Feb 1;23(2):197-204.

28. Murayama M. Orientation of sickled erythrocytes in a magnetic field. Nature. 1965 Apr 24;206(4982):420-2.

29. WHO (World Health Organization), Environmental Health Criteria 232, WHO Press, Geneva, Switzerland, 2004 Apr 26; ISBN 9241572329.

30. International Commission on Non-Ionizing Radiation Protection. Guidelines for limiting exposure to electric fields induced by movement of the human body in a static magnetic field and by time-varying magnetic fields below 1 Hz. Health physics. 2014 Mar 1;106(3):418-25.

31. Widder KJ, Senyei AE, inventors; Northwestern University, assignee. Method of delivering a therapeutic agent to a target capillary bed. United States patent US, 1982 Aug 244,345,588.

32. De Latour C. Magnetic separation in water pollution control. IEEE Transactions on Magnetics. 1973 Sep;9(3):314-6.

33. Kurinobu S, Uchiyama S. Recovery of plankton from red tide by HGMS. IEEE Transactions on Magnetics. 1982 Nov;18(6):1526-8.

34. Melville D, Paul F, Roath S. Direct magnetic separation of red cells from whole blood. Nature. 1975 Jun 26;255(5511):706.

35. Ichioka S, Minegishi M, Iwasaka M, Shibata M, Nakatsuka T, Harii K, Kamiya A, Ueno S. High-intensity static magnetic fields modulate skin microcirculation and temperature in vivo. Bioelectromagnetics. 2000 Apr 1;21(3):183-8.

36. Schul ten K. Magnetic field effects in chemistry and biology. Springer Berlin Heidelberg. InFestkörperprobleme 22 1982 (pp. 61-83).

37. Cozens FL, Scaiano JC. A comparative study of magnetic field effects on the dynamics of geminate and random radical pair processes in micelles. Journal of the American Chemical Society. 1993 Jun;115(12):5204-11.

38. Grissom CB. Magnetic field effects in biology: A survey of possible mechanisms with emphasis on radical-pair recombination. Chemical Reviews. 1995 Jan;95(1):3-24.

39. Ritz T, Adem S, Schulten K. A model for photoreceptor-based magnetoreception in birds. Biophysical journal. 2000 Feb 29;78(2):707-18.

40. Schaefer DJ, Bourland JD, Nyenhuis JA. Review of Patient Safety in Time-Varying Gradient Fields. Journal of magnetic resonance imaging. 2000 Jul 1;12(1):20-9.

41. Capstick M, McRobbie D, Hand J, Christ A, Kuhn S, Hanson Mild K, Cabot E, Li Y, Melzer A, Papadaki A, Prüssmann K. An investigation into occupational exposure to electromagnetic fields for personnel working with and around medical magnetic resonance imaging equipment. Report on Project VT/2007/017 of the European Commission, DG Employment, Social Affairs and Equal Opportunities http://www. myesr. org/html/img/pool/VT2007017FinalReportv04. pdf. 2008 Apr 4.

42. Ehrhardt JC, Lin CS, Magnotta VA, Fisher DJ, Yuh WT. Peripheral nerve stimulation in a whole-body echo-planar imaging system. Journal of Magnetic Resonance Imaging. 1997 Mar 1;7(2):405-9.

43. Ham CL, Engels JM, Van de Wiel GT, Machielsen A. Peripheral nerve stimulation during MRI: effects of high gradient amplitudes and switching rates. Journal of Magnetic Resonance Imaging. 1997 Sep 1;7(5):933-7.

44. Bourland JD, Nyenhuis JA, Schaefer DJ. Physiologic effects of intense MR imaging gradient fields. Neuroimaging Clinics of North America. 1999 May;9(2):363-77.

45. Den Boer JA, Bourland JD, Nyenhuis JA, Ham CL, Engels JM, Hebrank FX, Frese G, Schaefer DJ. Comparison of the threshold for peripheral nerve stimulation during gradient switching in whole body MR systems. Journal of Magnetic Resonance Imaging. 2002 May 1;15(5):520-5.

46. Zhang B, Yen YF, Chronik BA, McKinnon GC, Schaefer DJ, Rutt BK. Peripheral nerve stimulation properties of head and body gradient coils of various sizes. Magnetic resonance in medicine. 2003 Jul 1;50(1):50-8.

47. Heismann B, Ott M, Grodzki D. Sequence-based acoustic noise reduction of clinical MRI scans. Magnetic resonance in medicine. 2015 Mar 1;73(3):1104-9.

48. Murbach M, Neufeld E, Capstick M, Kainz W, Brunner DO, Samaras T, Pruessmann KP, Kuster N. Thermal Tissue Damage Model Analyzed for Different Whole-Body SAR and Scan Durations for Standard MR Body Coils. Magnetic resonance in medicine. 2014 Jan 1;71(1):421-31.

49. Murbach M, Neufeld E, Kainz W, Pruessmann KP, Kuster N. Whole-body and local RF absorption in human models as a function of anatomy and position within 1.5 T MR body coil. Magnetic resonance in medicine. 2014 Feb 1;71(2):839-45.

50. Foster KR, Glaser R. Thermal mechanisms of interaction of radiofrequency energy with biological systems with relevance to exposure guidelines. Health Physics. 2007 Jun 1;92(6):609-20.

51. Dewhirst MW, Vujaskovic Z, Jones E, Thrall D. Re-setting the biologic rationale for thermal therapy. International Journal of Hyperthermia. 2005 Dec 1;21(8):779-90.

52. Horsman MR, Overgaard J. Hyperthermia: a potent enhancer of radiotherapy. Clinical Oncology. 2007 Aug 31;19(6):418-26.

53. Ryan TP, Turner PF, Hamilton B. Interstitial microwave transition from hyperthermia to ablation: historical perspectives and current trends in thermal therapy. International Journal of Hyperthermia. 2010 Aug 1;26(5):415-33.

54. Rempp H, Hoffmann R, Roland J, Buck A, Kickhefel A, Claussen CD, Pereira PL, Schick F, Clasen S. Threshold-based prediction of the coagulation zone in sequential temperature mapping in MR-guided radiofrequency ablation of liver tumours. European radiology. 2012 May 1;22(5):1091-100.

55. Terraz S, Cernicanu A, Lepetit-Coiffé M, Viallon M, Salomir R, Mentha G, Becker CD. Radiofrequency ablation of small liver malignancies under magnetic resonance guidance: progress in targeting and preliminary observations with temperature monitoring. European radiology. 2010 Apr 1;20(4):886-97.

56. Lepetit-Coiffé, Matthieu, et al. "Real-time monitoring of radiofrequency ablation of liver tumors using thermal-dose calculation by MR temperature imaging: initial results in nine patients, including follow-up." *European radiology* 20.1 (2010): 193-201.

57. Qian GJ, Wang N, Shen Q, Sheng YH, Zhao JQ, Kuang M, Liu GJ, Wu MC. Efficacy of microwave versus radiofrequency ablation for treatment of small hepatocellular carcinoma: experimental and clinical studies. European radiology. 2012 Sep 1;22(9):1983-90.

58. Van Rhoon GC, Samaras T, Yarmolenko PS, Dewhirst MW, Neufeld E, Kuster N. CEM43° C thermal dose thresholds: a potential guide for magnetic resonance radiofrequency exposure levels?. European radiology. 2013 Aug 1;23(8):2215-27.

59. Shellock FG. Thermal responses in human subjects exposed to magnetic resonance imaging. Annals of the New York Academy of Sciences. 1992 Mar 1;649(1):260-72.

60. Athlas S. Magnetic resonance imaging of the brain and spine, Athlas S. New York: Raven Press; 1990.

61. Gordon CJ. Normalizing the thermal effects of radiofrequency radiation: body mass versus total body surface area. Bioelectromagnetics. 1987 Jan 1;8(2):111-8.

62. International Electrotechnical Commission. Amendment 2- Medical electrical equipment-Part 2-33: Particular requirements for the safety of magnetic resonance diagnostic devices. IEC 60601-2-33:2010/AMD: 2015 Jun 18.

63. U.S. Department of Health and Human Services, Food and Drug Administration, Center for Devices and Radiological Health. Criteria for significant risk investigations of magnetic resonance diagnostic devices. 2003.http://www.fda.gov/downloads/Medical Devices/DeviceRegulationandGuidance/GuidanceDocuments/ UCM072688.pdf. Accessed April 2016.

64. IEEE standard for safety levels with respect to human exposure to radio frequency electromagnetic fields, 3 KHz to 300 GHz. IEEE Standard C95.1-2005, 2006 Apr 16.

65. International Commission on Non-Ionising Radiation (ICNIRP), Medical Magnetic Resonance (MR) Procedures: Protection of patients. Health Physics t 2004 Aug, 87(2), pp 197-216.

66. Ahlbom A, Bridges J, De Seze R, Hillert L, Juutilainen J, Mattsson MO, Neubauer G, Schüz J, Simko M, Bromen K. Possible effects of electromagnetic fields (EMF) on human health--opinion of the scientific committee on emerging and newly identified health risks (SCENIHR). Toxicology. 2008 Apr 18;246(2-3):248-50.

67. International Electrotechnical Commission. Medical electrical equipment - particular requirements for the safety of magnetic resonance equipment for medical diagnosis. IEC 60601-2-33, 2002 May.

68. van Osch MJ, Webb AG. Safety of ultra-high field MRI: what are the specific risks?. Current Radiology Reports. 2014 Aug 1;2(8):1-8.

69. Speck O, Weigel M, Scheffler K. Contrasts, Mechanisms and Sequences. In: Hennig J, Speck O, editors. High Field MR Imaging. 1st ed. Berlin, Heidelberg: Springer Berlin Heidelberg; 2012. pp. 84–85. doi:10.1007/978-3-540-85090-8

70. Kraff O, Ladd ME. MR Safety Update 2015: Where Do the Risks Come From?. Current Radiology Reports. 2016 Jun 1;4(6):1-6.

71. Vijayalaxmi, Fatahi M, Speck O. Magnetic resonance imaging (MRI): A review of genetic damage investigations. Mutation Research/reviews in Mutation Research. 2015 Jun 30;764:51-63.72.

72. Winkler H Verbreitung und Ursache der Parthenogenesis im Pflanzen- und Tierreiche. Jena: Verlag Fischer, 1920.

73. Definition of Genome in Oxford dictionary. Retrieved 25 Oct 2016.

74. Luger K, Mäder AW, Richmond RK, Sargent DF, Richmond TJ. Crystal structure of the nucleosome core particle at 2.8 Å resolution. Nature. 1997 Sep 18;389(6648):251-60.

75. Pray L. Discovery of DNA structure and function: Watson and Crick. Nature Education. 2008;1(1):100.

76. Rossner P, Boffetta P, Ceppi M, Bonassi S, Smerhovsky Z, Landa K, Juzova D, Šrám RJ. Chromosomal aberrations in lymphocytes of healthy subjects and risk of cancer. Environmental health perspectives. 2005 May 1:517-20.

77. Clancy S. DNA damage & repair: mechanisms for maintaining DNA integrity. Nature Education 1 (1): 103 Email DNA integrity is always under attack from environmental agents like skin cancer-causing UV rays. How do DNA repair mechanisms detect and repair damaged DNA, and what happens when they fail. 2008:10-4.

78. Phillips JL, Singh NP, Lai H. Electromagnetic fields and DNA damage. Pathophysiology. 2009 Aug 31;16(2):79-88.

79. Khanna KK, Jackson SP. DNA double-strand breaks: signaling, repair and the cancer connection. Nature genetics. 2001 Mar 1;27(3):247-54.

80. Rogakou EP, Pilch DR, Orr AH, Ivanova VS, Bonner WM. DNA double-stranded breaks induce histone H2AX phosphorylation on serine 139. Journal of biological chemistry. 1998 Mar 6;273(10):5858-68.

81. Woolf DK, Williams NR, Bakshi R, Madani SY, Eaton DJ, Fawcitt S, Pigott K, Short S, Keshtgar M. Biological dosimetry for breast cancer radiotherapy: a comparison of external beam and intraoperative radiotherapy. Springer Plus. 2014 Jun 30;3(1):329.

82. Redon CE, Nakamura AJ, Martin OA, Parekh PR, Weyemi US, Bonner WM. Recent developments in the use of γ-H2AX as a quantitative DNA double-strand break biomarker. Aging (Albany NY). 2011 Feb 11;3(2):168-74.

83. Redon CE, Nakamura AJ, Sordet O, Dickey JS, Gouliaeva K, Tabb B, Lawrence S, Kinders RJ, Bonner WM, Sedelnikova OA. γ-H2AX detection in peripheral blood lymphocytes, splenocytes, bone marrow, xenografts, and skin. DNA Damage Detection In Situ, Ex Vivo, and In Vivo: Methods and Protocols. 2011:249-70.

84.Heylmann D, Kaina B. The γH2AX DNA damage assay from a drop of blood. Scientific reports. 2016;6.

85. Redon CE, Weyemi U, Parekh PR, Huang D, Burrell AS, Bonner WM. γ-H2AX and other histone post-translational modifications in the clinic. Biochimica et Biophysica Acta (BBA)-Gene Regulatory Mechanisms. 2012 Jul 31;1819(7):743-56.

86. Willitzki A, Hiemann R, Peters V, Sack U, Schierack P, Rödiger S, Anderer U, Conrad K, Bogdanos DP, Reinhold D, Roggenbuck D. New platform technology for comprehensive serological diagnostics of autoimmune diseases. Clinical and Developmental Immunology. 2012 Dec 19;2012.

87. Willitzki A, Lorenz S, Hiemann R, Guttek K, Goihl A, Hartig R, Conrad K, Feist E, Sack U, Schierack P, Heiserich L. Fully automated analysis of chemically induced γH2AX foci in human peripheral blood mononuclear cells by indirect immunofluorescence. Cytometry Part A. 2013 Nov 1;83(11):1017-26.

88. Runge R, Hiemann R, Wendisch M, Kasten-Pisula U, Storch K, Zoephel K, Fritz C, Roggenbuck D, Wunderlich G, Conrad K, Kotzerke J. Fully automated interpretation of ionizing radiation-induced γH2AX foci by the novel pattern recognition system AKLIDES®. International journal of radiation biology. 2012 May 1;88(5):439-47.

89. Heddle JA. A rapid in vivo test for chromosomal damage. Mutation Research/Fundamental and Molecular Mechanisms of Mutagenesis. 1973 May 31;18(2):18790.

90. Schmid W. The micronucleus test.Mutatin Research. 1975 Feb 31;1: 9–15.

91. Fenech, M. The in vitro micronucleus technique.Mutatation Research. 2000 Nov 20;455(1-2):81–95.

92. Fenech, M. & Morley, A.A. Solutions to the kinetic problem in the micronucleusassay.Cytobios43, 233–246 (1985).

93. Fenech M, Morley A. Solutions to the kinetic problem in the micronucleus assay. Cytobios. 1985 Jan 1;43(172-173):233-46.

94. Fenech M, Morley AA. Cytokinesis-block micronucleus method in human lymphocytes: effect of in vivo ageing and low dose X-irradiation. Mutation Research/Fundamental and Molecular Mechanisms of Mutagenesis. 1986 Jul 31;161(2):193-8.

95. Carter SB. Effects of cytochalasins on mammalian cells. Nature. 1967 Jan 21;213(5073):261-4.

96. Cornforth MN, Goodwin EH. Transmission of radiation-induced acentric chromosomal fragments to micronuclei in normal human fibroblasts. Radiation research. 1991 May 1;126(2):210-7.

97. Huang Y, Fenech M, Shi Q. Micronucleus formation detected by live-cell imaging. Mutagenesis. 2011 Jan 1;26(1):133-8.

98. Albertini RJ, Anderson D, Douglas GR, Hagmar L, Hemminki K, Merlo F, Natarajan AT, Norppa H, Shuker DE, Tice R, Waters MD. IPCS guidelines for the monitoring of genotoxic effects of carcinogens in humans. Mutation Research/Reviews in Mutation Research. 2000 Aug 31;463(2):111-72.

99. Crott JW, Mashiyama ST, Ames BN, Fenech MF. Methylenetetrahydrofolate reductase C677 T polymorphism does not alter folic acid deficiency-induced uracil incorporation into primary human lymphocyte DNA in vitro. Carcinogenesis. 2001 Jul 1;22(7):1019-25.

100. Fenech M. The role of folic acid and Vitamin B12 in genomic stability of human cells. Mutation Research/Fundamental and Molecular Mechanisms of Mutagenesis. 2001 Apr 18;475(1):57-67.

101. Fenech M. The Genome Health Clinic and Genome Health Nutrigenomics concepts: diagnosis and nutritional treatment of genome and epigenome damage on an individual basis. Mutagenesis. 2005 Jul 1;20(4):255-69.

102. Fenech M, Bonassi S. The effect of age, gender, diet and lifestyle on DNA damage measured using micronucleus frequency in human peripheral blood lymphocytes. Mutagenesis. 2011 Jan 1;26(1):43-9.

103. Fenech M. Important variables that influence base-line micronucleus frequency in cytokinesis-blocked lymphocytes—a biomarker for DNA damage in human populations. Mutation Research/Fundamental and Molecular Mechanisms of Mutagenesis. 1998 Aug 3;404(1):155-65.

104. Fenech M. Cytokinesis-block micronucleus cytome assay. Nature protocols. 2007 May 1;2(5):1084-104.

105. Kirsch-Volders M, Sofuni T, Aardema M, Albertini S, Eastmond D, Fenech M, Ishidate M, Lorge E, Norppa H, Surrallés J, von der Hude W. Report from the in vitro micronucleus assay working group. Environmental and molecular mutagenesis. 2000 Jan 1;35(3):167-72.

106. Meretoja T, Vainio H. The use of human lymphocyte tests in the evaluation of potential mutagens: clastogenic activity of styrene in occupational exposure. In Genetic Damage in Man Caused by Environmental Agents. Academic Press New York. 1979 (pp. 213-225).

107. Stich HF, Curtis JR, Parida BB. Application of the micronucleus test to exfoliated cells of high cancer risk groups: tobacco chewers. International Journal of Cancer. 1982 Nov 15;30(5):553-9.

108. Majer BJ, Laky B, Knasmüller S, Kassie F. Use of the micronucleus assay with exfoliated epithelial cells as a biomarker for monitoring individuals at elevated risk of genetic damage and in chemoprevention trials. Mutation Research/Reviews in Mutation Research. 2001 Dec 31;489(2):147-72.

109. Fenech M. The cytokinesis-block micronucleus technique: a detailed description of the method and its application to genotoxicity studies in human populations. Mutation Research/Fundamental and Molecular Mechanisms of Mutagenesis. 1993 Jan 31;285(1):35-44.

110. Bonassi S, Znaor A, Ceppi M, Lando C, Chang WP, Holland N, Kirsch-Volders M, Zeiger E, Ban S, Barale R, Bigatti MP. An increased micronucleus frequency in peripheral blood lymphocytes predicts the risk of cancer in humans. Carcinogenesis. 2006 Sep 14;28(3):625-31.

111. Bonassi S, El-Zein R, Bolognesi C, Fenech M. Micronuclei frequency in peripheral blood lymphocytes and cancer risk: evidence from human studies. Mutagenesis. 2011 Jan 1;26(1):93-100.

112. Countryman PI, Heddle JA. The production of micronuclei from chromosome aberrations in irradiated cultures of human lymphocytes. Mutation Research/Fundamental and Molecular Mechanisms of Mutagenesis. 1976 Dec 31;41(2):321-31.

113. Bolognesi C, Perrone E, Roggieri P, Pampanin DM, Sciutto A. Assessment of micronuclei induction in peripheral erythrocytes of fish exposed to xenobiotics under controlled conditions. Aquatic toxicology. 2006 Jun 1;78:S93-8.

114. Grover IS, Malhi PK. Genotoxic effects of some organophosphorous pesticides I. Induction of micronuclei in bone marrow cells in rat. Mutation Research/Genetic Toxicology. 1985 Mar 1;155(3):131-4.

115. Fenech M. The advantages and disadvantages of the cytokinesis-block micronucleus method. Mutation Research/Genetic Toxicology and Environmental Mutagenesis. 1997 Aug 1;392(1):11-8.

116. International Agency for Research on Cancer (IARC), Monographs on the Evaluation of Carcinogenic Risks to Humans. Non-Ionising Radiation. Part 1: Static and Extremely Low Frequency (ELF) Electric and Magnetic Fields, vol. 80, ISBN 9283212800, 2002.

117. Advice on limiting exposure to electromagnetic fields (0–300 GHz). NRPB (UK National Radiological Protection Board), Chilton, UK, vol. 15, no. 2, 2004.

118. Vijayalaxmi, Obe G. Controversial cytogenetic observations in mammalian somatic cells exposed to radiofrequency radiation. Radiation research. 2004 Nov;162(5):481-96.

119. Miyakoshi J. Effects of static magnetic fields at the cellular level. Progress in biophysics and molecular biology. 2005 Apr 30;87(2):213-23.

120. Verschaeve L. Genetic effects of radiofrequency radiation (RFR). Toxicology and applied pharmacology. 2005 Sep 1;207(2):336-41.

121. Juutilainen J, Kumlin T, Naarala J. Do extremely low frequency magnetic fields enhance the effects of environmental carcinogens? A meta-analysis of experimental studies. International journal of radiation biology. 2006 Jan 1;82(1):1-2.

122. Vijayalaxmi, Prihoda T,J . Genetic damage in mammalian somatic cells exposed to radiofrequency radiation: a meta-analysis of data from 63 publications (1990–2005). Radiation research. 2008 May;169(5):561-74.123.

123. Albert GC, Mcnamee JP, Marro L, Vijayalaxmi, Bellier PV, Prato FS, Thomas AW. Assessment of genetic damage in peripheral blood of human volunteers exposed (whole-body) to a 200 µT, 60 Hz magnetic field. International journal of radiation biology. 2009 Jan 1;85(2):144-52.

124. Wolf FI, Torsello A, Tedesco B, Fasanella S, Boninsegna A, D'Ascenzo M, Grassi C, Azzena GB, Cittadini A. 50-Hz extremely low frequency electromagnetic fields enhance cell proliferation and DNA damage: possible involvement of a redox mechanism. Biochimica et Biophysica Acta (BBA)-Molecular Cell Research. 2005 Mar 22;1743(1):120-9.

125. Ruediger HW. Genotoxic effects of radiofrequency electromagnetic fields. Pathophysiology. 2009 Aug 31;16(2):89-102.

126. Verschaeve L. Genetic damage in subjects exposed to radiofrequency radiation. Mutation Research/Reviews in Mutation Research. 2009 Jun 30;681(2):259-70.

127. Vijayalaxmi, Prihoda TJ. Genetic damage in mammalian somatic cells exposed to extremely low frequency electro-magnetic fields: A meta-analysis of data from 87 publications (1990–2007). International Journal of Radiation Biology. 2009 Jan 1;85(3):196-213.

128. Reddy SB, Weller J, Desjardins-Holmes D, Winters T, Keenliside L, Prato FS, Prihoda TJ, Thomas AW. Micronuclei in the blood and bone marrow cells of mice exposed to specific complex time-varying pulsed magnetic fields. Bioelectromagnetics. 2010 Sep 1;31(6):445-53.

129. Verschaeve L, Juutilainen J, Lagroye I, Miyakoshi J, Saunders R, De Seze R, Tenforde T, Van Rongen E, Veyret B, Xu Z. In vitro and in vivo genotoxicity of radiofrequency fields. Mutation Research/Reviews in Mutation Research. 2010 Dec 31;705(3):252-68.

130. Vijayalaxmi, Prihoda TJ. Genetic damage in human cells exposed to non-ionizing radiofrequency fields: a meta-analysis of the data from 88 publications (1990–2011). Mutation Research/Genetic Toxicology and Environmental Mutagenesis. 2012 Dec 12;749(1):1-6.131.

131. International Agency for Research on Cancer (IARC), Monographs on the Evaluation of Carcinogenic Risks to Humans.   Non-Ionising Radiation.   Part 2: Radiofrequency Electromagnetic Fields, vol. 102, ISBN 9789283213253. 2002.

132. The Scientific Committee on Emerging and Newly Identified Health Risks (SCENIHR). http://ec.europa.eu/health/ph_risk/committees/04_scenihr/docs/ scenihr_o_024.pdf (accessed 05.02.16).

133. Reddy AB, McKenzie RJ, McIntosh RL, Prihoda TJ, Wood AW. Incidence of micronuclei in human peripheral blood lymphocytes exposed to modulated and unmodulated 2450 MHz radiofrequency fields. Bioelectromagnetics. 2013 Oct 1;34(7):542-8.

134. Vijayalaxmi, Scarfi MR. International and national expert group evaluations: Biological/health effects of radiofrequency fields. International journal of environmental research and public health. 2014 Sep 10;11(9):9376-408.

135. Hill MA, O'neill P, McKenna WG. Comments on potential health effects of MRI-induced DNA lesions: quality is more important to consider than quantity. Eur Heart J Cardiovasc Imaging. 2016 Nov 1;17(11):1230-8.

136. Antonelli F, Belli M, Cuttone G, Dini V, Esposito G, Simone G, Sorrentino E, Tabocchini MA. Induction and repair of DNA double-strand breaks in human cells: dephosphorylation of histone H2AX and its inhibition by calyculin A. Radiation research. 2005 Oct;164(4):514-7.

137. Paul M. S. Monk Physical Chemistry. John Wiley and Sons. p. 435. ISBN 978-0-471-49180-4, 2004.

138. Aflatooni K, Gallup GA, Burrow PD. Electron attachment energies of the DNA bases. The Journal of Physical Chemistry A. 1998 Jul 30;102(31):6205-7.

139. Ptasińska S, Denifl S, Scheier P, Märk TD. Inelastic electron interaction (attachment/ionization) with deoxyribose. The Journal of chemical physics. 2004 May 8;120(18):8505-11.

140. Li X, Sevilla MD, Sanche L. Density functional theory studies of electron interaction with DNA: can zero eV electrons induce strand breaks?. Journal of the American Chemical Society. 2003 Nov 12;125(45):13668-9.

141. Scheer AM, Aflatooni K, Gallup GA, Burrow PD. Bond breaking and temporary anion states in uracil and halouracils: Implications for the DNA bases. Physical review letters. 2004 Feb 12;92(6):068102.

142. Bhaskaran R, Sarma M. The role of the shape resonance state in low energy electron induced single strand break in 2′-deoxycytidine-5′-monophosphate. Physical Chemistry Chemical Physics. 2015;17(23):15250-7.

143. Boudaïffa B, Cloutier P, Hunting D, Huels MA, Sanche L. Resonant formation of DNA strand breaks by low-energy (3 to 20 eV) electrons. Science. 2000 Mar 3;287(5458):1658-60.

144. Barrios R, Skurski P, Simons J. Mechanism for damage to DNA by low-energy electrons. The Journal of Physical Chemistry B. 2002 Aug 22;106(33):7991-4.

145. Mayer-Wagner S, Passberger A, Sievers B, Aigner J, Summer B, Schiergens TS, Jansson V, Müller PE. Effects of low frequency electromagnetic fields on the chondrogenic differentiation of human mesenchymal stem cells. Bioelectromagnetics. 2011 May 1;32(4):283-90.

146. Sannino A, Zeni O, Romeo S, Massa R, Gialanella G, Grossi G, Manti L, Scarfì MR. Adaptive response in human blood lymphocytes exposed to non-ionizing radiofrequency fields: resistance to ionizing radiation-induced damage. Journal of radiation research. 2014 Mar 1;55(2):210-7.

147. Tucker JD, Vadapalli M, Joiner MC, Ceppi M, Fenech M, Bonassi S. Estimating the lowest detectable dose of ionizing radiation by the cytokinesis-block micronucleus assay. Radiation research. 2013 Aug 9;180(3):284-91.

148. Fuentes MA, Trakic A, Wilson SJ, Crozier S. Analysis and measurements of magnetic field exposures for healthcare workers in selected MR environments. IEEE Transactions on Biomedical Engineering. 2008 Apr;55(4):1355-64.

149. Úbeda A, Martínez MA, Cid MA, Chacón L, Trillo MA, Leal J. Assessment of occupational exposure to extremely low frequency magnetic fields in hospital personnel. Bioelectromagnetics. 2011 Jul 1;32(5):378-87.

150. Yamaguchi-Sekino S, Nakai T, Imai S, Izawa S, Okuno T. Occupational exposure levels of static magnetic field during routine MRI examination in 3 T MR system. Bioelectromagnetics. 2014 Jan 1;35(1):70-5.

151. Karpowicz J, Gryz K. The pattern of exposure to static magnetic field of nurses involved in activities related to contrast administration into patients diagnosed in 1.5 T MRI scanners. Electromagnetic biology and medicine. 2013 Jun 1;32(2):182-91.

152. Bradley JK, Nyekiova M, Price DL, Lopez L, Crawley T. Occupational exposure to static and time-varying gradient magnetic fields in MR units. Journal of Magnetic Resonance Imaging. 2007 Nov 1;26(5):1204-9.

153. Groebner J, Umathum R, Bock M, Krafft AJ, Semmler W, Rauschenberg J. MR safety: simultaneous B 0, dΦ/dt, and dB/dt measurements on MR-workers up to 7 T. Magnetic Resonance Materials in Physics, Biology and Medicine. 2011 Dec 1;24(6):315-22.

154.McRobbie DW. Occupational exposure in MRI. British Journal of Radiology 2012,85:293–312.

155. Schaap K, Christopher-De Vries Y, Crozier S, De Vocht F, Kromhout H. Exposure to static and time-varying magnetic fields from working in the static magnetic stray fields of MRI scanners: a comprehensive survey in the Netherlands. Annals of occupational hygiene. 2014 Aug 18:meu057.

156. Zilberti L, Bottauscio O, Chiampi M. Assessment of exposure to MRI motion-induced fields based on the International Commission on Non-Ionizing Radiation Protection (ICNIRP) guidelines. Magnetic resonance in medicine. 2015 Nov 1, 76:1291–1300.

157. Fatahi M, Karpowicz J, Gryz K, Fattahi A, Rose G, Speck O. Evaluation of exposure to (ultra) high static magnetic fields during activities around human MRI scanners. Magnetic Resonance Materials in Physics, Biology and Medicine. 2016 Dec 16:1-0, DOI: 10.1007/s10334-016-0602-z.

158. Andreuccetti D, Contessa GM, Falsaperla R, Lodato R, Pinto R, Zoppetti N, Rossi P. Weighted-peak assessment of occupational exposure due to MRI gradient fields and movements in a nonhomogeneous static magnetic field. Medical physics. 2013 Jan 1;40(1), DOI: 10.1118/1.4771933.

158. Kännälä S, Toivo T, Alanko T, Jokela K. Occupational exposure measurements of static and pulsed gradient magnetic fields in the vicinity of MRI scanners. Physics in medicine and biology. 2009 Mar 17;54(7):2243.

160. Laakso I, Kännälä S, Jokela K. Computational dosimetry of induced electric fields during realistic movements in the vicinity of a 3 T MRI scanner. Physics in medicine and biology. 2013 Apr 2;58(8):2625.

161. Karpowicz J, Hietanen M, Gryz K. Occupational risk from static magnetic fields of MRI scanners. The Environmentalist. 2007 Dec 1;27(4):533-8.

162. Crozier S, Liu F. Numerical evaluation of the fields induced by body motion in or near high-field MRI scanners. Progress in biophysics and molecular biology. 2005 Apr 30;87(2):267-78.

163. Trakic A, Wang H, Liu F. Numerical study of currents in workers induced by body-motion around high-ultrahigh field MRI magnets. Journal of Magnetic Resonance Imaging. 2007 Nov 1;26(5):1261-77.

164. Fatah M, Demenescu LR, Speck O. Subjective perception of safety in healthy individuals working with 7 T MRI scanners: a retrospective multicenter survey. Magnetic Resonance Materials in Physics, Biology and Medicine. 2016 Jun 1;29(3):379-87.

165. Wilén J, de Vocht F. Health complaints among nurses working near MRI scanners- A descriptive pilot study. European journal of radiology. 2011 Nov 30;80(2):510-3.

166. Schaap K, Vries CD, Cambron-Goulet É, Kromhout H. Work-related factors associated with occupational exposure to static magnetic stray fields from MRI scanners. Magnetic resonance in medicine. 2015 Jun 1;75(5).2141–2155.

167. Batistatou E, Mölter A, Kromhout H, van Tongeren M, Crozier S, Schaap K, Gowland P, Keevil SF, de Vocht F. Personal exposure to static and time-varying magnetic fields during MRI procedures in clinical practice in the UK. Occupational and environmental medicine. 2016 Nov 1;73(11):779-86.

168. Acri G, Testagrossa B, Causa F, Tripepi MG, Vermiglio G, Novario R, Pozzi L, Quadrelli G. Evaluation of occupational exposure in magnetic resonance sites. La radiologia medica. 2014 Mar 1;119(3):208-13.

169. Theysohn JM, Maderwald S, Kraff O, Moenninghoff C, Ladd ME, Ladd SC. Subjective acceptance of 7 Tesla MRI for human imaging. Magnetic Resonance Materials in Physics, Biology and Medicine. 2008 Mar 1;21(1-2):63.

170. Warner R. Ultra-high field magnets for whole-body MRI. Superconductor Science and Technology. 2016 Aug 8;29(9):094006.

171. Heilmaier C, Theysohn JM, Maderwald S, Kraff O, Ladd ME, Ladd SC. A large-scale study on subjective perception of discomfort during 7 and 1.5 T MRI examinations. Bioelectromagnetics. 2011 Dec 1;32(8):610-9.

172. Moenninghoff C, Maderwald S, Theysohn JM, Kraff O, Ladd ME, El Hindy N, van de Nes J, Forsting M, Wanke I. Imaging of adult astrocytic brain tumours with 7 T MRI: preliminary results. European radiology. 2010 Mar 1;20(3):704-13.

173. Lupo JM, Chuang CF, Chang SM, Barani IJ, Jimenez B, Hess CP, Nelson SJ. 7 Tesla susceptibility-weighted imaging to assess the effects of radiotherapy on normal-appearing brain in patients with glioma. International Journal of Radiation Oncology* Biology* Physics. 2012 Mar 1;82(3):e493-500.173.

174. Visser F, Zwanenburg JJ, Hoogduin JM, Luijten PR. High-resolution magnetization-prepared 3D-FLAIR imaging at 7.0 Tesla. Magnetic resonance in medicine. 2010 Jul 1;64(1):194-202.

175. Rauschenberg J, Nagel AM, Ladd SC, Theysohn JM, Ladd ME, Möller HE, Trampel R, Turner R, Pohmann R, Scheffler K, Brechmann A. Multicenter study of subjective acceptance during magnetic resonance imaging at 7 and 9.4 T. Investigative radiology. 2014 May 1;49(5):249-59.

176. Versluis MJ, Teeuwisse WM, Kan HE, Buchem MA, Webb AG, Osch MJ. Subject tolerance of 7 T MRI examinations. Journal of Magnetic Resonance Imaging. 2013 Sep 1;38(3):722-5.

177. Williams S, Shiaw WT. Mood and organizational citizenship behavior: The effects of positive affect on employee organizational citizenship behavior intentions. The Journal of Psychology. 1999 Nov 1;133(6):656-68.

178. van Dongen D, Smid T, Timmermans DRM (2011) Perception of the health risks of electromagnetic fields by MRI radiographers and airport security officers compared to the

general Dutch working population: a cross sectional analysis. Environmental Health. 2011 Nov 10(1):95, Doi:10.1186/1476-069X-10-95.

179. Schaap K, Christopher-De Vries Y, Slottje P, Kromhout H. Inventory of MRI applications and workers exposed to MRI-related electromagnetic fields in the Netherlands. European journal of radiology. 2013 Dec 31;82(12):2279-85.

180. Thormann M, Amthauer H, Adolf D, Wollrab A, Ricke J, Speck O. Efficacy of diphenhydramine in the prevention of vertigo and nausea at 7 T MRI. European journal of radiology. 2013 May 31;82(5):768-72.

181. Koradecka D, Pośniak M, Widerszal-Bazyl M, Augustyńska D, Radkiewicz P. A comparative study of objective and subjective assessment of occupational risk. International journal of occupational safety and ergonomics. 2010 Jan 1;16(1):3-22.

182. Griffin MA, Neal A. Perceptions of safety at work: a framework for linking safety climate to safety performance, knowledge, and motivation. Journal of occupational health psychology. 2000 Jul;5(3):347.

183. Arezes PM, Miguel AS. Risk perception and safety behaviour: A study in an occupational environment. Safety Science. 2008 Jul 31;46(6):900-7.

184. Flin R, Mearns K, Gordon R, Fleming M. Risk perception by offshore workers on UK oil and gas platforms. Safety Science. 1996 Apr 30;22(1):131-45.

185. Friebe B, Wollrab A, Thormann M, Fischbach K, Ricke J, Grueschow M, Kropf S, Fischbach F, Speck O. Sensory perceptions of individuals exposed to the static field of a 7 T MRI: A controlled blinded study. Journal of Magnetic Resonance Imaging. 2015 Jun 1;41(6):1675-81.

186. Mian OS, Li Y, Antunes A, Glover PM, Day BL. On the vertigo due to static magnetic fields. PloS one. 2013 Oct 30;8(10):e78748.

187. International Commission on Non-Ionizing Radiation Protection. ICNIRP Statement on Diagnostic Devices Using Non-ionizing Radiation: Existing Regulations and Potential Health Risks. Health Physics. 2017 Mar 1;112(3):305-21.

Declaration of Honor

I hereby declare that I produced this thesis without prohibited external assistance and that none other than the listed references and tools have been used.

I did not make use of any commercial consultant concerning graduation. A third party did not receive any nonmonetary perquisites neither directly nor indirectly, for activities which are connected with the contents of the presented thesis.

All sources of information are clearly marked, including my own publications.

In particular, I have not consciously:

-Fabricated data or rejected undesired results

-Misused statistical methods with the aim of drawing other conclusions than those warranted by the available data

-Plagiarized data or publications

-Presented the results of other researchers in a distorted way

I do know that violations of copyright may lead to injunction and damage claims of the author and also to prosecution by the law enforcement authorities. I hereby agree that the thesis may need to be reviewed with an electronic data processing for plagiarism.

This work has not yet been submitted as a doctoral thesis in the same or a similar form in Germany or in any other country. It has not yet been published as a whole.

Magdeburg, 18 February 2017

Mahsa Fatahi

Curriculum Vitae

Personal Information

Date of birth: May 26th ,1985

Place of birth: Tehran, Iran

Education

2013-2017	Marie Curie Early Stage Researcher Ph.D. Candidate Magnetic Resonance Safety and Bio-effects, Otto-von-Guericke University, Magdeburg, Germany
2011-2013	Marie Curie Early Stage Researcher, Integrated Interventional Imaging Operating System (IIIOS) Initial Training Network, Institute for Medical Science and Technology, Dundee, Scotland, United Kingdom
2009-2011	Master of Medical Imaging, KTH Royal Institute of Technology, Stockholm, Sweden
2005-2008	Bachelor of Biomedical Engineering, Azad University, Science and Research Branch, Tehran, Iran